NAZARBAYEV
UNIVERSITY

MULTI-STAGE SENSITIVITY ANALYSIS OF EARLY DESIGN STAGE PARAMETERS FOR PCM-INTEGRATED BUILDINGS

by
Assemgul Saurbayeva

Submitted in partial fulfillment

of the requirements for the degree of
Doctor of Philosophy in Civil Engineering

April, 2023

MULTI-STAGE SENSITIVITY ANALYSIS OF EARLY DESIGN STAGE PARAMETERS FOR PCM-INTEGRATED BUILDINGS

by
Assemgul Saurbayeva

Submitted in partial fulfillment of the requirement for the degree of

Doctor of Philosophy in Civil Engineering

School of Engineering and Digital Sciences

Civil and Environmental Engineering Department

Nazarbayev University

April, 2023

Supervised by

Shazim Ali Memon

Declaration

I declare that the research contained in this thesis, unless otherwise formally indicated within the text, is the author's original work. The thesis has not been previously submitted to this or any other university for a degree and does not incorporate any material already submitted for a degree.

Signature:

Date: 10.04.2023

Abstract

Buildings are substantial contributors to greenhouse gas emissions and energy consumption. To meet the global carbon reduction goals, the enhancement of energy-efficiency of the buildings is vital. Early selection of key design parameters during building design offers the best opportunity for achieving energy-efficient buildings. Several studies have highlighted the importance of early design decisions in the building design process. However, the following issues have not been addressed yet: (a) How to develop a systematic framework for multi-stage sensitivity analysis and optimization of buildings to reduce total energy consumption in hot semi-arid climate zones? (b) Which early design stage parameters significantly impact the design of PCM-integrated buildings in hot semi-arid climate zones? (c) How do the early design stage parameters interact with total energy consumption? (d) What is the most effective combination of early design stage parameters that can reduce the total energy consumption of PCM-integrated buildings? (e) Are the optimal solutions for buildings economically feasible? (f) What is the impact of climate change on total energy consumption in PCM-integrated buildings? Thus, this research proposes a multi-stage sensitivity analysis and optimization framework to comprehensively explore the influence and relationship of early design stage parameters on total energy consumption in six cities in the hot semi-arid climate zone. For the multi-stage sensitivity analysis framework, three methods of global sensitivity analysis indices (Standardized rank regression coefficients, Partial rank correlation coefficient, and the Morris method), which are considered to be the most robust and efficient, were selected for the first stage while in the second stage, local sensitivity analysis was applied. The building layout, energy-efficiency measures, and envelope thermophysical properties of passive design measures were used as input parameters, while total energy consumption was selected as the output parameter. Thereafter, Evolutionary Algorithms were used to solve an optimization problem to find the best set of optimal solutions. Finally, an economic assessment of optimal solutions was applied to the current scenario. Based on the multi-stage sensitivity analysis results, the roof solar absorptance, wall solar absorptance, window conductivity, building orientation, and melting temperature of PCM were the most important early design stage parameters influencing total energy consumption. The rankings of certain early design stage characteristics may vary considerably between cities in the same climatic zone. The obtained single-objective optimization results showed that the total energy consumption was reduced by up to 19.7% and 5.6% for the current and future scenarios, respectively. For the current scenario, the payback period was between 25.7 and 63.7 years, respectively. Conclusively, this research presents design guidelines supported by data and can help engineers, designers, and architects use passive design measures from the early design stages in hot semi-arid climates.

ACKNOWLEDGMENTS

I must first and foremost express my gratitude to the Almighty for giving me the patience and strength to work through these years.

I wish to express my deep appreciation to Professor Shazim Ali Memon, my supervisor, for his invaluable advice, continuous support, and patience during my Ph.D. study. I have greatly benefited from your wealth of knowledge and meticulous editing. I am extremely grateful that you accepted me as a student and continued to have faith in me over the years.

I am grateful to Professor Jong Kim for providing resources and encouraging me to complete the thesis in a timely manner. I greatly appreciate my external supervisor, Professor Hongzhi CUI, for his feedback and guidance.

Finally, but most importantly, an enormous thanks to my parents, my grandmother, my brother, and his family, for supporting me emotionally throughout my Ph.D. experience and my life in general.

Furthermore, I extend my gratitude to my friends, NU groupmates, lab mates, and research group for their continuous support.

CONTENTS

LIST OF TABLES

LIST OF FIGURES

LIST OF SYMBOLS

Fully implicit scheme

C_p	Specific heat of material
ρ	Density of a material
Δx	Finite-difference layer thickness
i	Node being modelled
i-1	Adjacent node to exterior construction
I+1	Adjacent node to interior construction
j	Temperature at the end of previous time step
j+1	A new temperature at end of time step
Δt	Computation time step
k	Thermal conductivity
k_w	Thermal conductivity for the interface between nodes *i* and *i+1*
k_E	Thermal conductivity for the interface between nodes *i* and *i-1*
h	Enthalpy
α	Material's thermal diffusivity
c	Spatial discretization constant
Fo	Fourier number
T	Node temperature

Economic assessment

C_w	Cost of the wall
C_r	Cost of the roof
C_{win}	Cost of the window
C_{oo}	Operating cost for the optimal solution
C_{ob}	Operating cost for the base case
C_o	Operating cost
C_h	Operating cost for heating
C_c	Operating cost for cooling
C_{io}	Initial investment for the optimal solution
C_{ib}	Initial investment for the base case
C_i	Initial investment cost

Fanger thermal comfort model

h_c	Convective heat transfer coefficient
I_{cl}	Clothing insulation
f_{cl}	Clothing insulation surface area factor
M	Metabolic rate
$\mathrm{P_a}$	Water vapor partial pressure
W	Effective mechanical power
V_{ar}	Relative air velocity
$\mathrm{t_r}$	Mean radiant temperature
t_{cl}	Clothing surface temperature
$\mathrm{t_a}$	Air temperature

Local Sensitivity analysis

$S_{local,i}$	Local sensitivity index
$Y_{min,i}$	Minimum values of the output in the *i*-th input parameter
$Y_{max,*}$	Maximum global output among all the inputs of all the parameters
$Y_{max,i}$	Maximum values of the output in the *i*-th input parameter
n	Number of input parameters

Optimization

$EC_{cooling}$	Annual energy consumption for cooling
$EC_{heating}$	Annual energy consumption for heating
x_{ju}	upper limits of the decision variables
x_{jl}	lower and upper limits of the decision variables
x_j	jth value in this vector
x	Vector of decision variables
g_i	*ith* constraint function of vector *x*
f	Objective functions

Morris method

δ	Standard deviation of elementary effects
μ	Mean of elementary effects

$\mu*$	Mean of absolute elementary effects
n	Number of parameters
r	Number of trajectories
N	Number of model evaluations
x	Vector of design parameters

LIST OF ACRONYMS AND DEFINITIONS

A

ACH	Air change rate per hour
ANN	Artificial neural network
ASHRAE	American Society of Heating, Refrigerating, and Air-Conditioning Engineers
AR5	IPCC Fifth Assessment Report
ANOVA	Analysis of variance

B

BEM	Building energy modeling
BOPs	Building optimization problems
BO	Building orientation
BP	Statistical review of world energy
BPS	Building performance simulation
BPA	Building performance analysis
BSh	Hot semi-arid climate

C

CDFs	Cumulative distribution functions
Cfa	Humid subtropical climate
Cfb	Marine west coastal climate
CondFD	Conduction finite difference solution algorithm solution technique
CTF	Conduction transfer function
Csa	Hot-summer Mediterranean climate
Csb	Warm-summer Mediterranean climate

D

Dfa	Hot-summer humid continental climate
Dfb	Warm-summer humid continental climate
Dfc	Subarctic climate

DDH	Discomfort degree hour
DOE	U.S. Department of Energy

E

EAs	Evolutionary Algorithms
EDSP	Early design stage parameters
EE	Elementary effect
ES	Energy savings

F

FAST	Fourier Amplitude Sensitivity Test
FDM	Finite difference method
FS	Finkelstein-Schafer

G

GA	Genetic algorithm
GCM	Global circulation models
GSA	Global sensitivity analysis

H

HVAC	Heating ventilation and air conditioning

I

IEA	International Energy Agency
IWEC2	International Weather for Energy Calculation Version 2
ISH	Integrated Surface Hourly
IPCC	Intergovernmental Panel on Climate Change

L

LHS	Latin hypercube sampling
LCC	Life Cycle Cost
LSA	Local sensivity analysis
LSI	Local sensitivity index

M

MCDM	Multi-criteria decision making
MOO	Multi-objective optimization
MSA	Multi-stage sensitivity analysis

N

NREL	National Renewable Energy Laboratory

P

PB	Payback period
PCM	Phase change material
PMV	Predicted mean vote
PNNL	Pacific Northwest National Laboratory
PPD	Percentage of dissatisfied persons
PRCC	Partial rank correlation coefficient
PTHP	Packaged terminal heat pump
PTm	Melting temperature of PCM
Pt	Thickness of the PCM layer

O

OAT	One-parameter-at-a-time

R

RC	Roof conductivity
RCP	Representative concentration pathways
RSA	Roof solar absorptance
RSH	Roof specific heat

S

SA	Sensitivity analysis
SHS	Sensible heat storage
SHGC	Solar heat gain coefficient
SLR	Stepwise Linear Regression

SPEA II	Strength Pareto Evolutionary Algorithm II
SRC	Standard regression coefficients
SRRC	Standardized rank regression coefficient

T

TEC	Total energy consumption
TES	Thermal energy storage
TMY	Typical metrological years

W

WC	Wall conductivity
WinC	Window conductivity
WSA	Wall solar absorptance
WSH	Wall specific heat
WVT	Window visible transmittance

Preface

Ms. Assemgul Saurbayeva received her B.F.A. degree with honors in architecture from L.N. Gumilyov Eurasian National University, Astana, Kazakhstan, in July 2014. She received her MA degree in Architecture from L.N. Gumilyov Eurasian National University, Astana, Kazakhstan, in July 2016. From 2015-2016, she worked as an architect for the architectural company “SP Proekt Stroy”. From September 2016 to July 2019, she was an instructor at the Architecture Department of L.N. Gumilyov Eurasian National University, Astana, Kazakhstan. Since August 2019, she has been pursuing a Ph.D. in Civil Engineering at the Civil and Environmental Engineering Department of “Nazarbayev University” with a research topic on multi-stage sensitivity analysis of early design stage parameters for PCM-integrated buildings.

CHAPTER 1: INTRODUCTION

1.1. Research background and novelty

Global energy consumption has grown exponentially as a result of population and industry growth [1]. This process leads to growing concerns regarding the reduction of energy demand. Fossil fuels provided more than 60% of the world's energy in 2019 (Figure 1.1). According to the present and future scenarios provided by the International Energy Agency (IEA), Statistical Review of World Energy (BP), and the Intergovernmental Panel on Climate Change (IPCC), fossil fuels will remain dominant in the world's energy, with the percentage of non-carbon energy resources gradually increasing [2]. Using fossil fuels contributes to environmental issues such as global warming and air pollution, which negatively impact health and people's quality of life. Furthermore, they are nonrenewable resources, raising concerns about their viability for current and future generations. To deal with this situation, energy resources must be used properly [3].

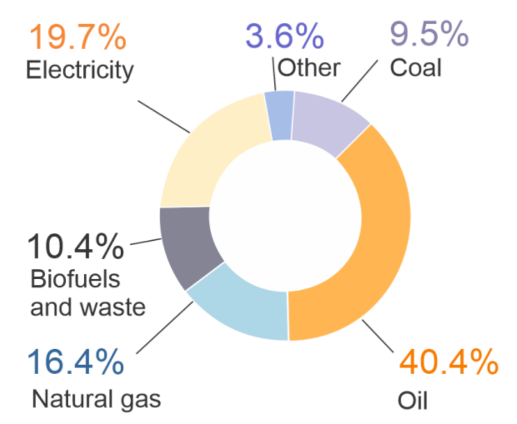

Figure 1.1: Share of world total final consumption by source, 2019. IEA, World Energy Balances, 2021. Adapted from [4].

Buildings represent the most significant energy consumers and greenhouse gas emitters [5]. Specifically, the building sector is responsible for over one-third of global energy usage and greenhouse gas (GHG) emissions (Figure 1.2) [6]. Nonetheless, buildings have a great capability to reduce the mentioned issues. Implementation of energy-efficient design measures can contribute to the solution of this problem. Passive design criteria, including building envelope features and techniques such as natural ventilation, sunshine, overhangs, and cooling systems, have gained considerable attention due to their ability to enhance building energy efficiency [7].

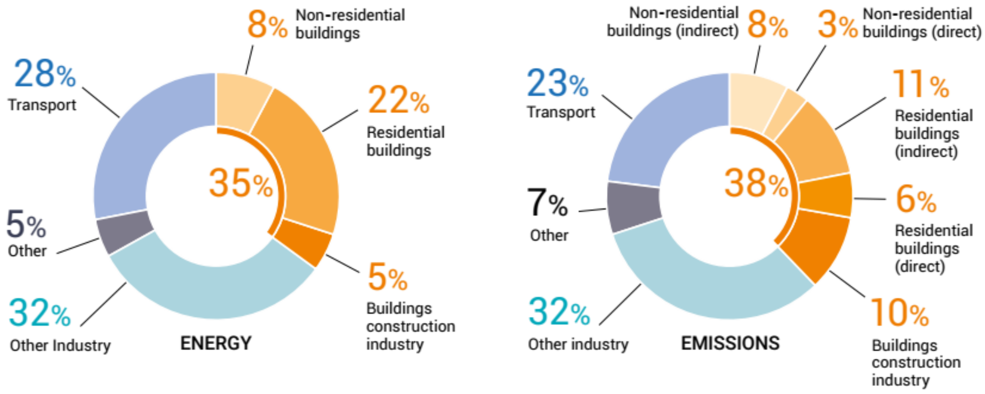

Figure 1.2: Global proportion of final energy and emissions from buildings and construction, 2019 (Sources: IEA 2020; IEA 2020b) [8].

Incorporating Thermal Energy Storage (TES) in buildings is also feasible to achieve energy-efficiency. TES is one of the innovative technologies that can significantly affect the growth of cooling and heating demand. Implementing this system in buildings contributes to better energy efficiency, reduced economic expenses and emissions, and improved system operation and reliability [9]. Latent heat TES employing phase change materials (PCMs) has received a lot of interest in building applications because of their high density of energy storage and capacity to store thermal energy in a constant temperature phase transition process [10]. It can reduce indoor temperature fluctuations, cooling loads, heat stress risks during extreme heat waves, and overall overheating hours [11,12]. The PCM-integrated into building materials such as plasterboard, concrete, or gypsum is a passive method requiring no extra equipment to function. Consequently, implementing passive design measures from an energy standpoint would significantly reduce energy consumption in buildings and decrease fossil fuel emissions.

Thus, investigation of the possible impact of passive design measures to optimize future energy consumption at the early design stage is vital. During this stage, many decisions are made due to the building design's flexibility, which plays a crucial role in determining the energy efficiency of the building [13]. In addition, it is widely acknowledged that the design process at this stage has a considerable effect on building energy efficiency, final costs, and overall performance [14]. Building simulation tools allow for detailed and systematic investigations and evaluations of several building design parameters [15]. Some input parameters used in the building modeling process cause larger variations in the overall energy output, suggesting they should receive more attention for enhancing building performance. Additionally, the complicated nature of buildings and occupant behavior makes the relationship between design parameters and building performance frequently unclear. However, if the uncertainty of significant parameters can be clearly identified, building performance may be easily improved by carefully selecting relevant design parameters and focusing on those elements [16]. As a result, determining the relative relevance of those input parameters necessitates a significant amount of work, which is referred to as sensitivity analysis.

The sensitivity analysis (SA) of model parameters is a key phase in the modeling method for obtaining trustworthy results and vital information and increasing confidence in the model results [17]. It is a valuable method for diagnosing modeling problems, identifying weak model components, and improving knowledge of the relationship between model inputs and outcomes [18]. The primary application of sensitivity analysis (SA) is to identify the input parameters that significantly impact the model outputs, while also assessing the uncertainty associated with these parameters [19,20]. Typically, it is executed at the early design stage because of its greater versatility [21]. Despite the worthwhile research that has been done in SA on building energy performance, most researchers have concentrated on using local or global sensitivity analysis techniques or both. However, the following issues still need to be addressed:

a) A few researchers have attempted to implement the SA in PCM-integrated buildings [22,23]. However, it appears that these investigations have focused only on PCM properties.
b) Past researchers frequently investigated the sensitivity of the building geometry and thermal properties on building performance integrated without PCM [24–28]. However, the combined impact of building geometry and thermal properties along with PCM has never been investigated.
c) The overall tendency in building energy analysis is to use a single sensitivity analysis method. However, applying a single sensitivity analysis can lead to neglecting the important design parameters [29]. To address the potential limitations of this method, multiple techniques can be employed to support

and validate the results. However, despite the benefits of multi-stage sensitivity analysis, its implementation in the literature is currently limited.

d) Studies have indicated that the sensitivity of total electricity demand is subject to fluctuations across different climates [30]. However, few researchers have investigated the effects of early design parameters on total energy consumption in buildings without PCM in hot semi-arid climates.

e) A combined sensitivity and optimization analysis of PCM-integrated buildings has never been conducted. Moreover, a set of optimal solutions for a climate zone has never been proposed. Implementing one optimal passive design approach for the whole climate is a critical strategy for assisting buildings in becoming more energy efficient.

f) Multi-stage sensitivity analysis and optimization of PCM-integrated buildings have never been performed to assess the impact of climate change on passive design measures on total energy consumption.

Therefore, an integrative multi-stage sensitivity analysis (MSA) and optimization framework for PCM-integrated buildings in a hot semi-arid climate zone will be proposed to address the related issues. The framework will consider the combined impact of building layout, thermal envelope characteristics, and energy efficiency measures on total energy consumption for current and future climate scenarios. The best optimal solution set will be proposed, and an economic assessment will be conducted to evaluate the viability of the optimal solutions for the current scenario.

1.2. Aim and objectives

To bridge the gaps in existing research, this research aims to develop a thorough MSA and optimization framework to explore the key early design stage parameters (EDSP) in PCM-integrated buildings, considering current and future scenarios. This will be accomplished by meeting the following objectives:

- To define the methodological framework for MSA and single-objective optimization for current and future climate scenarios.
- To find the most important EDSP in relation to the total energy consumption of PCM-integrated residential buildings in the hot semi-arid climate zone of the world for current and future climate scenarios.

- To identify the interaction between the EDSP and the total energy consumption of PCM-integrated residential buildings in a hot semi-arid climate zone of the world in current and future climate scenarios.
- To determine the best combination of optimal EDSP to provide the lowest feasible energy consumption for current and future climate scenarios. These findings might serve as a reference for the requirements of upcoming building regulations.
- To calculate the economic feasibility of optimal solutions for PCM-integrated residential buildings in a hot semi-arid climate zone of the world for the current scenario.
- To evaluate the impact of climate change on residential building energy consumption in a hot semi-arid climate zone and the possibility of a decrease in energy demand through the EDSP.

1.3. Research significance

- This research will utilize the MSA to identify the most important parameters, which can increase the effectiveness of the optimization process. Using MSA and optimization will result in a total energy reduction of buildings at the early design stages. Moreover, using passive design measures at the early design stage of the buildings will promote energy-efficiency, minimize environmental impact and costs, and maximize thermal comfort.
- Apart from identifying the most important EDSP, the MSA analysis and optimization will assist architects, engineers, and designers in the decision-making process during the initial design phase. Forecasting the consequences of initial decisions is notably challenging, yet crucial. Making errors during this phase will result in a limited design space, increasing the complexity and costs required to achieve high-performance objectives [31]. Thus, using MSA and optimization will provide design guidelines for constructing high-performance buildings.
- The application of the proposed approach can be extended on a broad scale. The methodology of the research is noteworthy and relevant to diverse regions of the world.

- The economic assessment of the EDSP of PCM-integrated buildings in a hot semi-arid climate zone would indicate the viability of using passive design measures in buildings.

1.4. Outline

Chapter 1 consists of the background of the research, objectives, and significance of the Thesis. The rest of the thesis is organized as follows:

Chapter 2 provides a literature review on building design stages, EDSP, and literature about PCM and SA techniques and their application in building energy analysis and optimization of building performance. The chapter also includes literature about the impact of climate change on the energy performance of buildings.

Chapter 3 describes the methodology of this thesis. The chapter describes the steps of the MSA and single-objective optimization framework, which can lead to the determination of the most important EDSP and optimal solutions for a hot semi-arid climate zone. It also describes the economic feasibility of optimal solutions.

Chapter 4 presents the MSA and single-objective optimization results for the semi-arid climate zone in the current and future scenarios and a comparative analysis of the MSA and single-objective optimization results in the current and future scenarios. It also presents economic assessment results for the hot semi-arid climate zone for the current scenario.

Chapter 5 includes the discussion and conclusions of this thesis. It also summarizes any limitations and makes recommendations for future research.

CHAPTER 2: LITERATURE REVIEW

This chapter aims to evaluate the pertinent literature to understand the nature and scope of current knowledge and determine the gaps that this research will address. In Section 2.1, the stages of the building design process are first discussed to understand the characteristics of each design stage. Section 2.2 analyzes the various EDSP to select the most suitable design parameters for sensitivity analysis. Section 2.3 examines the role, importance, and application of sensitivity analysis in building energy analysis. In Section 2.4, the building optimization methods and algorithms and their use in building performance analysis are summarized. The details regarding the implementation of phase change materials, sensitivity analysis, and optimization under the impact of climate change are summarized in Section 2.5. Finally, Section 2.6 summarizes the findings and limitations to which this research will contribute.

2.1. Building design stages

Generally, the design process is divided into three stages, such as the conceptual, schematic, and detailed design stages.

- ***The conceptual design stage*** creates the project's original building concept. During this phase of the design process, schematic drawings and layouts are created, defining the overall system structure and presenting an initial project configuration [32]. The basic geometrical dimensions of a building, such as its height, width, length, and orientation, are selected during this stage;
- ***In the schematic design stage,*** the schematic drawings are produced to estimate the major requirements for the building project. Decisions concerning the building's basic layout, number of storeys, important structural components, and room count are decided at this phase. The design criteria in the conceptual and schematic design processes can be considered mutually as **EDSP** [33].
- ***The detailed design stage*** includes all the details necessary to construct the structure and the data required for a sustainability evaluation. The measurements of roofs, walls, windows, and building materials are defined in the detailed stage.

Modifying early designs later is very hard and expensive, as thorough design decisions may have already been based on them (Figure 2.1). Detailed design decisions often make it difficult to cover for poor early design choices [33]. Consequently, it is crucial to examine the design possibilities, building performance simulation, and optimization in the early design stage of buildings [21]. Because of the limited data available during the conceptual design stage, any evaluation relies mostly on assumptions. The schematic design stage bridges the gap between the conceptual and detailed design stages. A more accurate solution assessment is possible at this stage due to the larger amount of data compared to the earlier stage. The methodology described in this research focuses on the conceptual and schematic design stages.

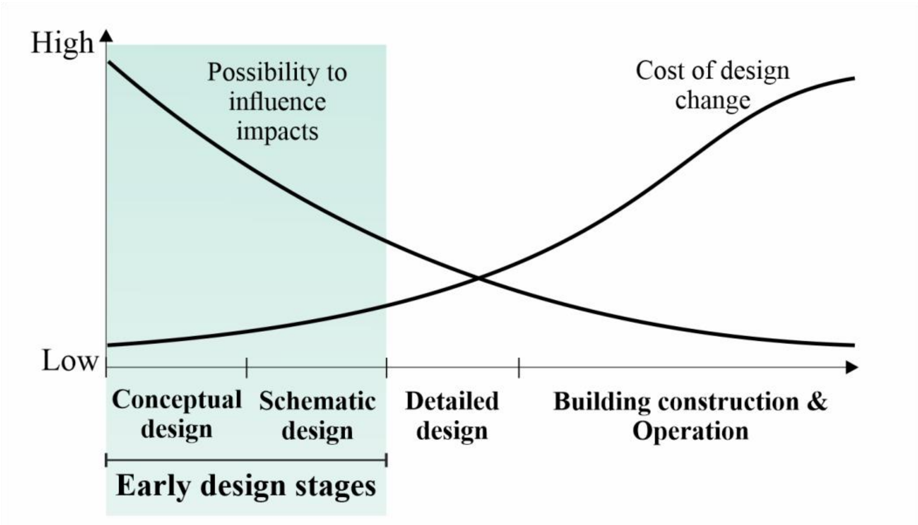

Figure 2.1: Building design stages. Adapted from [33].

2.2. Early design stage parameters

In the early design stages, SA can provide fundamental information about which input parameters should be concentrated on in the latter stages while providing information about parameters with a negligible effect on energy usage [34]. According to several studies, there is a better chance of minimizing the environmental effect of a building when decisions are taken early in the design process and when adjustments to those decisions are made less often later on [35]. For instance, Ochoa & Capeluto [36] varied the possible façade configurations of the building in hot climates. It was reported that intelligent facades could obtain energy savings (ES) of up to 20% and 60% in hot climates. In the research of Ciardiello et al. [37], optimization of the geometrical characteristics of the building enabled yearly energy consumption reductions of up to 60.6%. Thus, it follows that the building design parameters are significant and crucial in defining the energy performance of buildings. As a result, the building's energy consumption may be significantly decreased by choosing appropriate design parameters in the early design stages to enhance its energy performance.

The list of EDSP employed by different researchers is shown in Table 2.1. The summary includes the examined EDSP, building type, and location. Building size and layout, envelope composition and thermophysical properties, airtightness and infiltration, window-to-wall ratio, and overhang projection ratio are all common EDSP [6,33]. Measures such as building orientation and geometry, window-to-wall ratio, and building envelope can be passive strategies [38]. Building geometry is significant in designing energy-efficient buildings because it impacts the amount of energy required to keep the balance in the zones related to heat gains and losses governed by the surface area exposed to the outdoors. The building envelope, in conjunction with the building geometry, decreases energy transfers between the inside and outside caused by solar radiation and wind. Adopting passive techniques or climate-sensitive technologies is vital for buildings to gain energy efficiency. Passive techniques are closely related to the environment in which the building is located. Apart from these parameters, applying phase change materials (PCM) can reduce the cooling and heating load, improve indoor thermal comfort, reduce variations in temperature, and reduce overall overheating hours. Over the past two decades, there has been a sharp increase in interest in the usage of PCM. The next section discusses the PCM properties, typology, and application in buildings.

Table 2.1: Overview of EDSP used in the literature.

№	Building type	Location	EDSP	Reference
1	Office building	▪ Palermo ▪ Torino ▪ Frankfurt ▪ Oslo	▪ Thickness of the masonry walls ▪ Number/position of the windows ▪ Shape/type of the windows	[14]
2	Office building	▪ Harbin ▪ Chengdu	▪ Location ▪ Floor plan ▪ Orientation ▪ Building/room length ▪ Building/room width ▪ Building/floor height ▪ Floor area ▪ Floor height ▪ Floor/room number	[33]
3	Residential building (NZEB detached house)	▪ Madrid ▪ Naples ▪ Nice ▪ Athens	▪ External and internal shading systems ▪ Glazing components ▪ Window-to-wall ratio (WWR) ▪ Spectral characteristics (last layer, roof slab, opaque envelope) ▪ Type/thickness of insulation material	[6]
4	Archetype building	▪ Montreal ▪ Quebec	▪ WWR ▪ Plan shape ▪ Azimuth ▪ Wall/roof insulation ▪ Building-integrated photovoltaic/thermal roof systems ▪ Tilt angle	[39]
5	Multi-story building	▪ Tehran ▪ Kerman ▪ Bandar Abbas ▪ Tabriz	▪ Overhang depth/tilt angle ▪ Wall visible /solar/ thermal absorptance ▪ Wall/glazing conductivity ▪ Glazing solar/visible transmittance ▪ Window size ▪ Building orientation	[34]
6	Administrative building	▪ Beijing	▪ WWR ▪ U-value of wall/roof/window ▪ Solar heat gain coefficient ▪ Room depth ▪ Storey number ▪ Plan shapes	[40]

2.2.1. **Phase change materials**

Passive thermal energy storage (TES) integrated into the external walls offers a promising solution to enhance building envelope efficiency, reducing energy consumption and lowering carbon dioxide emissions [41]. The TES systems can be categorized into three groups: sensible heat storage, latent heat storage, and thermochemical heat storage [42]. Sensible heat storage (SHS) is an efficient technique for energy storage, which entails altering the temperature of the storage medium to conserve energy [43]. It is the most popular, straightforward, low-cost, and long-standing approach [44]. However, some drawbacks of this technique are the requirement of vast quantities of material and volumes, and the inability to store or deliver at a constant temperature [45]. Latent heat storage (LHS) is the method of storing heat energy via phase change materials, considered the most effective technology for enhancing the energy performance of the building envelope [46]. Compared to sensible heat storage, LHS has a greater density of energy storage and nearly no temperature change throughout the phase shift process [47]. As a result, the latent heat storage system may store more energy while utilizing the same quantity of resources. Furthermore, compared to the SHS, the constant temperature throughout the phase change in the LHS assists in significantly minimizing heat losses. Thermochemical heat storage systems (THS) store and release heat in a reversible endothermic and exothermic reaction process using thermochemical materials [48]. Due to their relatively high energy density, low heat loss, and long-term heat availability, these storage devices can be advantageous [49]. Nonetheless, the primary disadvantages of THS are their ineffective discharge power for building applications, low output temperature at the moment of equilibrium, delayed reaction kinetics, insufficient operating temperatures, costliness, and poor/moderate storage efficiency [49].

The application of LHS as thermal energy storage has received significant attention in recent decades because of its efficacy and superiority over other TES materials [50]. In most LHS applications, the cyclic solid-liquid physical transition of the so-called phase change material (PCM) activates the heat storage/release process [51]. PCMs can absorb and release energy through physical state changes [43]. Therefore, latent heat storage using PCM has been adopted as a passive design measure in this research. The following section discusses the various PCM transitions.

2.2.1.1. **PCM transition forms**

The concept of employing a PCM is straightforward: when the substance passes from solid to liquid, heat is absorbed at a constant temperature until it is entirely transformed into liquid. In contrast, heat is emitted when the substance transitions from liquid to solid; this occurs at a nearly constant temperature until the material is entirely solidified (Figure 2.2) [52].

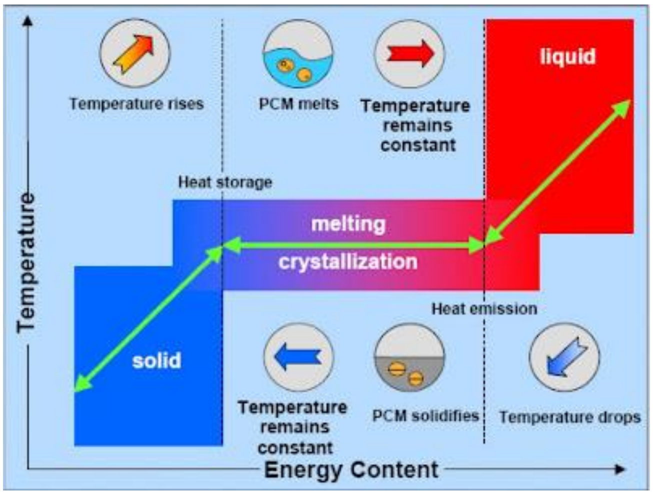

Figure 2.2: Principal of PCM [53].

PCMs are divided into four categories based on their phase change state: solid-solid PCMs, solid-liquid PCMs, gas-solid PCMs, and liquid-gas PCMs. In solid-solid transition, heat is trapped during the transition of a solid from one crystalline state to another. However, compared to the solid-liquid transition, the latent heat and volume variations in this transition are often less [54]. Due to various technological limitations, such as significant volume fluctuations during the phase transition process and high gas phase pressure within the system, employing solid-gas and liquid-gas phases as building materials is not advisable. The solid-liquid PCMs are often used in thermal energy storage systems due to their cost-effectiveness (the minor volume change is 10% or less) [54]. Only solid-liquid PCMs are employed in construction applications, particularly because they are incorporated into walls and wallboards and are readily accessible at a variety of phase change temperatures. Therefore, in this research, solid-liquid PCM will be employed.

2.2.1.2. **PCM classification**

PCMs in the solid-liquid phase are classified into three groups: organic, inorganic, and eutectic [55], as shown in Figure 2.3. These groups are further categorized based on the chemical components of the PCM. Organic PCMs are chemically stable, resistant to sub-cooling, and non-reactive. They comprise paraffin, polyethylene glycol, and fatty acids. Nevertheless, they have a low latent heat storage capacity, a low thermal conductivity, and may be combustible [52]. Inorganic PCM comprises hydrated salts and metallic [56]. Typically, they have a volumetric latent heat storage capacity roughly double that of organic molecules, and high latent heat of fusion. Nevertheless, degradation, corrosion, and supercooling are frequent downsides that might affect PCM qualities, lowering system efficiency in the long run [50]. Eutectic is composed of organic and inorganic compounds. The main benefit of eutectics over other PCMs is that varying component weight proportions may modify their melting points. Nevertheless, evidence on the thermophysical characteristics of eutectic PCMs is scarce [52]. Furthermore, certain fatty eutectics have a strong odor, making them unsuitable for use as PCM wallboard. This research used fictitious PCMs (instead of real Bio-PCMs) with phase transition temperatures ranging from 20 °C to 30 °C.

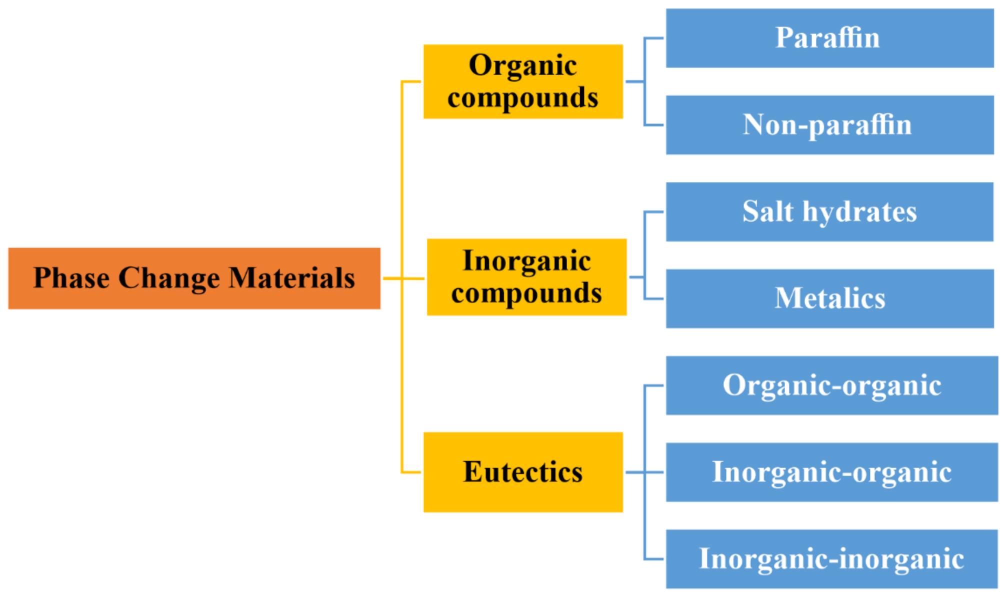

Figure 2.3: Classification of PCM [57].

2.2.1.3. **PCM in buildings**

This section presents the works related to PCM incorporation in buildings. PCMs are utilized to minimize cooling and heating demands via the building envelope while maintaining a suitable thermal comfort level due to their huge potential for energy storage during melting and solidification [58]. Because of the necessity to reduce building energy use, PCMs have gained increased attention recently. Various design parameters, including the layer thickness of the PCM, its position within the envelope structure, and the phase change temperature range, may impact the PCM's efficacy. The melting temperature must be appropriately selected to maximize the PCM's effectiveness [59]. Some noticeable studies are discussed herein, mainly focusing on incorporating the PCM layer into buildings and refining the location, thickness, and optimum melting temperature of PCM. Saffari et al. [60] examined the impact of PCM with different melting temperatures and layer thicknesses of building model prototypes on energy consumption for the climate of Madrid. Models were chosen from ANSI/ASHRAE Standard 140-2011. Three PCMs with melting temperatures of 23 °C, 25 °C, and 27 °C were selected. In addition, the payback period of PCM utilization was calculated. It was revealed that the PCMs with a melting temperature of 27 ℃ obtained the maximum energy savings of 10-15%, whereas the PCMs with a melting temperature of 23 ℃ and 25 ℃ achieved savings of 8-10% and 10-13%, respectively. Furthermore, buildings with a 10 mm PCM layer resulted in greater energy savings and shorter payback times. Hagenau & Jradi [61] investigated the influence of location and phase change temperature of PCM in office buildings located in Denmark to reduce energy consumption. For this research, 17 PCMs were selected. According to simulation results, PCM with a melting temperature of 21 ℃ showed the best performance. In addition, it was indicated that the installation of this PCM within the building envelope would result in yearly energy savings of about 9.7 GJ and a 2.3 kW decrease in the heating and cooling loads. Based on simulation results, the scenario with a 40 mm PCM layer placed on the inside surface of the building envelope was found to be the best.

It is important to note that prior studies have reported that the optimum location of PCM is between the interior surface and the midsection of the wall. For example, Kishore et al. [23] reported that the location of the PCM at 10% of the cavity width from the interior could reduce the peak period heat gain by 67% and 75%, respectively, with essentially no increase in the total heat gain. According to

Jin et al. [62], the optimal PCM position is 1/5 of the cavity thickness from the interior. Biswas & Abhari [63] reported that applying PCM to just the inside surface of an outside wall can provide superior thermal performance cheaper than adding PCM to the full wall cavity.

Therefore, for this research, PCM was installed on the inside surface of the outside wall. The melting temperature and thickness of the PCM layer were selected as the EDSP, and their range was considered to vary. Further details are provided in Section 3.3.

2.3. Sensitivity analysis

Parametric studies are commonly employed to analyze the effects of altering input design parameter values one at a time [64]. When the amount of input design parameters gets enormous, the constraints of such approaches become apparent. In this way, sensitivity analysis (SA) can be utilized to help with this type of design support. SA establishes a relationship between input variability or uncertainty and model output variability or uncertainty [39]. It is an analytical method that examines the relationship between design variables and objective output and improves the compromise of crucial variables within them [26,65]. In building energy analysis, SA is a valuable method for both observational research and energy simulation models. It has been commonly utilized to examine building thermal performance characteristics in different applications, such as energy model calibration, building design, building stock, building retrofit, and the impact of climate change on buildings [66]. Employing SA as a component of an integrated design process, the design team has the best opportunity to respond to such information and improve the design when such factors are identified early on. According to researchers, design modifications implemented early in the design stage have less negative time or financial outcomes than adjustments implemented later in the design process [39]. The following are the most prominent reasons for performing a sensitivity analysis:

- ***Model simplification:*** SA is useful for identifying model variables that seem to have negligible impact on desired outputs. The computational expenses and model complexity can be decreased by determining unimportant model variables and modifying them to simplified model forms and nominal values.

- ***Model refinement:*** SA can highlight the extremely significant variables on the output by estimating their relative importance. It can help identify which model components in the model evaluation framework need more analysis or assessment so the uncertainty surrounding them and the associated model outputs can be decreased.
- ***Model assessment:*** SA can be employed to evaluate model findings when inferences about the model's structure or parameterization are uncertain or have been modified. It helps determine which uncertain model variables are causing unfavorable model behavior.
- ***Exploratory modeling:*** SA may be extended to various additional issues after the model has gained enough credibility. It is possible to extrapolate model outputs to the actual system they portray and use this information as a guideline to assist model-based inferences by concluding the variables and processes that most (or least) influence outputs.

To conclude, a SA is a valuable method to simplify, refine, and assess the model variables in relation to the output. In building energy analysis, SA is considered an indispensable method to help concentrate on the most essential parameters of sustainable building design and optimization. Typically, it is performed at the initial design stage because of its greater versatility [15]. Several researchers recommended applying sensitivity analysis at the early design stage to determine the input parameters that have the greatest impact on building performance [39,67]. Therefore, in this research, different SA methods were applied. The next section describes the techniques of SA.

2.3.1. **Sensitivity analysis techniques**

Generally, sensitivity analysis methods have been divided into two basic categories: local and global [66]. The local sensitivity approach (LSA) is a one-factor-at-a -time approach where the impact of one input parameter is assessed while the others are kept fixed at their base case value. This technique has been frequently utilized in the literature due to its ease of application and low computing requirements; however, it has significant drawbacks [15,68]. For instance, the nature and behavior of the input parameters are ignored, which means that all values have an equal chance of appearing despite considering the impact of shape and range of the probability density function (PDF) [69].

Global sensitivity approaches (GSA) evaluate the importance of input parameters by altering all other model inputs simultaneously. The impact of the range and form of each design parameter's probability density function is considered, as well as the output variation caused by that design parameter [28]. The advantage of GSA is the ease of implementation through fast and effective evaluation of the building model by level-by-level discretization of inputs. Moreover, it assesses the input sensitivity globally to highlight the interaction between the inputs. It is particularly effective to differentiate the non-influential parameters with a limited sample size [70].

The four subcategories of GSAs are meta-models, variance-based, screening, and regression [34]. A collection of methods that can be employed to anticipate the desired outcome using inputs is referred to as a metamodel [71]. The simulation software's output data are fitted to specific locations in the sample space to create the metamodel [72]. Meta-modeling consists of two stages: creating regression without a predetermined form and calculating sensitivity measures by the variance-based technique [66]. The key advantage of employing meta-models is that they take substantially less time than simulations of specific building energy models. As a result, compared to the variance-based technique, this meta-modeling method can produce a more effective sensitivity measure [73]. TGP (treed Gaussian process), GP (Gaussian process), Support vector machine (SVM), ACOSSO (Adaptive Component Selection and Smoothing Operator), and MARS (Multivariate Adaptive Regression Splines) are frequently utilized meta-model types.

Variance-based methods depend on a breakdown of the model output variability and are referred to as ANOVA (analysis of variance) approaches. Since they are considered model-independent black-box approaches, these techniques may handle complicated non-additive and non-linear models. Nevertheless, these benefits come at a considerable computational cost compared to the screening approach [69]. FAST (Fourier Amplitude Sensitivity Test) and Sobol are widely utilized variance-based techniques. The Sobol approach provides two sensitivity indices: the main effect (first order) and the total effect. The main-effect index assesses the impact of a single parameter on the output while ignoring interactions with other parameters, while the total effect index displays the input parameter's impact after accounting for input correlations and interaction-related variation [70].

Screening techniques are employed in complicated circumstances with several design parameters and/or a computationally intensive evaluation. It is a cost-effective approach for identifying and ranking qualitatively the design parameters that govern the majority of the output variability [74]. These approaches aim to determine the least significant input parameters that may be set at any value without significantly affecting output variation. With only a few model assessments, these techniques may thereby rank input parameters by their relevance in descending order [75]. The Morris method is one of the most widely used screening SA methods in building energy modeling. Morris's approach produces two sensitivity indices: the mean value and the standard deviation. The mean value calculates the input component's overall impact on the output, while the standard deviation evaluates the input parameters' interactions with other factors.

The regression technique is the most often used sensitivity approach in analyzing building energy because of its simplicity and quick computation. They rate the relevance of the input parameters, calculating statistical indicators of regression analysis on a sample of distinct model simulation outcomes. The most commonly used regression analysis types are SRC (Standardised Regression Coefficients), PCC (Partial Correlation Coefficients), and stepwise regression. The rank transformations of SRC and PCC, SRRC (Standardized rank regression coefficient), and PRCC (Partial rank correlation coefficient) are also frequently utilized in research. The raw values of the inputs are replaced by their ranks via the rank transformation technique [76]. The impacts of extreme values are thought to be lessened by rank transformations, which have been utilized often in recent years.

The LSA and several GSA methods were selected for the proposed multi-stage sensitivity analysis (MSA) in this research. Applying a single sensitivity analysis approach may result in missing key design parameters [29]. As a result, MSA is useful for showing the magnitude and direction of the influence of EDSP on output. The selection of GSA methods was based on their adoption because of their high accuracy and low computational cost. Three GSA methods were selected, namely SRRC, PRCC, and the Morris method. SRRC and PRCC can avoid poor performance in regression analysis when the relationship between inputs is non-linear. The Morris method is notably effective at identifying non-influential parameters with a limited sample size and determining the interaction between the outputs. It could produce very accurate input sensitivity indices at a low computational cost.

2.3.2. **Application of sensitivity analysis in a building with and without PCM**

Several pieces of research have been conducted on SA methods and their implementation. However, only a few review papers are available on SA for building applications. Tian [66] provided a thorough overview of the many SA techniques used in building energy analysis, along with an explanation of the theoretical background of each technique and the investigations that have already been conducted using a particular technique. Pang et al. [70] presented a comprehensive critical review of the utilization of SA in building performance analysis (BPA) in terms of sampling and sensitivity analysis types. Furthermore, the significance of the SA in the BPA was thoroughly examined. In the research of Nguyen and Reiter [77], the efficiency of several sensitivity analysis methodologies has been compared using a combination of building energy modeling and computational experiments. Namely, nine sensitivity methods were considered: Morris, FAST, Sobol, SRC, SRRC, PCC, PRCC, SPEA (Spearman coefficient), and PEAR (Pearson product-moment correlation coefficient). According to the results, in comparison to SRRC, PRCC, and SPEA, the outcomes of SRC, PCC, and PEAR were more accurate. It was observed that Sobol and FAST generated the same ranking results. Compared to the variance-based techniques, the SRC, PCC, and PEAR produced high sensitivity rankings but were not completely precise sensitivity metrics.

A few researchers have performed the SA in PCM-integrated buildings. Al Janabi & Kavgic [22] applied local sensitivity analysis on the input parameters of hysteresis and material thickness of PCM-integrated public buildings in Manitoba. Thirteen parameters were used to perform sensitivity analysis: liquid-state specific heat, liquid-state thermal conductivity and density, latent heat, solid-state thermal conductivity, a low and high-temperature difference of the melting curve, and peak melting temperature, solid-state specific heat and density, peak freezing temperature, the high and low-temperature difference of the freezing curve. The results showed that the first eight parameters with the greatest impact on overall energy usage were the same in both zones. Kishore et al. [78] executed a thorough parametric and sensitivity analysis on major PCM parameters and investigated their impact on thermal efficiency regulation and wall-related heat gains in buildings in Arizona and

Nevada. For sensitivity analysis, the following eight parameters were selected: location, transition range, thickness, transition temperature, density, specific and latent heat, and thermal conductivity. It was indicated that the transition temperature of PCM, followed by the location and thickness of PCM, was the dominant parameter affecting the thermal efficiency regulation. However, specific heat and the thermal conductivity of PCM were insignificant. The findings from the literature review reveal a scarcity of research examining the effects of SA in buildings incorporating PCM, with a narrow emphasis on changes in PCM properties.

2.3.3. **Application of multiple sensitivity analysis in building performance studies**

This section presents a combination of several sensitivity analyses from building performance research. Gagnon et al. [79] utilized three sensitivity analysis methods (namely, Sobol, SRC, and Morris) to evaluate the influence of thirty variables on energy consumption and thermal comfort. The outcomes revealed that the primary parameters that significantly affect the total energy consumption include heat recovery efficiency, the properties and geometry of windows, and set points. Silva & Ghisi [68] applied two sensitivity analysis methods (LSA and Morris method) to develop an approach to assess the impact of design parameters on the energy and thermal performance of low-income houses in Brazil. Input parameters included the envelope construction details, the dimensions of heat zones and shading components, geometry, electrical equipment, and bioclimatic methods. Based on the results, the LSA and Morris methods showed an opposite sensitivity importance for heating and cooling consumption. Thermal transmittance of the roof was found to be the most influential parameter on energy consumption by LSA, whereas solar absorptance of the roof was an important parameter in the Morris method. To gain a comprehensive understanding of the inputs' behavior and their effect on outputs, employing local and global sensitivity techniques is highly recommended, as each provides distinctive information. Li et al. [80] applied four different sensitivity analysis techniques to indicate the impact of twenty-nine design parameters on the energy demand and winter thermal discomfort in China. Three different GSA (FAST, Morris, and regression methods) were applied, followed by the ranking of design parameters. Finally, the local sensitivity analysis was ultimately employed, and the findings indicated that the Morris method's ranking of the most critical design parameters aligned with regression techniques. Conversely, the FAST method significantly differed in ranking order relative to regression approaches. It can be observed that the determination of the most influential parameters by a single sensitivity analysis can lead to inaccurate results. Yang et al. [29] compared the four sensitivity analysis methods in a retail building located in Harbin. The global sensitivity analysis approaches known as the Morris method, SRC, FAST, and TGP (tree Gaussian Process) were used. In terms of computation cost and accuracy, the TGP method showed the best performance. The authors recommended using at least two sensitivity analysis methods in building performance analysis (BPA). Zeferina et al. [30] applied a two-stage sensitivity analysis to assess the eight design parameters of an office building located in Manchester. The initial sensitivity step used the Morris screening approach, which considered all 14 input characteristics and all six climates. The Sobol indices, a more intricate sensitivity approach, were used in the second sensitivity step, which required more computing resources but allowed for a more precise and quantitative evaluation of sensitivities. Lighting, equipment, and ventilation were important parameters for annual energy demand. According to Pianosi et al. [81], applying multiple sensitivity analysis methods has two benefits. At first, a more comprehensive understanding of a problem can be obtained by using several approaches that differ in their capability to address certain concerns. Further, using several approaches is a practical way to verify, accept, or support the results of global sensitivity analysis since techniques depend on many assumptions, the degree of accuracy of which is not clearly stated. This section provided important insight into the utilization, classification, and application of sensitivity analysis in building energy analysis. The following section will discuss the use of optimization and optimization algorithms and their application in the building.

2.4. Optimization

In recent years, there has been an increase in the number of research papers published on optimization analyses for improving building energy performance. Optimization makes it feasible to identify the best input parameters from a vast array of potential combinations that may fulfill the given constraint functions and accomplish the established conflicting objective functions. Various decision parameters can be examined in the building envelope, heating, ventilation, and air conditioning systems (HVAC), centralized/on-site energy generating systems, and so on [82].

A large number of reviews on the optimization of building performance were found. These studies offer a thorough understanding of the application of optimization in buildings, algorithms, objective functions, and input parameters, tools, etc. [16,83–88].

2.4.1. **Optimization algorithms**

The popularity of optimization for sustainable building design was enhanced by the rising computer power available to solve issues that were previously unsolved [84]. An optimization algorithm is a method that evaluates numerous solutions iteratively until an optimum or suitable one is identified. Optimization algorithms can be categorized in various ways depending on the subject or the features. Detailed information on optimization algorithms methods can be found in the reviews of Machairas et al. [83], Evins et al. [84], and Nguyen et al. [85]. The selection of an algorithm is influenced by the type of problem, the nature of the algorithm, the quality of solutions, the availability of the algorithm’s implementation, constraints, the competence of decision-makers, and computer resources [89]. This chapter discusses a small fraction of the wide variety of optimization algorithms.

In general, optimization algorithms are divided into two classes: deterministic and probabilistic. In deterministic optimization, each step of the algorithm's geometry is controlled by a deterministic rule. The sequence of points assessed is exclusively defined by the initial point (or starting point). In stochastic optimization, portions of the algorithm's stages are controlled by random decisions [90]. Deterministic algorithms are thought to be more efficient and exact for local optimization than stochastic algorithms, but stochastic methods are seen to be more dependable for global optimization and more resistant to numerical noise. Stochastic methods are often quicker than deterministic methods in identifying global optimum. Furthermore, it is more adaptable to black-box formulations and severely ill-behaved functions, while deterministic methods are generally based on certain theoretical assumptions about the problem formulation and its analytical features [91]. Many population-based optimization approaches, such as the genetic algorithm, particle swarm optimization, and genetic programming, use a stochastic process to find the best solution. Therefore, for this research, the stochastic algorithm was selected.

The optimization can be single- or multi-objective according to the number of objective functions used. In single-objective optimization issues aimed at minimization, the solution with the lower objective function value of the two alternatives might be considered optimal. In multi-objective optimization, multiple contradicting goals can be optimized concurrently by creating a collection of solutions. In this research, single-objective optimization of total energy consumption is selected.

2.4.2. **Sensitivity analysis in building optimization studies**

According to the literature, the sensitivity analysis may potentially be integrated with simulation-based optimization to improve the different objective functions or reduce the computational costs. For instance, Bre et al. [26] used the Morris sensitivity analysis to rank the most important parameters before the optimization. Objective functions related to energy and thermal performances were selected for minimization and maximization. The design parameters for thermal performance were: building azimuth, windows shading and type, the air infiltration rate of windows and doors, windows area fraction, the internal emissivity of the roof, window area fraction for natural ventilation, the solar absorptance of walls and roofs; and the thermal capacity of walls and roofs; the thermal transmittance of internal and external walls and roofs. According to the results, the window infiltration rate was the most significant design parameter. Fang & Cho [21] applied SRC as an indicator to optimize nine variables for daylighting and energy performance. The statistical analysis software R with the package 'sensitivity' was utilized to identify the key design variables by sensitivity analysis. The research outcome showed that the skylight length and width are the most influential parameters in all regions. Chen et al. [25] applied sensitivity analysis and optimization for passively designed high-rise buildings in five different climate zones in China. The optimization algorithm NGSA II was combined with the surrogate model SVM (Support Vector Machine). Optimization of total energy demand and comparison of FAST and MLR sensitivity analyses were conducted for each climate condition. The wall-specific heat and infiltration rate were defined as non-significant design inputs for all five climate regions established on the bootstrapped FAST total-order indices. The most influential geometry variables for Harbin city were window U-value, window-to-ground ratio, and wall thermal resistance. Using SA during the pre-optimization phase can help reduce the search space size and screen out minor parameters that have a little or negligible effect on the objectives.

2.4.3. **Optimization in early design stages of the buildings**

During the early design phases, when the information levels are limited, and design adjustments are constant, building energy optimizations create risks of high uncertainty and unnecessary computation [92]. The variety of variables in building geometry parameters is broad at the early stages of design, and the choice of material always comes from traditional design experience [93]. At this stage, planners deal with multi-disciplinary and conflicting goals and make decisions about general building performance. As the early design process offers the biggest potential for high-performance construction, planners need to be able to acquire accurate information on building results [14]. For this reason, the utilization of optimization in the early design stage should be sufficiently researched to decrease the complexity of inputs and computational time. In this regard, several researchers examined the implementation of optimization in the early design stage [14,94–96]. For instance, Echenagucia et al. [14] proposed an integrative approach to obtain the optimized envelope configuration for four European cities at an early design stage. Optimization was carried out by modifying the thickness of the masonry walls, and the number, type form, and position of windows. A multi-objective optimization was conducted using evolutionary algorithms to minimize the lighting and cooling energy consumption. Based on the results, a small WWR was an appropriate option in all locations. Delgarm et al. [96] carried out a simulation-based optimization study, employing mono- and multi-objective approaches, aiming to minimize the energy consumption of a room across four different climatic regions in Iran. The design parameters in the proposed optimization method were the wall characteristics, glass, window size, room orientation, and shade overhang requirements. According to the results, the optimal design reduces 1.6–11.3% of yearly total building energy usage. It was revealed that the energy consumption of the building might be significantly decreased by choosing suitable architectural design parameters in the early stages of a building's design to enhance its energy efficiency. Apart from parameters related to the building geometry and envelope characteristics, optimization was also performed in buildings integrated with PCM. The next section discusses the most important studies on optimizing PCM properties.

2.4.4. **Optimization in PCM studies**

Optimization approaches have been used to increase the performance of PCMs. Saffari et al. [12] applied the single-optimization method to find the optimum melting temperature of PCM incorporated in residential buildings in different climate zones. Optimizations were performed with the aim of improving the heating, cooling, and annual energy demand of PCM-integrated buildings. The results showed that the optimum melting temperature was around 20 °C and 26 °C in the dominant heating and cooling climates, respectively. Soares et al. [97] utilized the multi-dimensional optimization technique to determine the optimal solution for incorporating PCM into lightweight steel-framed residential buildings across various global climate zones (Csa, Cfa, CFb, Csb, Dfa, Dfb, and Dfc). Their findings indicated that a 4 cm thickness of PCM was optimal across all climate zones, but the optimum melting temperature of the PCM varied. In warmer areas, the optimal melting temperature ranged between 22 °C and 26 °C, whereas in colder climates, it ranged from 18 °C to 24 °C. From the incorporation of PCM, significant energy savings of 46 % and 62% were obtained in warm climates, while energy savings of 10% and 24% were achieved in cold regions. Arici et al. [98] conducted a study to analyze the effect of latent heat on wall thermal efficiency. They identified the optimal melting temperature of PCM and its placement and thickness to maximize the utilization of latent heat in different climatic conditions. Three cities in Turkey (Erzurum, Konya, and Diyarbakir) were selected for the research. Based on the results, Erzurum, Diyarbakir, and Konya had different yearly optimal PCM melting temperatures of 16 °C, 20 °C, and 25 °C, respectively. The PCM layer's optimal thickness was consistent across all cities. The placement of the PCM layer between the interior plaster and concrete yielded superior performance in terms of annual energy consumption for Diyarbakir and Konya. However, for Erzurum, greater yearly energy savings were attained by situating the PCM layer between the insulation and outside plaster. Kharbouch et al. [99] optimized the PCM-integrated envelope of a residential building located in the Moroccan climate. For optimization, seven input parameters were selected: PCM melting temperature and thickness, building orientation, air infiltration rate, external wall solar absorptance, rate of glazing area, and window glazing type. The results indicated that the optimum melting temperature was 20 °C, the thickness of the PCM layer was 0.02 m, the building orientation was 0 °, the glazing area was 10%, the window glazing type was double glazing, the air infiltration rate was 0.1, and the solar absorptance was 0.2. For energy savings evaluation, the index of energy efficiency was utilized, which showed a reduction of about 3.34% due to optimization.

It is observed that building performance optimization is a common and effective way of providing a comprehensive framework for enhancing energy-efficient measures. External thermal loads can significantly impact a building's energy efficiency and the thermal comfort of its occupants, especially during hot seasons. Thus, accounting for climate change effects is crucial when optimizing a building's energy performance to ensure reliable results. The following chapter outlines the process of generating weather data and research findings regarding the impact of climate change on buildings.

2.5. Impact of climate change

2.5.1. **Future climate change scenarios**

Extreme weather conditions are predicted to occur more frequently and intensely because of climate change. To study climate change, the IPCC used a variety of potential future emission scenarios. Using different socio-economic scenarios, various scenarios were produced by altering the rate of greenhouse gas production. These emission scenarios have been developed into representative concentration pathways (RCPs) as a result of the IPCC Fifth Assessment Report (AR5) [100]. The RCPs provide several trajectories for GHG emissions, land use air, pollutant emissions, and atmospheric concentrations in the twenty-first century. The number following "RCP" denotes the amount of radiative forcing (i.e., the total amount of greenhouse gas emissions from all sources represented in Watts per square meter in the tropopause as a result of human activity in 2100) that has been observed in the published research, ranging from 2.6 to 8.5 W/m^2 [101]. The RCPs have four emission scenarios: A strict scenario is RCP 2.6, intermediate scenarios are RCP 4.5 and RCP 6.0, and a scenario with extremely high GHG emissions is RCP 8.5 (Figure 2.4) [102].

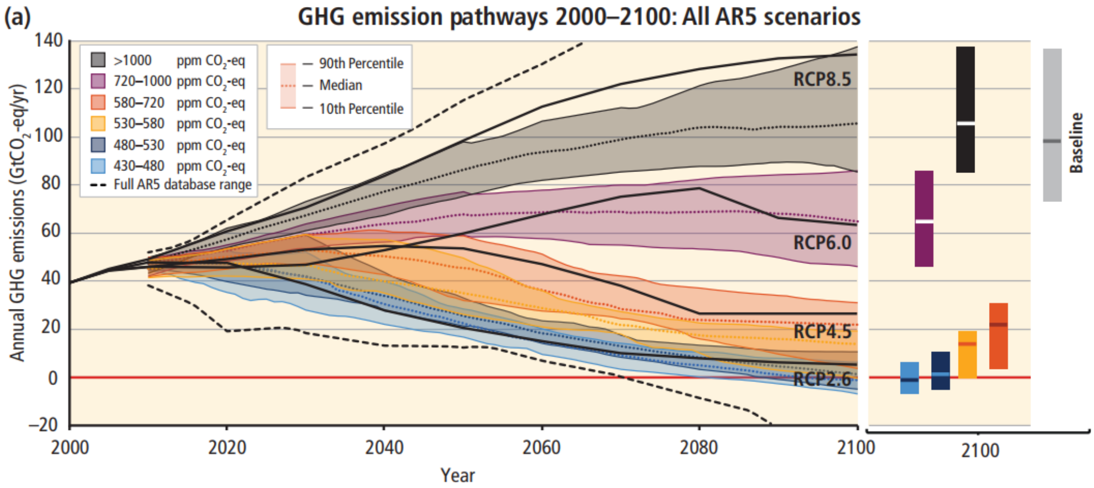

Figure 2.4: Global greenhouse gas emissions (gigatonnes of CO2-equivalent per year, GtCO2-eq/yr) under the base case and mitigation scenarios for various long-term concentration levels [103].

As per AR5, the extent of the global temperature rises in steps from RCP 2.6 to RCP 8.5. By the end of the twenty-first century, the global surface temperatures of RCP 2.6, RCP 4.5, RCP 6.0, and RCP 8.5 are predicted to climb by 0.3 - 1.7 °C, 1.1- 2.6 °C, 1.4 - 3.1 °C, and 2.6 - 4.8 °C, in comparison to 1986–2005 [104].

2.5.2. **Global circulation models**

The emission scenarios do not necessarily include climate change forecasts; instead, they illustrate potential human growth routes and simulate the factors contributing to climate change using possible scenarios and underlying assumptions. These scenarios may then be utilized as a future climate change modeling starting point. To anticipate the future climate, Global Circulation Models (GCMs) are provided with emission scenarios as input [105]. GCMs are mathematical representations of the fundamental processes and interactions of the climate system. With a fair amount of geographical and temporal precision, the GCMs can forecast the climate [105]. Global Climate Models (GCMs) are becoming increasingly popular for forecasting future climate conditions. However, their limitations in providing accurate and trustworthy monthly data at a broad geographical scale render them unsuitable for building performance simulation tools requiring precise hourly weather data. To address this, it is necessary to spatially and temporally downscale GCMs to provide hourly data appropriate for building modeling tools [106]. In fact, downscaling has been applied to all meteorological data with a geographical resolution of less than 100 km^2 and a temporal resolution of less than monthly values [107]. The downscaling method requires the typical metrological year to generate future weather data.

2.5.2.1. **Typical metrological year**

During the early design stage, the building sector utilizes meteorological data to evaluate the design and performance of the building. A typical meteorological year (TMY), according to the National Renewable Energy Laboratory (NREL), is defined as a data collection of solar radiation and other meteorological parameters at hourly intervals across a year. It comprises months selected out of several years combined to create an entire year [28].

Typical weather files utilized for simulation contain 8,760 hourly values of a few selected climate factors, such as temperature, relative humidity, solar radiation, and wind speed. In the past, numerous techniques for averaging or generating meteorological data were employed to establish typical climatic conditions. TMY was generated by the most utilized technique of the Finkelstein-Schafer (FS) statistical method. A brief description of the generation of TMY is given. The approach entails choosing five candidate years most similar to the combination of all the years being studied for each of the twelve months. The first step of the statistical analysis is the creation of nine daily weather metrics for each daily record: a mean, minimum and maximum dew point and dry bulb temperature, total horizontal solar radiation, and mean and maximum wind velocity. The short-term cumulative distribution functions (CDFs) for certain months in particular years, as well as the twelve long-term cumulative distribution functions (CDFs), one for each month covering the whole time of record, are created by sorting each of the nine sets of daily metrics into bins according to the month [108].

2.5.2.2. **Downscaling global climate models**

For incorporating the effects of climate change into weather data, various techniques have been widely employed [106]. There are two basic strategies for analyzing climate change in greater spatial detail: statistical downscaling and dynamical downscaling, respectively [109]. A third strategy is a hybrid approach, combining both approaches. The classification of downscaling methods is given in Figure 2.5.

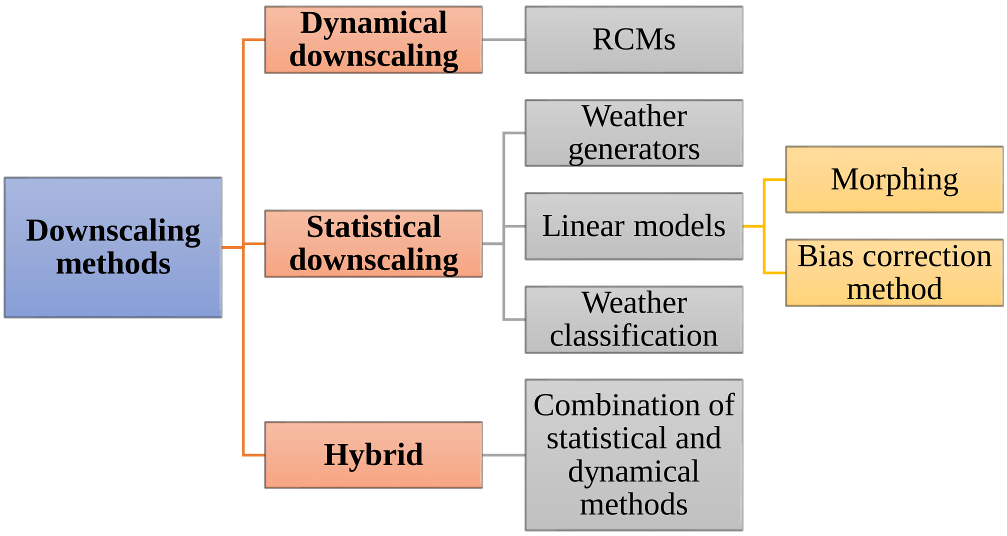

Figure 2.5: Downscaling global climate models [110].

2.5.2.3. **Dynamical downscaling**

Using a Regional Climatic Model, dynamic downscaling obtains local or regional climate information (RCM). RCMs are numerical models that need GCM or observation-based data set boundary constraints to be explicitly established [107]. The dependency on the physical process instead of statistical correlations and the lack of stationarity conditions are important advantages [109]. Nonetheless, it has several disadvantages, such as requiring a substantial amount of computer resources, especially for extremely high-resolution simulations, and its performance is also heavily dependent on GCM boundary-forcing data. This approach may introduce systemic bias; consequently, it is advised that the equations be solved, and statistical adjustments be applied to better match the RCM outputs and the observed data [111].

2.5.2.4. **Statistical downscaling**

Statistical downscaling uses statistical approaches to demonstrate empirical correlations between large-scale and local climates [109]. It needs less processing power and effort to execute, but it is constrained by the assumption of a steady link between current data and the current model climate in a modified future climate [112]. It is a diverse set of approaches with varying levels of complexity and application. Although they are all quite easy to implement, they all need a significant amount of reliable observational data.

Stochastic weather generators are statistical algorithms that can fill in missing data and produce infinitely lengthy synthetic weather series [113]. Local meteorological variables are grouped with respect to distinct atmospheric circulation types in the weather classification method [112]. Linear models determine linear connections between the predictor(s) and the predictand. The bias correction method is necessary to assess if the datasets should be modified to account for systematic variations between model results and observations [114]. Statistical downscaling methods are essential for adjusting time series to anticipate future trends. Among these methods, Morphing stands out as a widely adopted approach. It was introduced by Belcher et al. [115], and involves transforming hourly values of selected meteorological variables using three algorithms that adjust for monthly trends and variances in GCM or RCM outputs for a specific region. This technique has proven effective in providing accurate predictions of future climate scenarios [107].

2.5.2.5. **Hybrid downscaling**

The application of the hybrid approach is becoming popular in the studies of the impact of climate change. It combines the advantages of both statistical and dynamical downscaling approaches. In some situations, a hybrid strategy can decrease the computing power and storage space needed for dynamic downscaling. The hybrid downscaling technique involves utilizing statistical methods to refine the spatial and temporal resolution of outputs generated by a regional climate model (RCM) that have been initially saved at a coarse level. This process results in more accurate and detailed information for climate analyses and projections [107]. There are several studies related to the use of the hybrid downscaling approach. For example, Tu et al. [116] propose a hybrid downscaling approach that combines deep learning with a weather research forecasting method to produce precipitation in Japan. It was reported that the hybrid downscaling process could resolve the issue between reducing the computing burden and maintaining the downscaling's physical mechanics. Colette et al. [117] presented a unique downscaling methodology that includes dynamical and statistical methods, albeit in a different sequence than is often used. The proposed hybrid technique entails statistically correcting GCM fields in relation to atmospheric reanalyses before conducting dynamical downscaling on these adjusted fields. A novel hybrid statistical/dynamical climate downscaling method was reported to provide significant prospects for climate impact studies that need balanced, unbiased, high-resolution 3D fields. Thus, for this research, a hybrid downscaling method will be applied.

2.6. Impact of climate change on buildings

2.6.1. **Impact of climate change on PCM buildings**

Despite its potential to mitigate the detrimental effects of climate change on buildings, there has been a lack of research on using PCM in this context. Ramakrishnan et al. [118] studied the influence of building renovation using PCMs on heat stress hazards in residential buildings during heat waves in 2030 and 2050 in Melbourne. Results showed that the buildings with PCM and night ventilation reduced the discomfort hours by 48% and 46% in 2030 and 2050, respectively. Nurlybekova et al. [119] investigated the influence of PCM integration in buildings in six cities in the subtropical climate zone under current and future climate scenarios (RCP 8.5). The energy and thermal performance of buildings were studied. Results showed that for selected cities (Chengdu, Hanoi, and Kathmandu), the optimum PCM ranged from 28 °C to 30 °C, while the optimum PCM for Zhengzhou was 18 °C for both scenarios. However, the optimum PCM was different for current and future scenarios (29 °C and 18 °C) in Islamabad. The implementation of PCM resulted in up to 37 % of energy savings for both scenarios. Adilkhanova et al. [120] investigated the efficacy of PCM in decreasing summer energy consumption in lightweight relocatable buildings with natural ventilation in six cities of Kazakhstan under a high greenhouse gas emissions scenario (RCP 8.5). Their findings revealed that using PCM with a high melting point (26 °C to 28 °C) resulted in the greatest reduction in thermal discomfort hours. Meanwhile, Kharbouch [59] examined the impact of PCM on improving the summer thermal performance of an office building, taking into account the effects of climate change in Morocco under a moderate GHG emissions scenario (RCP 4.5) for the next three decades (2020, 2030, and 2040). Two types of buildings were selected for the study: a free-running office building and an air-conditioned office building. An economic evaluation of the cost of PCM was also conducted for the air-conditioned building. Finally, for the air-conditioned building, an economic evaluation of the PCM cost was performed. Results indicated that for 2040, the optimum PCM melting temperature was 26 °C for the air-conditioned office building, whereas the optimum PCM melting temperature for a free-running building was 28 °C. Maximum energy reductions of 20.5% were achieved in air- conditioned office building, while for free-running building, the energy reduction was about 9.87 %. The threshold of PCM installation was 263.6 MAD/ m^2.

2.6.2. **Impact of climate change in sensitivity analysis and optimization studies**

Based on the literature review, few investigations are related to the application of SA under the impact of climate change in buildings without PCM. Yildiz et al. [121] used sensitivity analysis to find the most robust and sensitive parameters for cooling energy consumption in hot and humid climates in 2012, the 2020s, the 2050s, and 2080. For this purpose, a low-rise apartment building located in Turkey was selected. SRRC was selected for performing the SA, while Monte Carlo Analysis and Latin HyberCube were selected for sampling. Typical Meteorological Year 2 (TMY2) was chosen for simulations, while the future weather files were derived by the morphing method using the Climate Change Weather File Generator (CCWorldWeatherGen). Several building design parameters were considered for sensitivity analysis: natural ventilation, zone height, insulation (thickness of wall and roof), thermophysical properties of the building (U-value, SHGC, specific heat, thermal conductivity), window to external wall area (south, north, east, and west), building shape (length and width), envelope color (wall and roof), and air infiltration. SRRC results showed that the most significant parameters for all selected periods were: natural ventilation, the thickness of insulation, window area (east, west, north, south), air infiltration, length and width of the building, SHGC (east, south, west, north), and space height. The most essential design criteria were the same throughout all historical periods, with only minor variations in the order of priority. These modifications were anticipated since the sensitivity of design parameters varies with climate conditions. Apart from sensitivity analysis under the impact of climate change, some investigations were provided in the area of the optimization of buildings. Rubio-Belido et al. [122] conducted a study to analyze the influence of climate change on the energy usage of buildings across nine regions in Chile during 2020, 2050, and 2080. The authors employed a mathematical model following the calculation method of ISO-13790:2008 to perform optimization. Two parameters, namely WWR and form ratio (building length/wide ratio), were selected for optimization. According to the results, optimized structures will inevitably increase yearly energy use in some locations. However, attaining an optimal equilibrium between WWR and shading with fenestration ratio (FR) can considerably curtail energy consumption, decreasing from 0.13 to 0.27 kWh/year per square meter. Bilardo et al. [123] examined the impact of global cost optimization of the multi-family building design subjected to several future climate scenarios (RCP 4.5 and RCP 8.5) from 2026 to 2045 in Italy. The single-objective optimization method was utilized. Overall, the results indicate a slight reduction in the overall cost of the building under study in future climate assessments. However, from the standpoint of primary energy, the drop is significant. Nguyen et al. [124] assessed energy consumption and thermal comfort by using multi-objective optimization in the regions of Southeast Asia. According to the results, the optimal models consistently exhibit greater performance in the current or future regarding energy conservation and overheating avoidance under the same environmental circumstances. However, no perfect solution exists that can sustain overheating and energy consumption at the current level of the basic building and the majority of its changes in the future. From the literature review mentioned above, it is clear that there are only a few studies on sensitivity analysis and optimization under the impact of climate change.

2.7. Chapter summary

Chapter 2 investigated the EDSP related to the building geometry, building envelope thermophysical properties, and energy-efficiency measures that influence the performance of the building during the design process and, therefore, should be incorporated into the building design optimization process. Several pieces of research demonstrated the significance of the examination of EDSP. The results of the investigations showed that selecting appropriate design parameters enabled the energy-efficient functioning of heating and cooling systems. However, the combination of building geometry, building envelope thermophysical properties, and PCM parameters to improve the energy-efficiency of buildings is neglected.

This chapter highlights the significance of sensitivity analysis and simulation-based optimization in the initial design phase. The sensitivity analysis identifies critical parameters that significantly affect the model's output. In turn, this knowledge enables the elimination of irrelevant parameters and offers guidance for future research to decrease parameter uncertainties and improve the validity of the model. The two main approaches of sensitivity analysis were identified: local and global. In local sensitivity analysis, one design parameter is altered over its entire range, while the other parameters are maintained constant in their initial states. It is a widely used approach because of its simplicity of application and low computer demands; however, it has substantial limitations (linearity and normalcy assumptions, local variations). Another group of methods in a statistical framework has been established to address the constraints of local approaches. Global sensitivity analysis examines output changes caused by a single input variable by simultaneously altering complete parameters throughout their full input space. As a result, global approaches examine parameter interaction and give reliable sensitivity measurements for nonlinear models. Using single sensitivity analysis (local or global) prevails in the existing research. However, it was reported that using only one sensitivity analysis approach could miss some important design parameters. As a result, it was suggested that at least two sensitivity analyses be performed. Additionally, the use of sensitivity analysis in PCM-integrated buildings is limited.

In addition, existing optimization methods, algorithms, and their applications in building energy analysis were presented. Optimization techniques are used to solve issues systematically by generating solutions based on specific objectives that are functions of design parameters. The two main optimization approaches were determined: deterministic and stochastic. Deterministic rules govern each step of the algorithm's geometry in deterministic optimization, and the initial point alone determines the entire sequence of evaluated points. Stochastic optimization uses random judgments to influence some of the algorithm's phases. Determining the proper values by optimizing the design parameters at the early design stage results in considerable improvements in the energy consumption of a building. Consequently, optimizing in the early design stage should be thoroughly investigated to decrease the complexity of inputs and computing time.

The studies related to climate change's impact on buildings' energy consumption were summarized. The generation of weather data includes three methods: dynamical, statistical, and hybrid. Dynamical downscaling uses RCMs to provide climate data at a smaller geographic scale than GCMs. Statistical downscaling transforms large-scale predictors into fine-scale predictands by using empirical mathematical correlations. The hybrid downscaling method combines statistical and dynamical downscaling. Based on the review, numerous investigations have explored how climate change impacts building performance using various techniques and scenarios for generating weather data. It was revealed that a few researches have attempted to identify the most important design parameters and optimize building design for future climate change. Furthermore, the most common limitation of prior studies on optimization under the impact of climate change is the small number of design parameters. Ignoring long-term change can lead to incorrect outcomes. As a result, it is critical to develop a process that would aid architects in maximizing building design while considering climate change.

The findings of this chapter are summarized below:

- Incorporating PCM into the building envelope is acknowledged as a successful strategy for reducing energy usage and enhancing thermal comfort;
- Utilizing sensitivity analysis during the initial stages of the design phase allows for the identification of the most critical parameters related to building performance;
- According to several studies, the ranking outcome of the same model may vary depending on various SA approaches. Whenever computing tools are available, using at least two SA approaches is suggested to find the essential parameters. The advantage of this strategy is that it can make use of numerous SA approaches while providing a dependable result when the model is intricate, or the model attribute is unclear;
- Typically, the application of optimization techniques during the early design stage of a building aids in achieving high performance;
- Climate change can significantly influence increasing energy requirements, according to an examination of building energy consumption.

CHAPTER 3: METHODOLOGY

This chapter demonstrates the research methodology used to address the thesis goal. The sections start with an introduction outlining the method (section 3.1). Section 3.2 describes the analyzed regions' climate conditions and current and future weather data generation methods. Section 3.3 summarizes the selected EDSP. The sampling methods for MSA are described in Section 3.4. At the same time, the selected building model and the construction materials are reported in Section 3.5. The description of the applied thermal comfort model, details of the validation of the developed model, and the software used are given in Sections 3.6-3.8. Section 3.9 describes the integrated MSA approach to identify the most significant EDSP related to total energy consumption and their interaction. The single-objective optimization method was carried out to find the best combination of optimal EDSP that would provide the lowest feasible energy consumption (Section 3.11). The economic assessment of optimal solutions is described in Section 3.11. Finally, the summary of the chapter is given in Section 3.12.

3.1. Overview

The following section provides an overall framework of the proposed methodology, which consists of four main stages: model construction, MSA for both present and future climate scenarios, optimization and post-optimization analysis for present and future scenarios, and assessment of the impact of climate change. Figure 3.1 illustrates this framework.

As outlined in subsequent sections, the building modeling phase involves identifying the building type, EDSP, performance objectives, and climatic conditions. Following building energy modeling, the MSA technique is employed to identify key EDSP, utilizing multiple sensitivity methodologies to reduce the optimization search space. The results of multiple sensitivity techniques might result in a varied sensitivity ranking, which can help to avoid overlooking the most crucial design parameter. The MSA produces rankings of EDSP and identifies their relationship with the objective.

The MSA consists of two stages. To determine the magnitudes of the effect of EDSP on energy consumption, the first stage utilizes three GSA methods: Standardized rank regression coefficients (SRRC), Partial rank correlation coefficient

(PRCC), and the Morris method. The MSA is divided into two stages. According to Saltelli & Marivoret [125], the PRCC and SRRC were the most efficient and reliable among the sampling-based indexes. Furthermore, the regression method has a low computational cost, while the Morris method suits problems with many inputs. In the second stage, LSA is utilized to analyze the impact trajectory of the most sensitive parameters acquired in the first stage. The significance of EDSP for each SA approach was subsequently assessed. EnergyPlus, jEPlus, and R were employed in the simulation-based SA implementation. jEPlus runs EnergyPlus for simultaneous simulations and generates the necessary input files. Finally, the simulation data was transferred to the R program to execute the SA.

In the early design stages, a single-objective optimization of crucial parameters was carried out using jEPlus and Evolutionary Algorithms (EA). This was achieved by combining jEPlus with EA (jEPlus+EA), efficiently optimizing building operations and design [15]. Thereafter, the economic assessment of optimal solutions for the current scenario was applied.

Finally, the evaluation of the impact of climate change in the selected zones was completed. For analysis, the typical metrological year and RCP 8.5 data were utilized. Also, a comparative analysis of MSA and optimization was carried out for current and future climate scenarios. A detailed description of each stage of the methodology is presented in the following sub-sections.

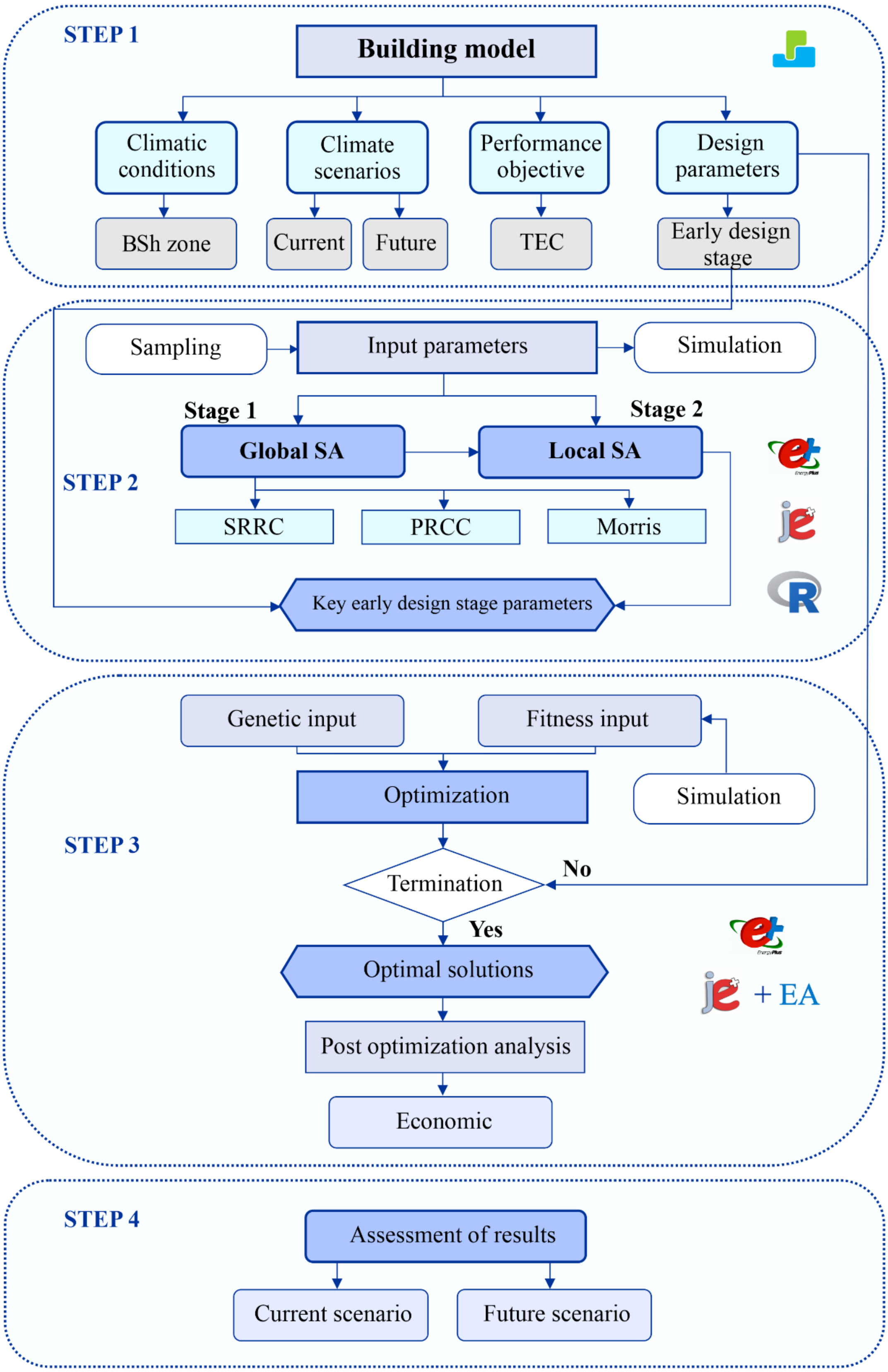

Figure 3.1: Research framework

3.2. Climate conditions

The Köppen-Geiger climatic classification [126] was employed in the current research (Figure 3.2). In this classification, the primary climates are divided into five groups: equatorial (A), dry (B), warm temperate (C), snowy (D), and polar (E). The second alphabet represents precipitation, classified as S: steppe, W: desert, m: monsoonal, w: winter dry, s: summer dry, and f: fully humid. Additional information is given on temperature: *h* for hot and dry, *k* for cold and dry, *a* for hot and cool summers, *b* for warm and cool summers, *d* for severely continental, and *F* for polar frost [127]. The BSh zone from the Köppen-Geiger map, characterized by consistently high temperatures and solar radiation throughout the year, was selected for this research. In order to represent the whole climate zone, the six cities located in various regions of the BSh zone were selected. Cities in BSh zones are Ahmadabad, Lahore, Marrakesh, Port Elizabeth, Tripoli, and Windhoek. More detailed information on geographical data is given in Table 3.1. BSh (hot semi-arid) climates are transition zones between BW and humid climates. In the BSh zone, the winters are generally mild; summers may be hot, sometimes extremely hot [128].

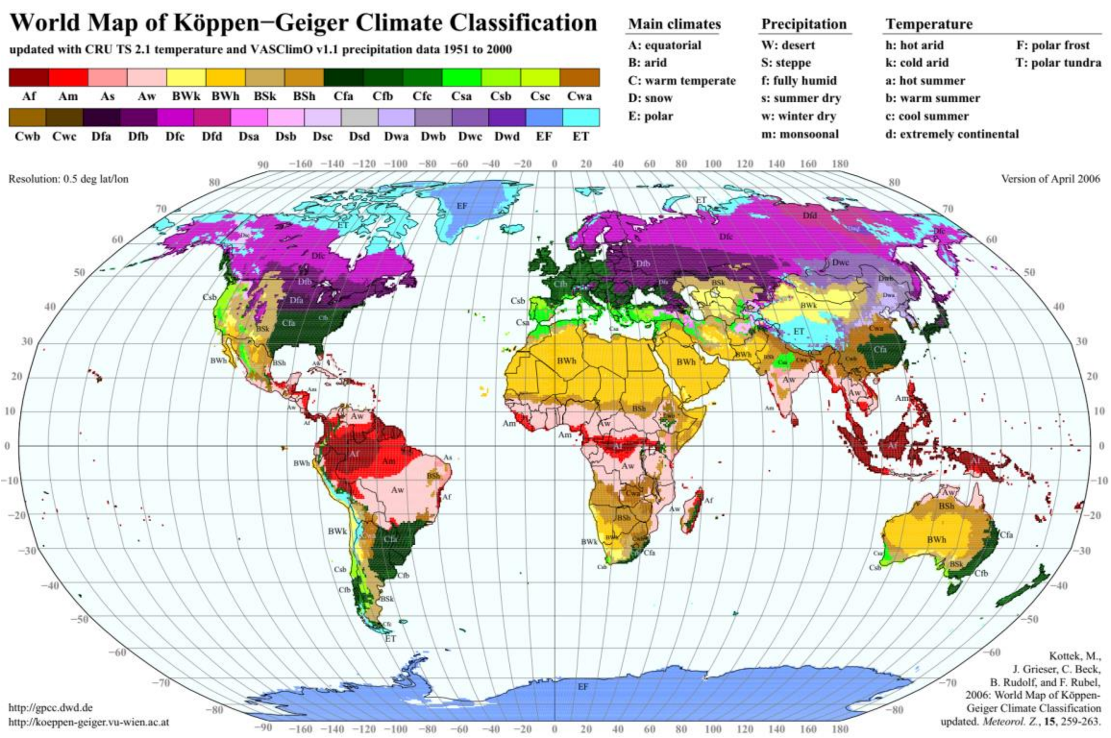

Figure 3.2: World Map of Köppen–Geiger climate classification [127].

Table 3.1: Selected locations and climate characteristics.

Climate	City	Country	Latitude	Longitude	Time zone	Elevation, m
BSh	Ahmadabad	India	23.0225	72.5713	+5:30	53
	Lahore	Pakistan	31.5203	74.3587	+5:00	210
	Marrakesh	Morocco	31.6294	-7.9810	+1:00	458
	Port Elizabeth	South Africa	39.3134	-74.9809	+2:00	67
	Tripoli	Libya	32.8872	13.1913	+2:00	31
	Windhoek	Namibia	-22.5608	17.0657	+2:00	1687

3.2.1. **Weather data**

For the simulation, weather files for the selected location are required. The weather files contain information about geographical factors, such as latitude, longitude, elevation, time-zone, data source, holidays, and daylight saving time, as well as meteorological factors like dew point and dry bulb temperature, solar radiation (direct, diffuse global, extraterrestrial, horizontal infrared), sky cover, wind speed and direction, station pressure, and relative humidity [129]. For this research, two types of weather data were used:

- The current weather data, which represents the typical meteorological year (TMY);
- The future weather data generated by the hybrid method.

3.2.1.1. **Current weather data**

For this research, TMY data from IWEC2 (International Weather for Energy Calculation Version 2) was utilized. TMY can accurately depict the long-term usual weather patterns throughout the year [108]. IWEC2 weather files for 3012 international locations outside of the United States and Canada were prepared utilizing fresh data from 2007 to 2011 and evaluated using ASHRAE 1477-RP [130]. These files were developed from Integrated Surface Hourly (ISH) meteorological data originally maintained at the National Climatic Data Center. The ISH database comprises weather observations of current weather, dew-point and dry-bulb temperature, sky cover, ceiling height, visibility, liquid precipitation, atmospheric pressure, wind speed, and direction for at least 12 years and up to 25 years for these selected areas [131]. Due to the lack of recorded solar radiation in the ISH database, the hourly total horizontal solar radiation is computed based on the empirical Zhang-Huang Model [132] on the sun-earth geometry, reported cloud cover, wind speed, relative humidity, and temperature change from three hours prior. Using the sun angle and the ratio of the determined total global horizontal to the extraterrestrial solar radiation, an empirical Gompertz Function Model [133] is utilized to determine the direct normal solar radiation. Following that, other models employ these deduced solar radiation values to compute different illuminances (diffuse horizontal, direct normal global horizontal), as well as zenith luminance, which is helpful for daylighting investigations. The weather files for this research were purchased from White Box Technologies, Ltd. (Moraga, USA) [134]. Figure 3.3 shows the monthly averages of outdoor air drybulb temperature, direct solar radiation, and humidity for six cities for the current scenario.

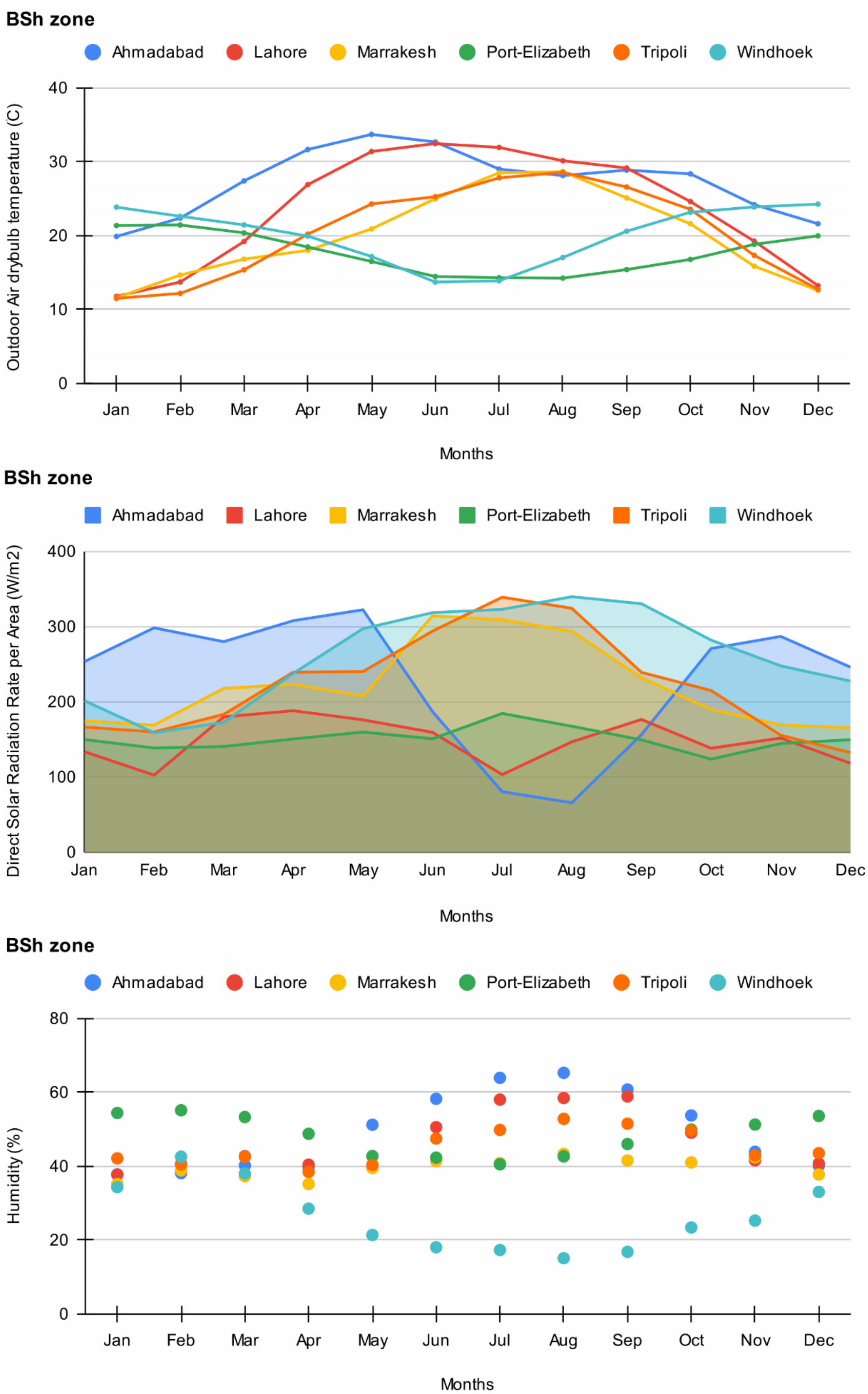

Figure 3.3: The average outdoor air-dry bulb temperature, direct solar radiation, and humidity for the BSh zone.

3.2.1.2. **Future weather data**

Buildings will be particularly vulnerable to the anticipated future climate changes since they are an essential infrastructure component. Therefore, it is essential to statistically forecast the potential effects of the future climate on the total energy consumption of the building. Thus, the impact of climate change on energy consumption was assessed. To conduct an analysis, the simulations were evaluated using a high-emissions scenario known as RCP 8.5. This approach was adopted to ascertain the simulations' most extreme possible result.

Typically, future weather files are produced by downscaling spatial scale weather data for future months and years forecasted by Global Climate Models (GCMs). As mentioned earlier (Section 2), there are three main methods to generate future weather data: dynamic, statistical (deterministic and stochastic), and hybrid. The dynamic method demands huge computing power and storage space to create data sets [135].

The morphing statistical method has been popular for generating future weather data for several decades. Nevertheless, one drawback of the morphing process is that certain variables are generated separately, so their correlations in the new weather series could not be identical to those in the historical weather series. Furthermore, new sequences of occurrences cannot be formed, and future weather series are restricted to observed events. A new sequence of events could not be formed, and future weather series are only allowed to include recorded events [105]. The stochastic technique produces artificial future weather data using a few weather factors. In addition, it is necessary to collect meteorological data over several years to be relevant to the weather trends over the appropriate time period. Precisely modeling some variables may also be problematic for this strategy [136]. The hybrid method combines the first two strategies by employing statistical methods to downscale the RCM's results. The benefit of this technique is that it enables the simulation of a broad variety of potential climatic conditions, including extreme weather events that have not yet been reported [120]. This research utilized future weather files derived through a hybrid downscaling methodology. The weather data were purchased from White Box Technologies, an expert in generating future weather data based on a hybrid downscale approach. The monthly averages of outdoor air dry bulb temperature, solar radiation, and humidity for future climate scenarios (RCP 8.5) in the BSh zone are presented in Figure 3.4.

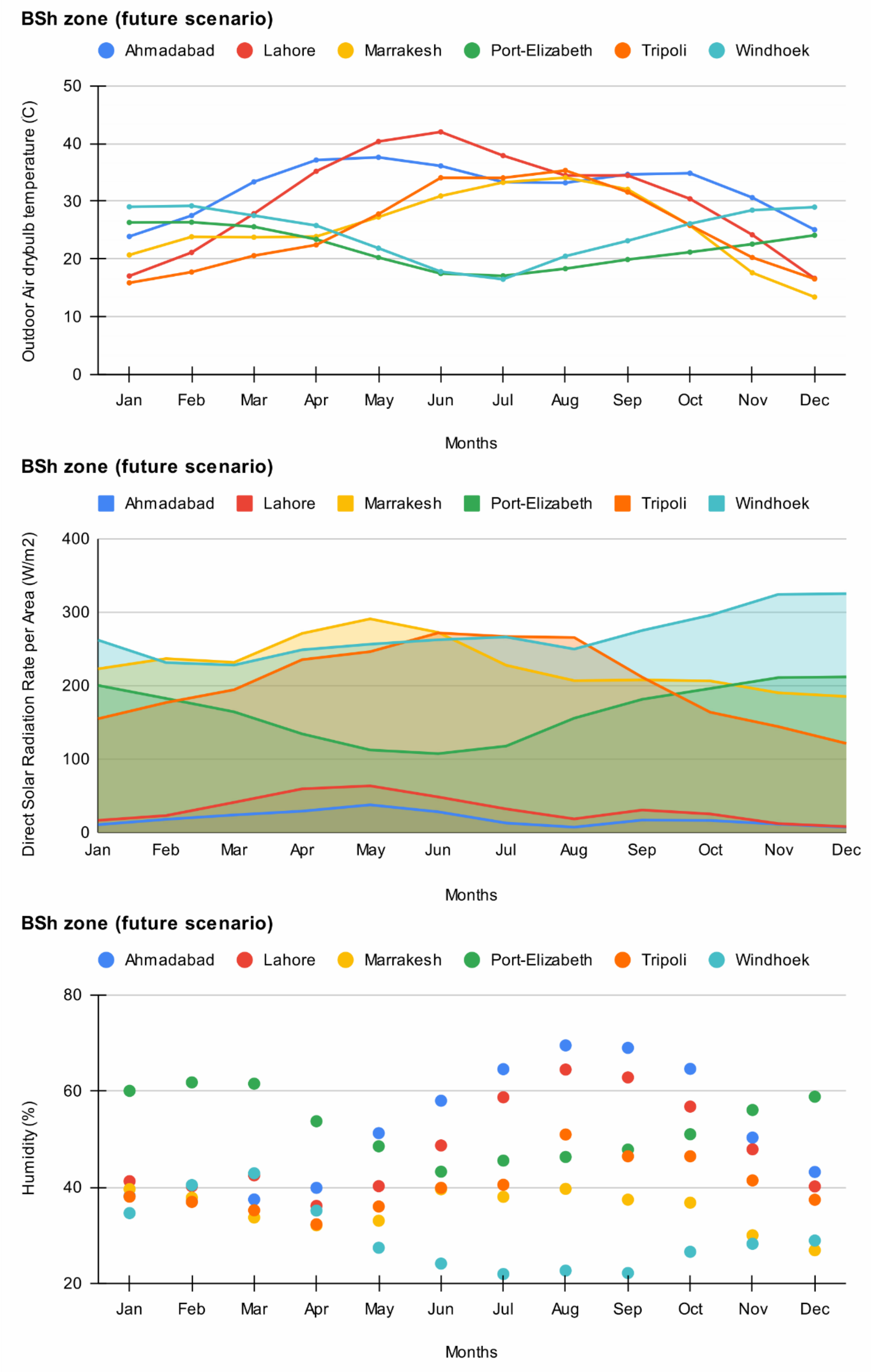

Figure 3.4: The average outdoor air dry-bulb temperature, direct solar radiation, and humidity for the BSh zone (RCP 8.5).

3.3. Input parameters, sampling, and objective function for sensitivity analysis and optimization

3.3.1. **Early design stage parameters**

In sensitivity analysis and optimization, the parameters subject to variation are called design parameters. For this research, emphasis was placed on selecting relevant passive design parameters during the early stages of building design. These typically encompass key parameters such as building size and layout, thermophysical characteristics and composition of the building envelope, airtightness, and infiltration, overhang projection ratio, and the window-to-wall ratio [6,33].

According to the literature, the most significant components influencing energy consumption in buildings throughout the operational stage are the thermal characteristics of the external building envelope, including the wall, windows, and roof. This is due to the transmission of cooling and heating loads of buildings externally through the building envelope from the exterior environment [137]. Apart from the building envelope's thermal characteristics, building orientation's impact on energy consumption is substantial. A building's ability to naturally heat the building envelope via solar gain can be influenced by its position in relation to the sun's path [138]. Moreover, the impact of thermal energy storage systems on energy consumption cannot be neglected. Incorporating phase change materials is an efficient way to save energy while improving interior comfort [139]. Therefore, several EDSP related to the building layout, thermal envelope characteristics, and energy-efficiency measures were examined in this research (Figure 3.5). Notably, the aforementioned combination of design parameters in the early stages has not been investigated in any research concerning buildings integrated with PCM. The building layout includes the building orientation (BO), while the thermal envelope characteristics refer to wall conductivity (WC), wall solar absorptance (WSA), wall specific heat (WSH), window visible transmittance (WVT), window conductivity (WinC), roof specific heat (RSH), roof conductivity (RC), and roof solar absorptance (RSA). The energy efficiency measures include the melting temperature (PTm) and thickness of the PCM layer (Pt).

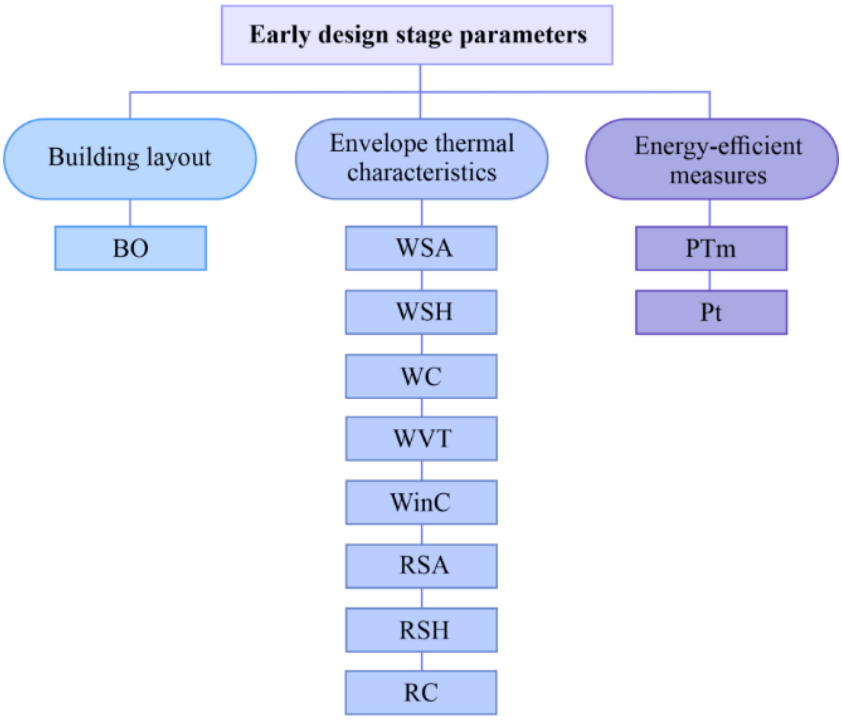

Figure 3.5: EDSP classification.

Specifically, eleven EDSP have been selected for the MSA. Table 3.2 lists the inputs considered, their initial values employed, and the range across which they were adjusted. The ranges of parameters are based on previous literature [80,140–142]. The base case values of the corresponding DOE reference model were used to determine the base settings for the building.

Each parameter has been adjusted between a lower and upper range value for the sensitivity analysis. BO varies from 0◦ to 360° to maximize or minimize the solar gain. The thermal characteristics of the first construction layer were selected for the adjustment. WSA and RSA are often associated with light- to dark-colored walls or roofs and vary from 0.1 to 0.9 [143]. WVT measures the amount of daylight that enters the glass and ranges from 0.06 to 0.81. WinC varies from 0.1 to 1 W/m K and displays the glass heat transfer rate. Single pane window was selected for this research. WSH and RSH vary from 800 to 2000 J/kg·K and 450 to 1400 J/kg·K, and refer to the amount of heat in a material that can be stored. WC and RC indicate the wall and roof's capacity to transfer heat and vary from 0.1 to 1 W/m K. PTm has a temperature range of 20 to 30 °C, a melting point range of 4 °C, and a latent heat capacity of 219 kJ/kg whereas Pt varies between 0.01 and 0.03 m. Each input parameter was modified using the appropriate step size; for instance, building orientation was altered from 0° to 30° to 60° and so on until 360°.

Table 3.2: Sampling ranges and distribution of input parameters.

	Input parameters*	**Abbreviation**	**Units**	**Range**	**Step size**	**Base case**
Layout	Building orientation	BO	°	[0, 360]	30	0
Envelope thermal characteristics	Window visible transmittance	WVT	-	[0.06, 0.81]	0.06	0.8
	Wall specific heat	WSH	J/kg·K	[800, 2000]	100	840
	Window conductivity	WinC	W/m K	[0.1, 1]	0.1	0.9
	Wall solar absorptance	WSA	-	[0.1, 0.9]	0.1	0.7
	Wall conductivity	WC	W/m K	[0.1, 1]	0.1	1
	Roof solar absorptance	RSA	-	[0.1, 0.9]	0.1	0.7
	Roof specific heat	RSH	J/kg·K	[450, 1400]	100	1360
	Roof conductivity	RC	W/m K	[0.1, 1]	0.1	0.16
Energy-efficient measures	Melting temperature of PCM	PTm	ºC	[20, 30]	1	-
	Thickness of PCM layer	Pt	m	[0.01, 0.03]	0.002	0.02

Note: * *- All parameters are continuous uniform*

3.3.2. **Sampling**

Effective sampling methodologies are essential for accurate results in the initial analysis of a project's design parameters and their range [69]. Certain GSA methods require specific sampling techniques, and as such, the Latin Hypercube Sampling method was used for SRRC and PRCC, while Morris factorial sampling was utilized for the Morris method to construct the datasets for SA. These approaches were selected after defining the EDSP to ensure the validity of the final outcomes.

3.3.2.1. **Latin Hypercube sampling**

Latin Hypercube sampling (LHS) is a Monte Carlo sampling technique invented by Mckay et al. [144]. LHS adopts the concept of a Latin square, where each row and each column contain a single sample. It broadens the use of this idea to any number of dimensions [145]. LHS is a compromise between stratified sampling and simple random sampling (Figure 3.6). As a result, it is frequently regarded as a particular type of stratified sampling [70]. The advantage of LHS is the combination of simple random and stratified sampling, which yields more reliable results and simplifies its use. LHS is often employed with computationally intensive models due to its efficient stratification characteristics, which enable the extraction of a substantial amount of sensitivity with a relatively small sample size. It operates by separating inputs into strata, and after producing samples, each parameter's value is derived from a distinct stratum [146]. In LHS, the random parameter distributions are separated into N equal probability intervals, which are subsequently sampled. N denotes the size of the sample. The sample must be at least k+1, where k is the number of parameters being modified, but is often significantly larger to assure reliability [144]. Then, N model solutions are simulated using every combination of parameter values (each). For each model run, the model output of interest is compiled. LHS guarantees that the whole range of each input variable is covered, regardless of which variable or combination of variables dominates the computer model responses. This indicates that a single sample will be informative when certain input factors dominate other responses. By sampling throughout the whole range, each variable can emerge as significant [147].

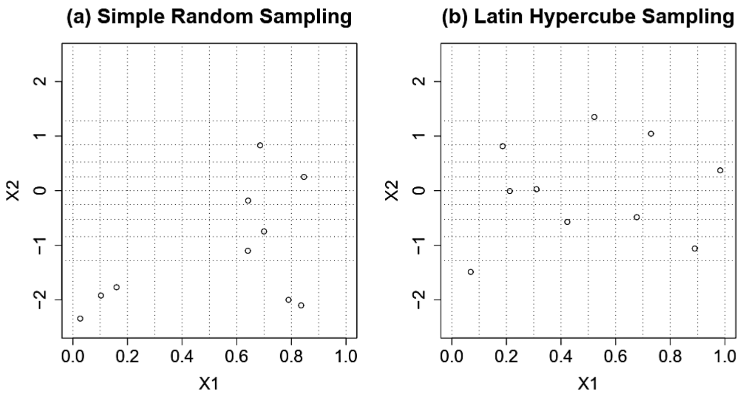

Figure 3.6: Example of a) simple random sampling b) LHS (generation of a sample of size n = 10 from two variables X = [X1,X2]) [148].

LHS works by separating the subspace of each vector component $S_i i$; = 1,2,..., *N* into *M* = *n* distinct subsets (strata) of equal probability: Ω_{ik};i = 1, 2,..., *N; k* = 1, 2, . . . , *M*. Each vector component's samples are drawn from the corresponding strata in accordance with [149]:

$$x_{ik} = D_{Xi}^{-1}(U_{ik}); i = 1,2, \dots, N; k = 1,2, \dots, M \tag{3.1}$$

Where, S_i is the sample space, and where U_{ik} denotes iid (independent and identically distributed realizations) uniformly distributed samples on $[\varepsilon_k^l,\ \varepsilon_k^u]$ with $\varepsilon_k^l = \frac{k-1}{M}$ and $\varepsilon_k^u = \frac{k}{M}$. The terms of the produced vector components are grouped at random to construct the samples *x*. In other words, each vector component's term x_{ik} is randomly chosen (without replacement), and these terms are then aggregated to create a sample. This procedure is carried out *M* = *n* times.

The difference between the influential and non-influential characteristics becomes stronger as the sample size increases, according to [150,151]. To generate more reliable findings for each city, a sample size of 1000 was used. For twelve cities under current and future climate scenarios in the SRRC and PRCC, 24000 samples were obtained.

3.3.2.2. **Trajectory-based sampling strategy of Morris method**

The sampling process begins by discretizing the parameter space by transforming the input parameters *k* into dimensionless parameters in the range (0;1) and dividing each parameter range into a number of p levels, which leads to producing a regular grid in the unit-length hypercube H*k*. The starting point is selected randomly from the grid with a difference in one coordinate. Δ is a trajectory, a collection of k+1 points, where each parameter varies by a predefined value [17].

The following method is used to construct the trajectories. The *p*-level grid **Ω** randomly chooses a base value x^* for the vector *X*. All of the trajectory points are generated from x^* by rising one or more of its *k* components by Δ, even if x^* is not a part of the trajectory itself. To ensure that the initial trajectory point, $x^{(1)}$, is still in **Ω**, one or more components of x^* are increased by Δ until $x^{(1)}$ is attained. The second trajectory point, $x^{(2)}$, is produced from x^* with the condition that it varies from $x^{(1)}$ in its ith component, which has either been increased or lowered by Δ ,

$x^{(2)}=x^{(1)} + e_i\Delta$ or $x^{(2)}=x^{(1)} - e_i\Delta$. In the set {1, 2, ..., k}, the index i is randomly chosen. The process is continued until the trajectory is closed by $x^{(k+1)}$. The strategy generates a trajectory of (k+1) sampling points $x^{(1)}$with the important characteristics that every value of the base vector x^* has been chosen at least once to be raised by Δ , and that two consecutive points vary in only one component [73]. Figure 3.7 shows an example of a trajectory with k = 3.

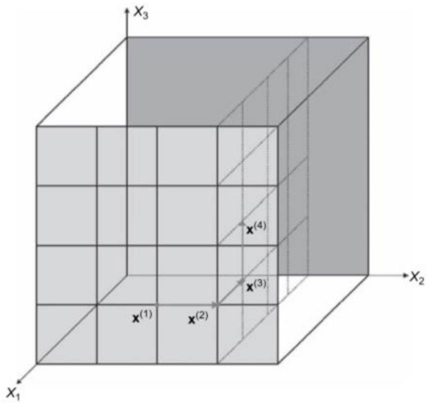

Figure 3.7: A trajectory with k = 3 [75].

A practical method for producing a trajectory with the needed elements is as follows. A *B* matrix can be used to represent a trajectory of size *k*-by-*(k + 1),* whose rows denote input vectors *xs*, for which the corresponding experiment offers *k* elementary effects, one for each input factor, from *(k+1)* runs. Initially, the base matrix is created using ones in its lower triangular section and zeros in the remaining section [152].

$$B = \begin{bmatrix} 0 & 0 & 0 & ... & 0 \\ 1 & 0 & 0 & ... & 0 \\ 1 & 1 & 0 & ... & 0 \\ 1 & 1 & 1 & 0 & ... \\ ... & ... & ... & ... & ... \end{bmatrix} \tag{3.2}$$

The matrix *B'*, denoted by,

$$B' = J_{k+1,k}\, x^* + \Delta B \tag{3.3}$$

where x^* is a base value that was selected randomly and $J_{k+1,k}$ is a k +1 k matrix of ones. The intended design matrix has a possible candidate in the value of X, however, B' with the drawback that its kth elementary impact would not be chosen randomly.

The sampling matrix is shown in a randomized form by:

$$B^* = (J_{k+1,k}\, x^* + \left(\frac{\Delta}{2}\right)[\, 2B - J_{k+1,k}\big)\, D^* + J_{k+1,k}])P^* \tag{3.4}$$

where each element of the k-dimensional diagonal matrix D^* is either +1 or 1 with equal probability, P^* is a k-by-k random permutation matrix in which no two columns have any 1s in the same location, and each row includes one element equal to 1, all others are 0. B^* offers a single, randomly chosen elementary effect for each input, D^* indicates the rise or fall of factors along the trajectory, P^* indicates the sequence in which the components are moved and, when read, row by row.

In this study, r = 10 was utilized to represent ten repetitions or trajectories of the EE for each input value. The literature recommends a minimum value of r = 4 to ensure proper representation of the zone of variation for all design parameters. However, r = 10 is recommended for obtaining highly reliable results [28]. The minimal number of simulations is:

$$N = r\,(k+1) = 10\,(11+1) = 120 \tag{3.5}$$

where N is the number of samples, k is the number of design parameters, and r is the number of EE per factor.

The Morris technique requires a minimum of 120 simulations for the set of 11 parameters, 10 elementary effects for each parameter for one city. In total, outputs were generated from 2880 simulations.

3.3.3. **Objective function**

The EDSP for the MSA and optimization were derived from building energy consumption. The objective function of the research is represented by the total energy consumption (TEC) of the building. TEC is the sum of annual heating and cooling loads, which are calculated through the following equation:

$$\text{TEC} = EC_{heating} + EC_{cooling} \tag{3.6}$$

Where,

$EC_{heating}$: the annual energy consumption for space heating (kWh/year);

$EC_{cooling}$: the annual energy consumption for space cooling (kWh/year).

Since it was anticipated that these energy consumptions would not vary much throughout the optimization periods, electronic equipment, artificial lighting, and domestic hot water were not considered.

3.4. Building model

Choosing an appropriate building model was necessary to run the simulation in various weather scenarios. For this purpose, the four-story mid-rise apartment from the ASHRAE 90.1-2003 prototype building models [153] was chosen. With the assistance of the U.S. Department of Energy's (DOE) Building Energy Codes Program, the Pacific Northwest National Laboratory (PNNL) developed these prototype building models. Thus, building prototypes can be used in different climatic conditions because they are modeled in many climatic regions. For entire building energy simulation analysis, these prototype buildings that comply with ANSI/ASHRAE/IES Standard 90.1 are frequently utilized as a reliable benchmark (U.S. Department of Energy, 2016a). Figure 3.10 provides a three-dimensional view of the building.

Except for the ground floor, each storey includes 8 apartments (7 apartments and 1 lobby). The corridor is located in the center of the building (Figure 3.8). The zone depth is 7.62 m from the side walls. The building dimensions are 46.329 x 16.916 m, with an aspect ratio of 2.74. Table 3.3 gives the building's basic information.

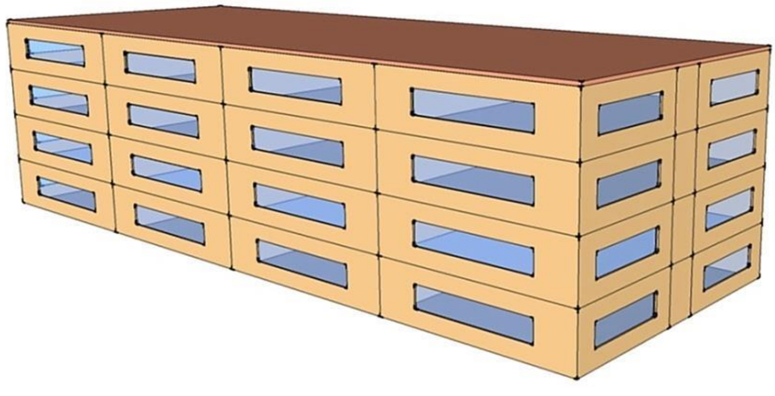

Figure 3.8: Mid-rise apartment building (base case).

Table 3.3: Basic information of the base case building model.

Aspects	Description
Orientation	The building's long axis is oriented to the north
Building storeys	4
Heights	3 m/storey
Dimensions	46.329 x 16.916 m
Aspect ratio	2.74
Floor areas	Total floor area 3130.83 m^2
Window-to-wall ratio	20 %
HVAC system	Packaged Terminal Heat Pump (PTHP)

In compliance with ASHRAE Standard 90.1.2010, the packaged terminal heat pump system (PTHP) was chosen to provide HVAC services, and the humidification and dehumidification relative humidity ratios were set at 25% and 60%, respectively, according to BS EN 15251. The ACH was also fixed at 0.7. The residential building's HVAC activation schedule from 00:00-8:00 and 16:00-24:00 hours was determined based on the suggested guidelines [60] (Figure 3.9).

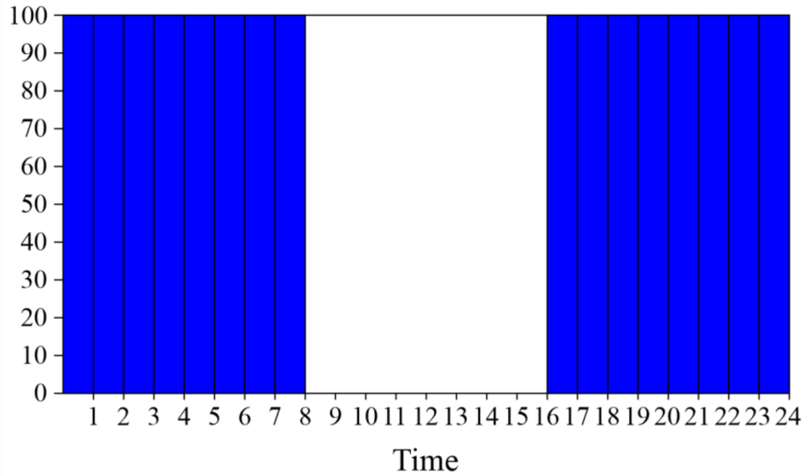

Figure 3.9: HVAC activation schedule.

3.4.1. **Construction materials**

The walls of the building are made from stucco, gypsum board, and an insulation layer, while the roof is made of built-up roofing, an insulation layer, and a metal surface. In order to incorporate PCM into the building envelope, PCM gypsum boards were mounted to the inside surfaces of the outer walls and roof. On the wall, PCM was placed between the insulation layer and gypsum board, while on the roof, it was positioned between insulation and metal surfaces. Five layers build up the external walls with PCM: stucco (25.40 mm), gypsum board (15.90 mm), insulation (50.80 mm), PCM, and gypsum board (15.90 mm). Four layers were used to build up the roof composition: built-up roofing (9.50 mm), insulation (58 mm), and metal surface (0.80 mm). The thicknesses of layers were selected according to building model prototypes [154]. Each building element's layers are listed in the table from the exterior to the interior (Figure 3.10). These layers are specified by thickness, density, specific heat, conductivity, and thermal resistance (Table 3.4).

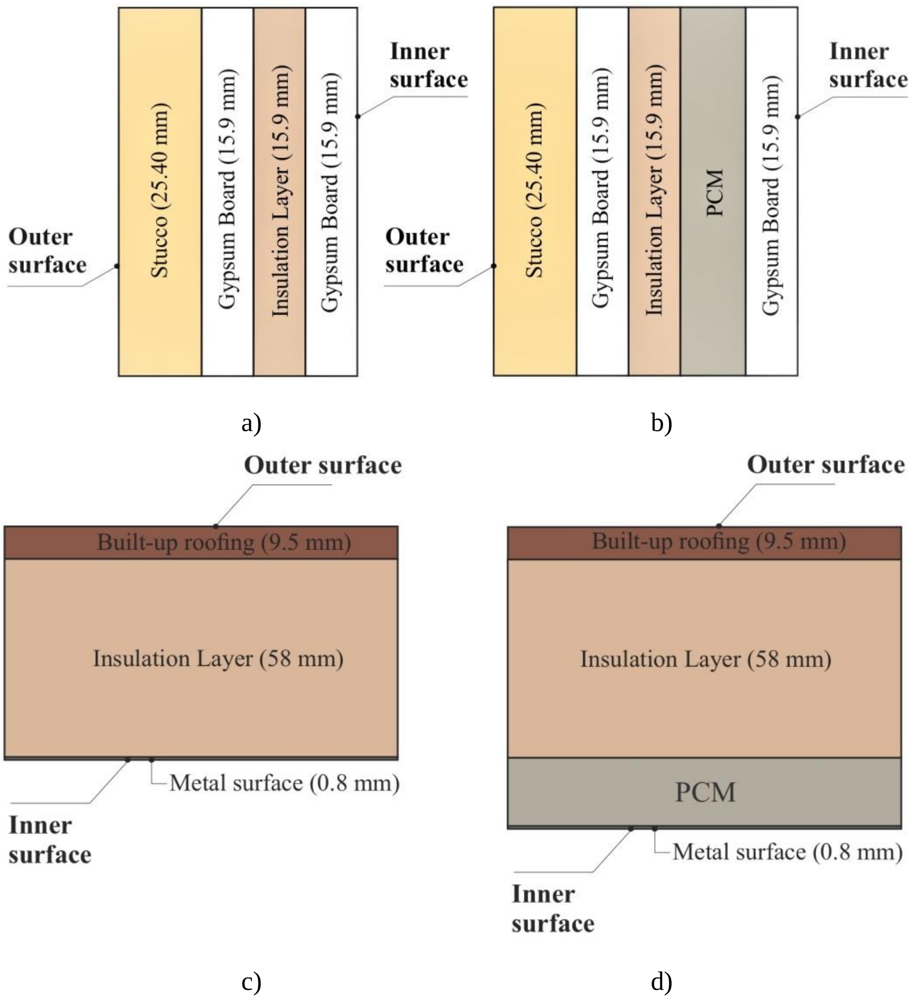

Figure 3.10: Wall composition of a) base case; b) PCM-integrated building (mm); Roof composition of c) base case; d) PCM-integrated building (mm).

Table 3.4: Thermal properties of building elements.

Element	Thickness (m)	Density (kg/m^3)	Specific heat (J/kg K)	Conductivity (W/m K)
Exterior wall				
Stucco	0.0254	1856	840	0.72
Gypsum board	0.0159	800	1090	0.16
Insulation	0.058	24	1037	0.036
PCM	0.0200	860	1970	0.20
Gypsum board	0.0159	800	1090	0.16
Roof				
Built-up roofing	0.0095	1120	1460	0.16
Insulation	0.058	24	1037	0.036
PCM	0.0200	860	1970	0.20
Metal surface	0.0008	7824	500	45.28

3.5. Thermal comfort model

The health and efficiency of building occupants are significantly impacted by thermal comfort. To measure the thermal comfort of inhabitants in commercial and residential buildings, Fanger developed the projected mean vote (PMV) model in the late 1960s. Fanger’s thermal comfort model is an indicator based on two personal (clothing insulation and metabolic rate) and four environmental parameters (humidity, air speed, mean radiant temperature, and air temperature) (Figure 3.11) [155]. The PMV value can also be used to calculate thermal acceptability or the predicted percentage of dissatisfaction (PPD). By estimating the proportion of persons expected to feel too warm or cold in a specific setting, the predicted percentage dissatisfied (PPD) index gives information on people's thermal discomfort or thermal dissatisfaction. According to ASHRAE 55 recommendations, thermally appropriate interior settings must satisfy at least 80% of space occupants. Additionally, it is advised that the appropriate PPD for thermal comfort should be lower than 10% and that the PMV should be between - 0.5 and +0.5 [156]. A 7-point scale of thermal sensations is used to illustrate the PMV model (Figure 3.12). It ranges from - 3 (too cold) to +3 (too warm). A PMV value of zero is anticipated to give the lowest percentage of dissatisfied persons (PPD) within a community [157].

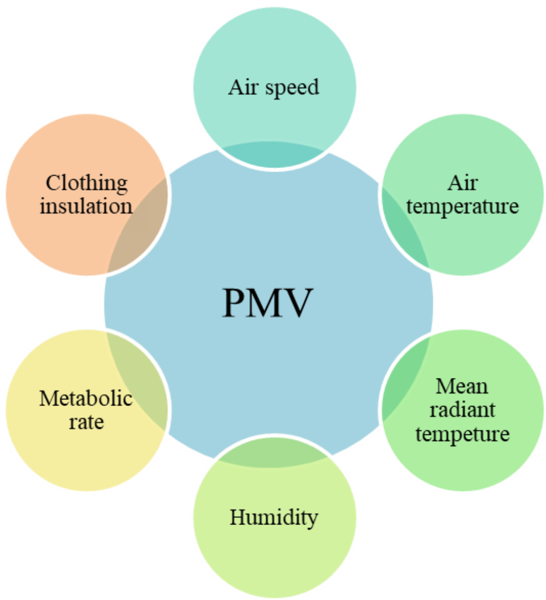

Figure 3.11: Thermal comfort parameters of Fanger PMV model.

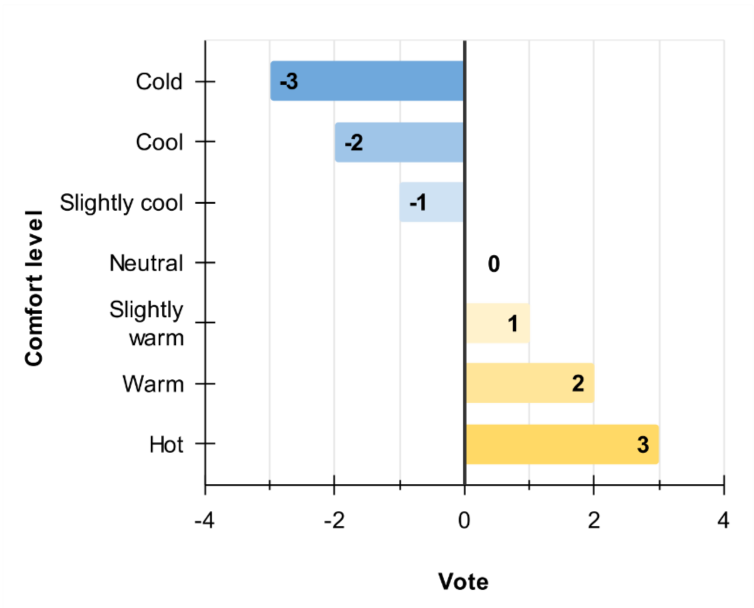

Figure 3.12: Thermal sensation scale.

The PMV and PPD [158] can be evaluated as follows:

$$\text{PMV} = [0.303 \exp(-0.036M) + 0.028] * \{(M - W) - 3.05 * 10^{-3} * [5733 - 6.99\,(M - W) - P_a] - 0.42 * [(M - W) - 58.15] - 1.7 * 10^{-5}\,M\,(5867 - P_a) - 0.0014M(34 - t_a) - 3.96 * 10^{-8} f_{cl} * [(t_{cl} + 273)^4 - (t_r + 273)^4] - f_{cl} h_c\,(t_{cl} - t_a)\} \tag{3.7}$$

$$f_{cl} = \begin{cases} 1.00 + 1.290 * I_{cl} \ for \ I_{cl} \ \leq 0.078 \ m^2.K/W \\ 1.05 + 0.645 * I_{cl} \ for \ I_{cl} \ \leq 0.078 \ m^2.K/W \end{cases} \tag{3.8}$$

$$t_{cl} = 35.7 - 0.028\,(M - W) - I_{cl}\ \{3.96 * 10^{-8} f_{cl} * [(t_{cl}+273)^4 - (t_r+273)^4\,] + f_{cl} h_c\,(t_{cl} - t_a)\} \tag{3.9}$$

$$h_c = \begin{cases} 2.38(t_{cl} - t_a)^{0.25} for\ 2.38 * \left|t_{cl} - t_a\right|^{0.25} > 12.1\sqrt{V_{ar}} \\ \quad 12.1\sqrt{V_{ar}}\, for\ 2.38(t_{cl} - t_a)^{0.25} < 12.1\sqrt{V_{ar}} \end{cases} \tag{3.10}$$

$$P_a = P_{sv} * (\frac{RH}{100}) \tag{3.11}$$

$$P_{sv} = \exp(72.55 - \frac{7206.7}{T_a+273.15} - 7.1385 * \ln{(t_a + 273.15)} + 0.000004046 * (T_a+273.15)^2) \tag{3.12}$$

$$\text{PPD} = 100–95 * \exp\left[-(0.03353 * PMV^4 + 0.2179 * PMV^{2)}\right] \tag{3.13}$$

Where:

t_r – mean radiant temperature (^oC);

t_a – air temperature (^oC);

P_a – water vapor partial pressure (Pa);

W – effective mechanical power (W/m^2);

M - the metabolic rate (W/m^2);

f_{cl} – clothing insulation surface area factor;

t_{cl} – clothing surface temperature (^oC);

I_{cl} - clothing insulation ($m^2 \ K/W$);

h_c – convective heat transfer coefficient [W/(m^2K)];

V_{ar} – relative air velocity (m/s).

The recommended PMV and PPD categories are presented in Table 3.5. Instead of using a preset thermostat temperature to regulate the interior thermal environment, the PMV values were chosen following the thermal comfort criteria for heating and cooling periods (Cat.I, Cat.II, Cat.III, and Cat.IV) to manage the HVAC operation using the Fanger model (Table 3.5). The thresholds for new buildings are between -0.5 and +0.5, while those for existing buildings are between -0.7 and +0.7. The -0.2 and +0.2 thresholds are for spaces occupied by very sensitive people, while PMV < -0.7 and PMV < +0.7 are for buildings that do not meet the criteria for the aforementioned categories [60]. For this research, the thresholds for new buildings between -0.5 and +0.5 were selected.

Table 3.5: Thermal requirement of the four categories of indoor environment.

Categories	I	II	III	IV
PMV	-0.2<PMV<+0.2	-0.5<PMV<+0.5	-0.7<PMV<+0.7	PMV < -0.7; or +0.7< PMV
PPD (%)	<6	<10	<15	>15

3.6. Building energy simulation

The conduction finite difference solution algorithm solution technique (CondFD) uses the finite difference method to calculate the heat transfer equations numerically while discretizing the building envelope layers into several nodes [159]. The user can select between the Crank-Nicolson or totally implicit approach for numerical simulation. This research used an enthalpy-temperature function with a completely implicit finite difference method to account for phase transition energy. Initially, it was developed by Pederson and modified by Tabares-Velasco et al. [160]. The fully implicit scheme is calculated using the following formula:

$$C_p \Delta x \frac{T_i^{j+1} - T_i^j}{\Delta t} = k_{int} \frac{T_{i+1}^{j+1} - T_i^{j+1}}{\Delta x} + k_{ext} \frac{T_{i-1}^{j+1} - T_i^{j+1}}{\Delta x} \tag{3.14}$$

Where,

$$k_w = \frac{(k_{i+1}^{j+1} + k_i^{j+1})}{2} \tag{3.15}$$

$$k_E = \frac{(k_{i-1}^{j+1} + k_i^{j+1})}{2} \tag{3.16}$$

$$k_i = k(T_i^{j+1}) \tag{3.17}$$

Where:

T is the node temperature;

k is the thermal conductivity:

k_{int} is the internal nodes thermal conductivity;

k_{ext} is the external nodes thermal conductivity;

k_E is thermal conductivity for the interface between nodes *i* and *i-1;*

k_w is thermal conductivity for the interface between nodes *i* and *i+1;*

Δt is the computation time step;

Δx is the finite-difference layer thickness;

ρ is the density of a material;

$C_p$is the specific heat of material;

i is a node being modeled;

j is simulation time step;

j+1 previous simulation time step;

i+1 is adjacent node to exterior construction;

i-1 is adjacent node to interior construction.

In the CondFD technique, all components are automatically separated into discrete parts using the following equation, which depends on the time step, the material's thermal diffusivity (α), and a spatial discretization constant (c). The spatial discretization value of 3 (corresponding to a Fourier number (Fo) of 1/3) can be kept as the default or changed to additional values.

$$\Delta x = \sqrt{c * \alpha * \Delta t} = \sqrt{\frac{\alpha * \Delta t}{Fo}} \tag{3.18}$$

In order to account for enthalpy variations that occur during phase transition for the PCM technique, the user enters an enthalpy-temperature function in conjunction with the CondFD approach. At each time step, an equivalent specific heat is calculated using the enthalpy-temperature function [160].

$$h = h(T) \tag{3.19}$$

where,

h is enthalpy.

$$C_p^*(T) = \frac{h_i^j - h_i^{j-1}}{T_i^j - T_i^{j-1}} \tag{3.20}$$

In this research, PCM has a latent heat of 219 kJ/kg [161]. The PCM's enthalpy-temperature graph in Figure 3.13 accounted for phase transition. By repositioning the curve in accordance with the PCM melting ranges, the enthalpy-temperature graphs for every other PCM were created. Due to the built-in constraints of EnergyPlus, input values were limited to a maximum of 16 points. These points were chosen to ensure the least deviation from the analytical curve. According to Tabares-Velasco et al., the time step should be set to three minutes (20 time-steps per hour) for accurate modeling with a discretization factor of three [160].

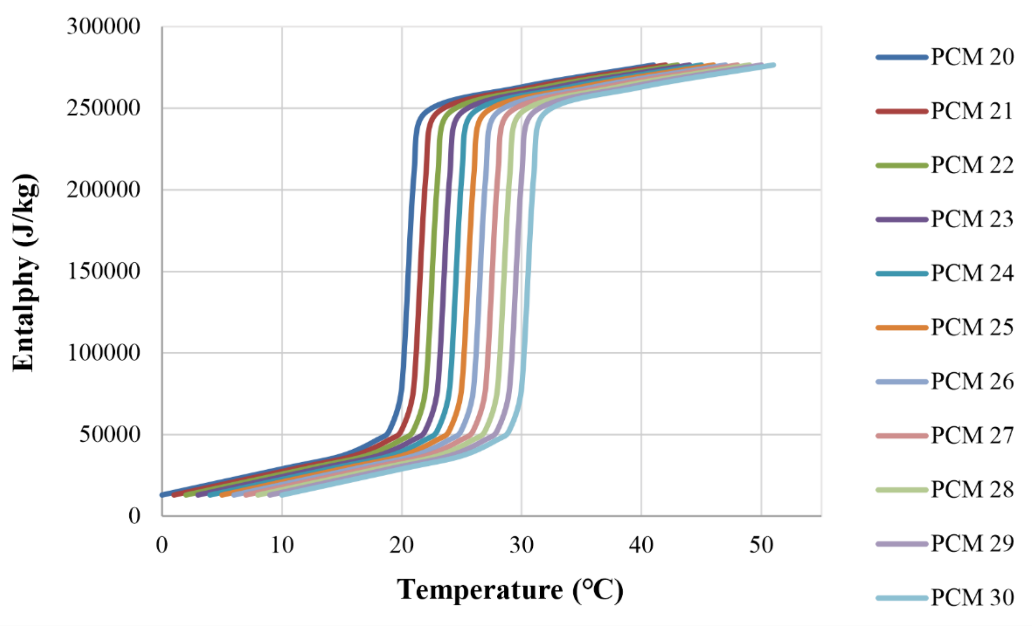

Figure 3.13: Enthalpy–temperature graph of PCM.

3.7. Software

This section discusses the tools utilized in this research. DesignBuilder v 6.1 was employed to perform the building modeling and simulations. It is one of the most reliable graphical user interfaces in EnergyPlus. The program can simulate modern building materials with various thermophysical characteristics, including PCM [162]. It determines most of the building's physical envelope components, including the structure and materials, loads, weather conditions, equipment, occupancy, schedules, set-point temperatures, and modeling of HVAC systems. For the building energy simulations, EnergyPlus 9.2 software was utilized. EnergyPlus is a widely used and recognized software in the building energy community. This software combines the greatest features and capabilities from DOE-2 and BLAST, along with additional features. Besides water flow in buildings, EnergyPlus models cooling, heating, ventilation, lighting, and other energy flows [163]. The heat balance model used in EnergyPlus's building thermal zone calculation method is based on the following presumptions: heat conduction across surfaces is one-dimensional, surface irradiation is diffuse, each surface's temperature is constant, and the air in the thermal zone is uniformly heated [14]. EnergyPlus was widely used in different studies to estimate the energy consumption of PCM-integrated buildings. For instance, Hagenau & Jradi [61] utilized EnergyPlus software to find the best PCM for a typical office in Denmark among seventeen PCMs. Wang et al. [164] assessed the performance of PCM in air-conditioned lightweight buildings located in Shanghai using EnergyPlus. Al-Janabi & Kavgic [22] used the hysteresis approach in EnergyPlus to examine the viability of incorporating PCMs into the suspended ceiling. It can be noted that the most often employed energy modeling software in the literature is DesignBuilder and EnergyPlus [165]. Despite having a wide range of capabilities, EnergyPlus cannot carry out any optimization tasks. As a result, additional software is required for this process. jEPlus+EA was employed as an optimization program in this research. This software, driven by the Java programming language, was initially published in 2009 by Yi Zhang at De Montfort University's Institute of Energy and Sustainable Development [166]. Several studies applied jEPlus+EA to perform the optimization [142,167].

The sensitivity analysis is carried out using the statistical analysis program R. New advancements created by prominent statisticians worldwide are available in R, an open-source and free software environment [168]. By utilizing R and distributing R code in building performance analysis, R advances the goal of reproducible research [66]. The package "sensitivity" was adopted in this research (Appendix A). Numerous sensitivity analysis techniques are included in this package [21]. It has been used extensively in building performance simulation (BPS) [70]. For instance, Bre et al. [26] employed the sensitivity package of R software to evaluate the impact of design parameters on the energy and thermal efficiency of residential buildings in the Argentine Littoral region. The Morris method was used to rank the design parameters.

3.8. Validation

Many scholars have studied the capability of EnergyPlus to model PCMs; therefore, extensive validation and verification experiments have been carried out [169]. For instance, a 3% variation in zone temperature was noted for both PCM and no PCM buildings when the findings of the EnergyPlus program were compared to the experimental data collected by Kuznik and Virgone [170].

In this research, to confirm the preciseness of the EnergyPlus model, the PCM model was verified by comparative analysis of simulation data with the experimental results of Cui et al. [171] and the recurrence of analytical and numerical solutions to Stefan's problems conducted by Tabares Velasco et al. [160]. To verify the DesignBuilder model, simulation and experimental results were compared. Figure 3.14 demonstrates the simulation room model and the experimental model. A concrete test room with measurements of 500 mm x 500 mm x 500 mm and 20 mm thickness was constructed in DesignBuilder software. In the research of Cui et al. [171] the effect of macro-encapsulated PCM with a melting temperature of 23 °C on the room air temperature of the concrete cubicle for the climate of Shenzhen was investigated by placing the sensor at the center of the room. Temperature measurements were taken with temperature sensors with a precision of 0.3 °C. The values of room air temperature acquired from numerical models and experimentation are shown in Figure 3.15. The results indicate that the difference between the simulation's and experiment's results was less than 4.5%. In the research of Souayfane et al. [172] a 3.63% difference between simulation and experimental data was attained.

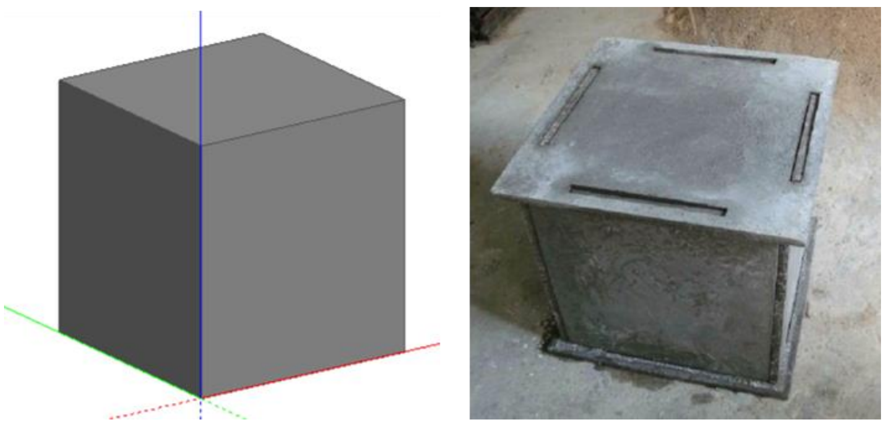

Figure 3.14: Numerical vs. experimental model.

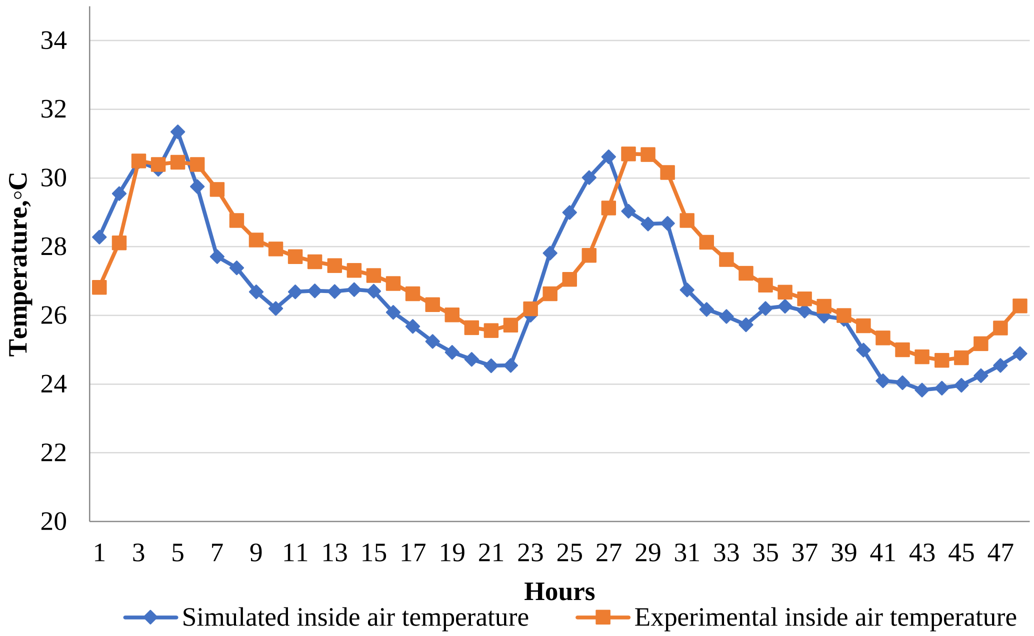

Figure 3.15: Experimental and simulated values.

The analytical and numerical solutions to Stefan's problem are shown in Figure 3.16. According to the results, the two solutions are in good agreement, showing that PCM implementation is accurate. The numerical model correctly predicted the heat flow with a Root Mean Squared Error (RMSE) of 18.1 W/m2.

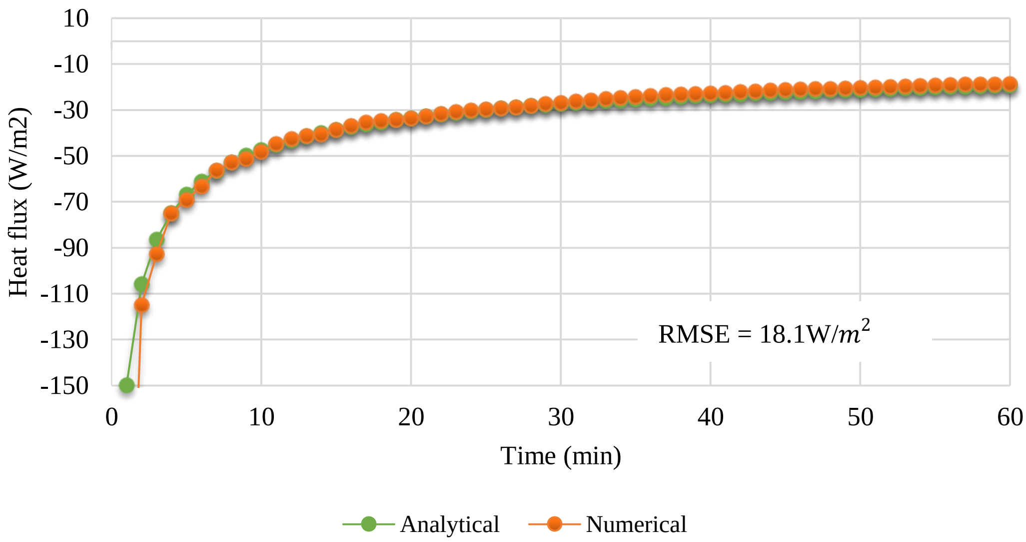

Figure 3.16: Analytical vs. numerical solution to Stefan's problem.

3.9. Multi-stage sensitivity analysis

An MSA was proposed to determine the significant EDSP and their interaction. It employs two-stage sensitivity analysis methods: global and local (Figure 3.17). In the first stage, eleven EDSP are subjected to sensitivity analysis using global sensitivity analysis methods to evaluate their impact on energy consumption. Three global sensitivity analysis methods, namely SRRC, PRCC, and the Morris method, are proposed to find the most significant EDSP and their relationship. Global sensitivity analysis techniques are focused on simultaneous alterations to all design parameters and evaluate the magnitudes of the effects of EDSP on energy consumption. The local sensitivity analysis is then conducted to determine each parameter's effect independently and analyze the trajectory of the most sensitive parameters. Key EDSP are identified using Latin HyberCybe Sampling and Morris factorial sampling. The MSA and optimization approach are detailed in the subsequent section.

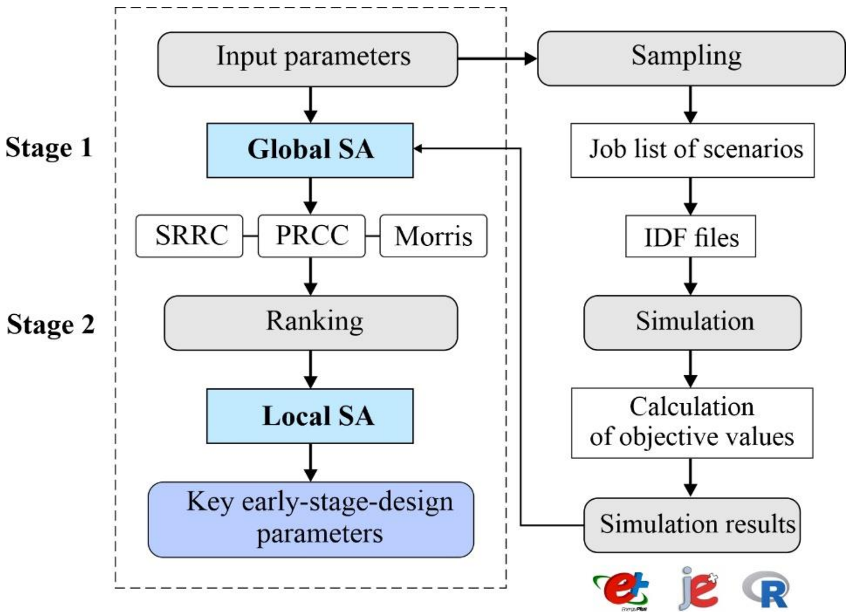

Figure 3.17: Workflow of MSA.

3.9.1. **Rank transformation**

The analysis based on a linear regression model is expected to perform inadequately when the connections between the input parameters and outputs are nonlinear. However, by employing rank transformation, the poor performance of the regression model can be improved without acquiring additional processing costs [173]. In contrast to other sensitivity analysis techniques, rank regression is simple to comprehend and quick to compute [34]. The rank transformations of the Standardized Regression Coefficient (SRC) and Partial Correlation Coefficients (PCC) were employed in this research. SRC computes regression equations utilizing normalized data. PCC is the correlation coefficient between two parameters after controlling for the influence of other parameters [174]. Standardized rank regression coefficient (SRRC) and Partial rank correlation coefficient (PRCC) are rank transformations of SRC and PCC, respectively, that can be used in nonlinear monotonic functions.

3.9.2. **First-stage sensitivity analysis**

3.9.2.1. Standardized rank regression coefficient

The Standardized Rank Regression Coefficient (SRRC) is a widely used method in the building performance simulation field to assess models that exhibit non-linear relationships between inputs and outputs [121]. The use of SRRCs is common in the building performance simulation community [15,140,175]. It helps determine the sensitivity of each EDSP by performing a regression analysis on rank-transformed data. The original parameter values are replaced with their corresponding ranks [151]. A regression model can then be used to investigate the relationship between the model output and input parameters. The following is a regression model for investigating the relationship between model output on input parameters:

$$\frac{(y_i - y_m)}{S_y} = b_1^{(s)} \frac{(y_i - y_m)}{S_{x1}} + b_k^{(s)} \frac{(x_k - x_{i,m})}{S_{xk}} = \sum_{i=1}^{k} SRC(y, x_i) \frac{(x_k - x_{i,m})}{S_{x1}} \tag{3.21}$$

where $x_{i,m}$, y_m represents the average value of model output: Y=(y_1,..., y_N); X_i = (x_{1i},..., x_{Ni}) represents input parameter; S_y , S_{xi} indicates the standard deviations of model output (Y) and input parameter (X_i); $b_1^{(s)}$, …$b_k^{(s)}$ indicate the standardized regression; N represents the number of model runs.

3.9.2.2. Partial rank correlation coefficient

By calculating the Partial rank correlation coefficient (PRCC), it is possible to identify the statistical correlations between each input parameter and the output parameters while maintaining the other input parameters at their predetermined values [176]. Regardless of whether the parameters are correlated, this technique identifies each parameter's independent impacts. Thus, only output parameters that are monotonically correlated to the input parameters should be included in this analysis. A PRCC reflects the degree of monotonicity between a given input parameter and an outcome [177]. Examining scatterplots where each input variable is shown as a function of the parameter allows one to determine the monotonicity of a model.

In particular, PRCC is determined by applying the formulas for PCC, but replacing X and Y with the rank values of those parameters. The following is the calculation for each input and output parameter for PRCC. For a single outcome parameter, the procedure would be described. The outcome vector is first considered in addition to the input values as a second column in column K+1. Where i=run number, the set (r_{1i}, r_{2i}, ..., r_{ki}, R_i) denotes the ordinal number designating the rank (1 to N) of each of these columns. $\mu=\frac{(1+N)}{2}$ is the average rank. Elements c_{ij} were used to determine the symmetric matrix (C) of K+1 by K+1.

$$c_{ij} = \frac{\sum_{t=1}^{N}(r_{it}-\mu)(r_{jt}-\mu)}{\sqrt{\sum_{t=1}^{N}(r_{it}-\mu)^2\sum_{s=1}^{N}(r_{js}-\mu)^2}} \; i,j = 1,2 \ldots, K. \tag{3.22}$$

R_i substitutes r_{jt} and r_{js} in the $c_{i,k+1}$ elements. All of C's leading diagonal components are one. The inverse of C is defined as matrix B.

$$B=[b_{ij}]=C^{-1} \tag{3.23}$$

Between the ith input parameter and the yth output parameter, the PRCC (γ_{iy}) is specified as:

$$\gamma_{iy} = \frac{-\,b_{i,K+1}}{\sqrt{b_{ii}b_{\,K+1,K+1}}}. \tag{3.24}$$

3.9.2.3. Morris method

The Morris technique leverages the Elementary effects (EE) concept to represent a model's sensitivity to its input parameters [17]. The approach entails discretizing the input space for each parameter and then completing a certain number of OAT designs. In the input space, these experimental designs are picked at random, and the direction of the change is similarly determined at random. It is possible to evaluate the elementary effects of each input by repeating these processes. Sensitivity indices are generated from these effects [178]. The Morris method aims to create a computationally cheap experiment with a modest number of model assessments [179]. This method divides inputs into three categories: those with minor impact, those with substantial linear effects but no interactions, and those with strong non-linear and/or interaction effects [178]. For further information on the Morris approach, see [75]. Based on the currently available information, the Morris method is considered the most promising for sensitivity analysis in sustainable building design [18]. The advantages of using the Morris method are listed below:

1. The approach can deal with a huge number of parameters;
2. It is cost-effective since there aren't many simulations relative to the number of parameters;
3. It doesn't rely on presumptions about linearity or correlations between parameters and model outputs;
4. Within the constraints, parameters are adjusted globally;
5. The graphic representation of the results makes them simple to understand;
6. This method determines if parameter fluctuation is mutually correlated or non-linear.

The parameters for the model are X_1, X_2, ... X_k = X, where *k* is the size of the input space, and each can take X_i values from the range {0, 1/(*p*-1), 2/(*p*-1)…,1}. The experimental region **Ω** is a *k*-dimensional *p*-level grid, with a sample point designated by x =(x_1, x_2, ... x_k). Scaling the normalized values with a parameter's maximum and lowest limits yields the actual parameter values for model assessment. *N* is the total number of model evaluations, and the model output of one evaluation is given by *y (x)*, where *x* is a sample point. Finally, each input is linked to r elementary effects (EE), representing the output change observed at *r* distinct points in the design space. Consequently, the basic consequence of the *i*th input factor at position X may be written as [67]:

$$EE_i = \frac{y(x+e_i\Delta_i)-y(x)}{\Delta_i} \tag{3.25}$$

where, e_i is a vector of zeros, except for the *i*-th component, which equals ±1 and signifies an incremental change in parameter *i* [17].

The model's sensitivity to each design parameter is calculated using the EE's mean value and standard deviation. The average impact of the input parameter examined on the model output is measured by the mean μ*. The standard deviation δ evaluates the impact of variables resulting from their interaction with other parameters [180].

$$\mu_i = \frac{1}{r}\sum_{t=1}^{r} EE_{it} \tag{3.26}$$

$$\delta_i = \sqrt{\frac{1}{(r-1)}\ d\ \sum_{t=1}^{r}(EE_{it} - \mu_i)^2} \tag{3.27}$$

$$\mu_i^* = \frac{1}{r}\sum_{t=1}^{r}|EE_{it}| \tag{3.28}$$

According to Morris, there are three categories of parameters:

1) Noninfluential parameters, i.e., those having relatively low values of both μ_i (or μ_i^*) and δ_i. The low values suggest that the parameter has little overall impact on model output.
2) Parameters having linear and/or additive effects, i.e., parameters with a relatively high μ_i (or μ_i^*) and a relatively small δ_i. The low value of δ_i and the high value of μ_i (or μ_i^*) suggest that the variety of elementary effects is minimal. However, the size of the effect itself is constantly significant for the variations in the parameter space.
3) Nonlinear and/or interaction effects, i.e., parameters with a relatively small value of μ_i (or μ_i^*) and a relatively high value of δ_i. In contrast to the preceding scenario, a small value of μ_i (or μ_i^*) implies that the aggregate impact of perturbations is small, but a high value of δ_i shows that the variation of the effect is considerable; the effect can be substantial or negligibly small depending on the other parameters at which the model is assessed. Such wide variance indicates nonlinear effects and/or parameter interaction.

This categorization enables parameter significance ranking and, as a result, the screening of non-influential parameters. This is exemplified in Figure 3.18, which shows a typical parameter categorization generated from a visual examination of the elementary effect statistics on the δ_i vs μ_i plane. Nevertheless, the technique is employed relatively qualitatively. The relative positions of the statistics in the plane are used to define influential and non-influential parameters. Non-influential ones are often concentrated closer to the origin (compared to more influential ones) with a prominent border. To be sure, if these statistics are distributed equally throughout the plane, the difference becomes more confusing (in this case, a more advanced classification might be essential) [181].

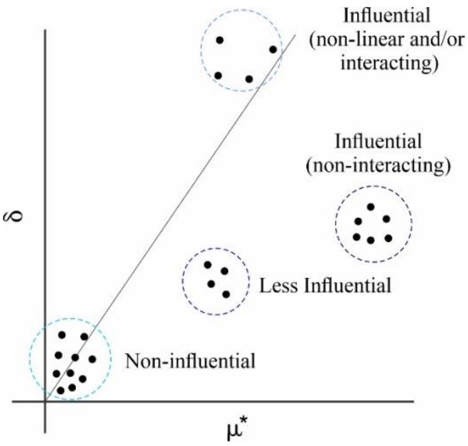

Figure 3.18: Parameter importance in Morris method. Adapted from [181].

To analyze the sensitivity using the Morris approach, the following processes must be fulfilled [68]:

1. Clearly define the input parameters and their range of values;
2. Determine each input parameter's degree of variation, p, using a discrete distribution. Ensure that all input parameters have the same degree of variation, *k*;
3. Generate a Morris sample consisting of $n=r(k+1)$ observations, where r is the number of trajectories and *k* is the number of input parameters;
4. Develop n simulation models, execute them, and collect output parameters;
5. Arrange the data based on the input and output;
6. Calculate the mean and standard deviation of elementary effects (μ, μ*, and δ) for each input parameter and output;
7. Create scatterplots of {μ* x δ} to classify input parameters as linear, monotonic, non-monotonic, or non-linear.

3.9.2.4. **Ranking of early design stage parameters**

The SRRC, PRCC, and Morris methods are ranked to identify the most important parameters derived from the first stage of sensitivity analysis. SRRC and PRCC are the rank transformation methods of SRC and PCC, where inputs and outputs are sorted in ascending order, and their values are replaced with their rankings. At the same time, the Morris method presents the ranking of parameters obtained by μ*. The average value of the global sensitivity analysis rankings is utilized to select the significant EDSP for the next stage.

3.9.3. **Second stage sensitivity analysis**

3.9.3.1. **Local sensitivity analysis**

The local sensitivity analysis, also known as the one-parameter-at-a-time (OAT) method, examines the impact on the model output by modifying a single input element at a time. A baseline scenario should be chosen for comparison, and a sensitivity coefficient should be used to interpret the output. This method is relatively straightforward and requires fewer simulation runs than global sensitivity analysis [15]. To determine the local sensitivity index (LSI), the output difference for the extreme values of the design parameter can be calculated using a simple method [182]:

- Determine input parameters and their ranges of variation;
- In a discrete distribution, set variation level *m* for each input parameter;
- Generate $p = m$ x n observations using a one-parameter-at-a-time (OAT) approach, where *n* is the number of input parameters;
- Run *n* simulations to obtain output parameters;
- Create a visual representation of the output distribution.

A simple method to determine how sensitive a design parameter is to calculate the output difference for the design parameter's extreme values. These steps may be used to calculate the local sensitivity index:

$$S_{local,i} = \frac{Y_{max,i} - Y_{min,i}}{Y_{max,*}} \tag{3.29}$$

where:

$S_{local,i}$ is the local sensitivity index;

$Y_{min,i}$ is the minimum value of the output in the *i*-th input parameter;

$Y_{max,i}$ is the maximum value of the output in the i-th input parameter;

$Y_{max,*}$ which is the maximum global output among all the inputs of all the parameters.

3.10. Simulation-based optimization

A rigorous framework for investigating alternative, effective designs is provided by building optimization techniques. These strategies attempt to discover the most energy-efficient design by intelligently evaluating different options. Simulation-based building optimization (combining an optimization algorithm with building simulation software) is a popular and successful strategy that can systematically handle the multiple trade-offs involved in design [183]. In this technique, building simulation software is used to evaluate the objective function, and an optimization algorithm adjusts the optimization parameters to improve the value of the objective function in an iterative process. Optimization aims to find a feasible set of decision variables that maximizes or minimizes the values of the objective function.

maximize f(x)
subject to

$$g_i(x) \leq 0, i = 1, 2 \dots, m \tag{3.30}$$

$$x_{jl} \leq x_j \leq x_{ju} j = 1,2 \dots, n$$

where, *f* represents the objective function, x_{jl} and x_{ju} represent the lower and upper limits of the decision variables, x_j is the jth value in this vector, x is the vector of decision variables, and g_i represents the *ith* constraint function of vector *x*.

3.10.1. **Problem formulation**

The three fundamental components of every optimization model are the objective function, decision parameters, and constraints.

- ***Objective function*** - the output parameters that should be minimized or maximized;
- ***Decision parameters*** - values that may be changed to maximize or minimize the objective functions;

- ***Constraints*** that can often be used to prevent unpleasant or impractical system responses limit the values that decision variables can take, or both [184].

According to Prowler [185], it is critical to identify the project objectives early in the design process and keep them balanced through the conceptual and detailed design phases to obtain a successful design solution. The objective function of the optimization process is an indicator of the performance of the buildings when optimization methodologies are employed to explore the design space. The nature of the problem governs the selection of an objective function. The literature on building design exploration frequently discusses energy usage, thermal comfort, and cost among the building performance indicators [84–86]. Thus, in this thesis, the performance of potential solutions is evaluated in terms of energy consumption.

$$\text{TEC} = EC_{heating} + EC_{cooling} \tag{3.31}$$

Where,

$EC_{cooling}$: the annual energy consumption for space cooling (kWh/year);

$EC_{heating}$: the annual energy consumption for space heating (kWh/year).

The total energy consumption indicates the sum of the heating and cooling consumption of the building and is calculated in KWh/year. Hence, the optimization aims to minimize the space heating and cooling demand.

After determining the objective function, the constraints and decision parameters should be defined. Decision parameters for optimization are the key EDSP that MSA indicates. They might have discrete (integer) or continuous (real) values depending on the purpose. Continuous data consists of complex numbers and fluctuating data values taken over a certain time interval. Discrete data is a sort of numerical data that consists of whole, tangible numbers with particular and definite data values that are determined by counting. For optimization, the continuous parameters were selected.

3.10.2. **Evolutionary Algorithms**

The efficiency of simulation-based optimization greatly depends on the optimization method, several of which have been used in recent years to design/retrofit structures [86]. Even though several studies on building optimization problems (BOPs) exist, selecting an effective optimization technique is critical for achieving an optimized solution in an appropriate computing time [186]. Evolutionary algorithms (EAs), known as genetic algorithms (GAs), are the most widely used optimizers in building performance optimization research due to their benefits throughout the optimization process. EAs have a relatively simple concept: randomly selected solutions are frequently evaluated, and the best ones are selected to create new variations until either a sufficiently good solution has been identified or the time limit has expired. Figure 3.19 presents the general EAs processes. The procedures begin with implementing an encoding scheme for numerically expressing the answers (the issue variables) so that EAs can handle them. Each variable is represented as a "gene" in a "chromosome," which encodes a solution. The initial population of solutions is often drawn randomly from the whole solution space. Each response in the population will have its "fitness" for a certain set of requirements assessed. The ranking stage cooperates with the selection approach to guarantee that the 'better' solutions are more likely to be employed in creating new versions [187].

Continuous variables are discretized into finite and indexed values using integer encoding. After that, it displays a solution by indexing the values of all the problem parameters. Integer encoding efficiently lowers the solution space of the problem from infinite to finite by splitting continuous parameters [187].

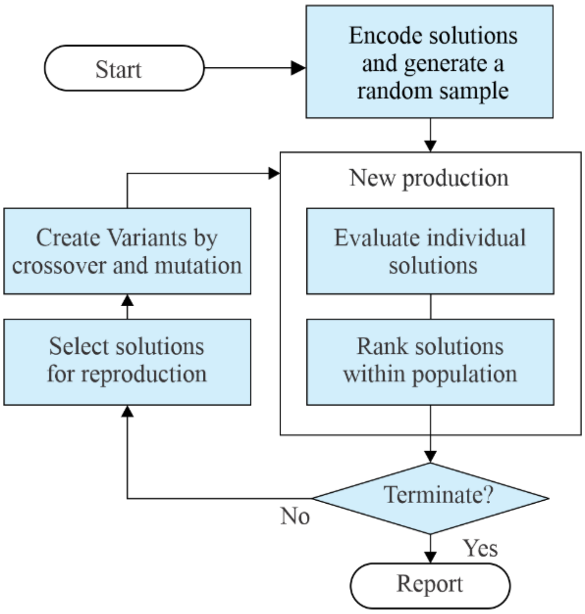

Figure 3.19: The EA process flowchart. Adapted from [187].

3.11. Economic assessment

Economic analysis is used to determine whether the optimal solutions are cost-effective. The initial investment, payback period, and operational costs are used to assess the economic benefits of the optimal solutions.

The cost of electricity cost [188] and the cost of materials are reported in Table 3.6, respectively. The cost of the materials was assumed to be constant, even though prices vary depending on location. The cost of material installation was embedded in the cost of the material. The initial investment cost was computed simply by considering the building envelope-related material and installation expenses. The cost of PCM was selected as the constant in the whole zone. Since it was anticipated that the value of the HVAC system installation costs and other expenditures would be the same for all candidate solutions in the same area, these costs were not considered. The annual energy consumption cost was included in the analysis. The main initial investment expenditures and yearly HVAC operating costs are as follows:

$$C_i = C_w + C_r + C_{win} \tag{3.32}$$

$$C_o = C_h + C_c \tag{3.33}$$

$$PB = \frac{(C_{io} - C_{ib})}{(C_{ob} - C_{oo})} \tag{3.34}$$

Where:

C_i – initial investment cost;

C_w – cost of the wall;

C_r – cost of the roof;

C_{win} – cost of the window;

C_o – operating cost;

C_{ob} – operating cost for the base case;

C_{oo} – operating cost for the optimal solution;

C_{ib} - initial investment for the base case;

C_{io} – initial investment for the optimal solution;

C_c - operating cost for cooling;

C_h - operating cost for heating;

PB – payback period.

Table 3.6: Electricity prices for the selected zone [189].

BSh zone	
Cities	Electricity price (kWh, $)
Ahmadabad	0.073
Lahore	0.055
Marrakesh	0.107
Port Elizabeth	0.141
Tripoli	0.004
Windhoek	0.110

Table 3.7: The initial investment cost for materials [190–193].

Layers	**Materials**	**Initial investment cost for m^2 , $**
	Stucco	163

Wall	Gypsum plasterboard	20.6
	Insulation	18.8
	Wall color	0-16.2
Roof	Built-up roofing	66.9
	Insulation	9.7
	Metal surface	1.2
	Roof color	0-16.2
Window	Window	300-404
PCM	PCM (kg)	2

3.12. Chapter summary

The current chapter presents the research methodology employed to address the thesis's aims and objectives. The methodology consists of four main stages. The first stage focused on the selection of the building model, weather data, and EDSP and objective function. The second stage focused on the MSA methods to recognize the impact of EDSP on total energy consumption. For this, three different global sensitivity and local sensitivity analyses were employed. EDSP were sampled by applying LHS and factorial sampling. A total of 26880 simulations were performed for current and future climate scenarios. Following MSA, the third stage employed single-objective optimization. Optimization was performed to generate the optimal EDSP for each climate zone. The last stage comprised post-optimization analysis and evaluation of the impact of climate change.

CHAPTER 4: MULTI-CHANGE SENSITIVITY ANALYSIS AND OPTIMIZATION UNDER CURRENT AND FUTURE CLIMATE SCENARIOS

This chapter presents the results of MSA and optimization in the current and future climate scenarios for residential buildings in six BSh zone cities. Section 4.1 summarizes the variations in weather data and the results of the energy analysis of the base case for the current and future climate scenarios. Section 4.2 presents the results of MSA and single-objective optimization for current and future scenarios. Then, an economic assessment of the current climate scenario is introduced in Section 4.2.4. Finally, Section 4.3 presents the summary of this chapter.

4.1. Impact of climate change

This part of the chapter depicts the weather data for the current and future climate scenarios. This analysis set out to examine the variation of weather data in the selected zones as well as the patterns of alterations in weather factors caused by the effect of climate change. The variation of annual energy demand from current to future scenarios was also examined. It should be noted that the "current scenario" refers to the weather files of TMY, while the "future scenario" refers to the simulations based on future climate weather files for the year 2095 (RCP 8.5).

4.1.1. **Future weather change analysis**

This subsection analyzes the typical metrological year (TMY) and downscaled future weather data for RCP 8.5 in 2095 for different locations. Table 4.1 demonstrates the annual average temperature, relative humidity, wind speed, and solar radiation for the current and future climate scenarios in the BSh zone. Table 4.1 shows that, compared to the current weather files, the average temperature increased by 5.07 ℃ in RCP 8.5. The average temperatures in Ahmadabad, Lahore, Marrakesh, Port Elizabeth, Tripoli, and Windhoek increased by 4.9℃, 6.4℃ , 5.6 ℃, 4.2 ℃ , 4.7 ℃ , and 4.4 ℃, respectively. However, a decreasing trend of solar radiation was observed in Ahmadabad and Lahore, which is thought to be caused by increased cloud cover and precipitation. An increase of between 0.1 m/s to 0.6 m/s was predicted for wind speed, except for Windhoek. The variations in relative humidity were not particularly substantial in RCP 8.5 compared to the current climate scenario. In summary, as expected, the increase in average temperature for the future scenario was observed. However, the changes of the solar radiation, wind speed, and humidity values in the future in BSh zone were negligible.

Table 4.1: Annual average values of climate parameters in six cities of the BSh zone in 2020 and 2095

Bsh zone	**Ahmadabad**		**Lahore**		**Marrakesh**		**Port Elizabeth**		**Tripoli**		**Windhoek**	
Weather	TMY	2095	TMY	2095	TMY	2095	TMY	2095	TMY	2095	TMY	2095
Dry-bulb temperature (℃)	27.3	32.3	23.7	30.2	19.9	25.5	17.7	21.9	20.5	25.2	20.1	24.6
Solar radiation (W/m^2)	229.6	18.2	147.9	31.4	222.1	229.1	150.8	195.2	224.1	204.3	261.4	286.7
Wind speed (m/s)	2.1	2.7	2.2	2.3	2.3	2.5	5.1	5.4	3.6	3.8	2.8	2.6
Humidity (%)	49.4	51.9	46.5	48.3	39.5	35.6	48.4	52.9	45.2	40.1	26.2	29.6

4.1.2. **Building energy simulation results for the current and future climate scenarios**

This section describes the total energy consumption for the base case for the current and future climatic scenarios for the BSh zone. The results of TEC of the base case in six different cities of the BSh zone are presented in Table 4.2. In the current climate scenario, the TEC ranged from 53589 to 218352 kWh, while for the future climate scenario, the TEC varied from 108916 to 238686 kWh, respectively. According to the results, the total energy consumption increased by 1.5% to 89.8% in the BSh zone.

Table 4.2: Performance of baseline model under current and future climate scenarios in the BSh zone.

Cities/TEC	**Ahmadabad**	**Lahore**	**Marrakesh**	**Port Elizabeth**	**Tripoli**	**Windhoek**
TMY (kWh)	218621	172466	93596	57370	105638	91956
2095 (kWh)	221807	234156	169165	108916	164687	140424
Difference (%)	1.5	35.8	80.7	89.8	55.9	52.7

4.2 Multi-stage sensitivity analysis results

This section presents the results of the MSA for the current and future climate scenarios, followed by a comparative analysis of the MSA for the current and future scenarios.

4.2.1. **Results of first-stage sensitivity analysis for current and future climate scenarios**

4.2.1.1. **Morris method results in the current climate scenario**

The Morris sensitivity analysis method determined the most significant EDSP related to total energy consumption. The eleven EDSP were ranked considering their impact on TEC, as indicated by μ*. Regardless of the direction of the variation, the μ* measure can reveal the qualitative impact of each parameter. It is frequently employed to rank the parameters according to their significance [75]. The greater the μ* value, the more essential the input parameter will be in subsequent energy design analysis. Figure 4.1 presents the results of μ* measure for different cities located in the BSh zone. The highest μ* values were obtained for the BO, RSA, and WSA. The parameter PTm had a lower value but can be considered as important. Apart from these parameters, Pt and WinC showed significance, but to a lesser extent. The remaining parameters demonstrated a negligible impact on the total energy consumption. Overall, BO, RSA, WSA, and PTm were the parameters that contributed the most to the sensitivity of the results of the building model for total energy consumption.

The mean of the elementary effects (μ) was used to determine the sign of indicators (positive or negative). When a parameter has a positive sign, it is directly proportional to the performance criteria, meaning that as the parameter's value rises, so does the output's value. Indirect proportionality is indicated when a parameter has a negative sign (if the parameter value increases, the output value decreases) [194]. From Table 4.3, the parameters WSA, WC, RSH, RC, and Pt (highlighted in yellow color) showed a negative relationship with the TEC. Increase of Pt can cause a delay in the transfer of heat through the envelope, resulting in a lag in the building's reaction to variations in external temperature. As a result, the HVAC system may have to work more to maintain a reasonable inside temperature, resulting in higher energy usage. In addition, WSH demonstrated a negative relationship with TEC in Port Elizabeth and Windhoek. It is pertinent to mention here that the cities showing the higher value of μ* and the lower value of μ indicate a non-monotonic impact on the output.

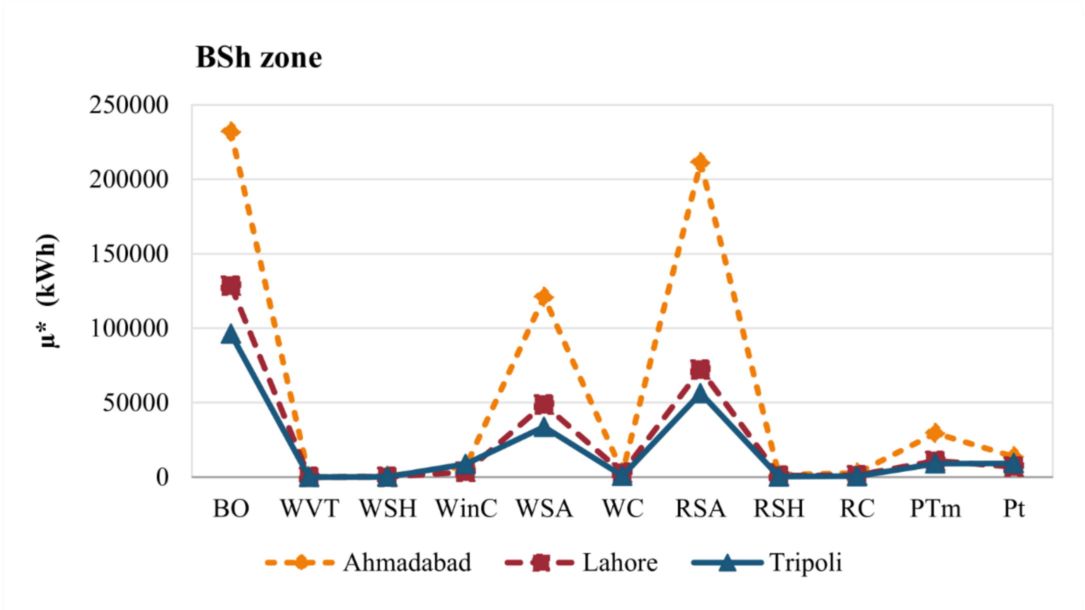

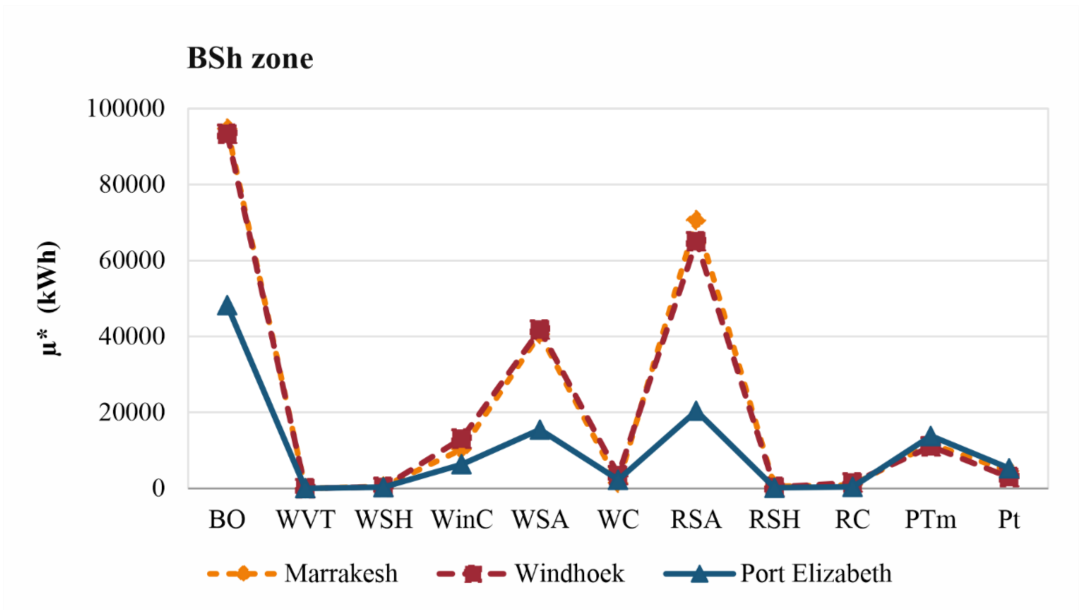

Figure 4.1: μ* indices for each input parameter relative to TEC in the BSh zone for the current climate scenario.

Table 4.3: μ signs in BSh zone for the current climate scenario.

Cities/ Parameters	Ahmadabad	Lahore	Marrakesh	Port Elizabeth	Tripoli	Windhoek

BO	71111	41122	19872	19594	30404	37029
WVT	0	0	0	0	0	0
WSH	184	104	8	-87.5	4	-234
WinC	840	306	1089	892	943	1322
WSA	-6865	-3703	-3050	-683	-2634	-2567
WC	985	-1410	-1214	-2082	-693	995
RSA	45527	18064	17608	6583	14110	14862
RSH	-58	-93	-167	1	-97	-66
RC	-1882	-394	69	-134	-145	-211
PTm	2530	44447	4227	7542	1113	-711
Pt	-5614	-1668	-851	2115	-2747	1515

Figure 4.2 presents the μ^* and δ for each EDSP derived from the Morris method in the BSh zone. In the figure, three straight lines with slopes of $\delta/\mu^* > 0.1$, 0.5, and 1 were used to represent the influence in the scatter plot graphically. According to Sanchez et al. [195], four effects may be distinguished between the standard deviation (δ) and μ^*: almost linear ($\delta/\mu^* \leq 0.1$), monotonic ($0.5 > \delta/\mu^* > 0.1$), almost monotonic ($1 > \delta/\mu^* > 0.5$), nonlinear ($\delta/\mu^* > 1$). According to Figure 4.2, almost all parameters (BO, WSA, WSH, WC, WinC, WVT, RSH, RC, PTm and Pt lie in the range of $\delta/\mu^* > 1$, indicating non-linear/correlated effects on the total energy consumption. However, RSA lies between $0.5 > \delta/\mu^* > 0.1$, indicating a monotonic relationship to the total energy consumption. Furthermore, except for Port Elizabeth, it was demonstrated that BO and WSA are the design parameters most significantly impacting each other or having a nonlinear influence on TEC. Additionally, PTm displayed substantial non-linearity in Port Elizabeth.

Several studies employed the Morris method to evaluate the effect of EDSP on objective functions in residential buildings without PCM. For instance, Bre et al. [47] applied the Morris method to residential buildings in the Argentine Littoral area to assess the effect of design parameters on thermal and energy performance. The findings indicated that the building's azimuth, window infiltration rate, and the solar absorptance of outside walls were the key parameters in reducing overall energy usage. Silva & Ghisi [68] used the Morris approach and local sensitivity analysis to determine the sensitivity of design elements in the energy and thermal performance of low-income dwellings in Brazil.

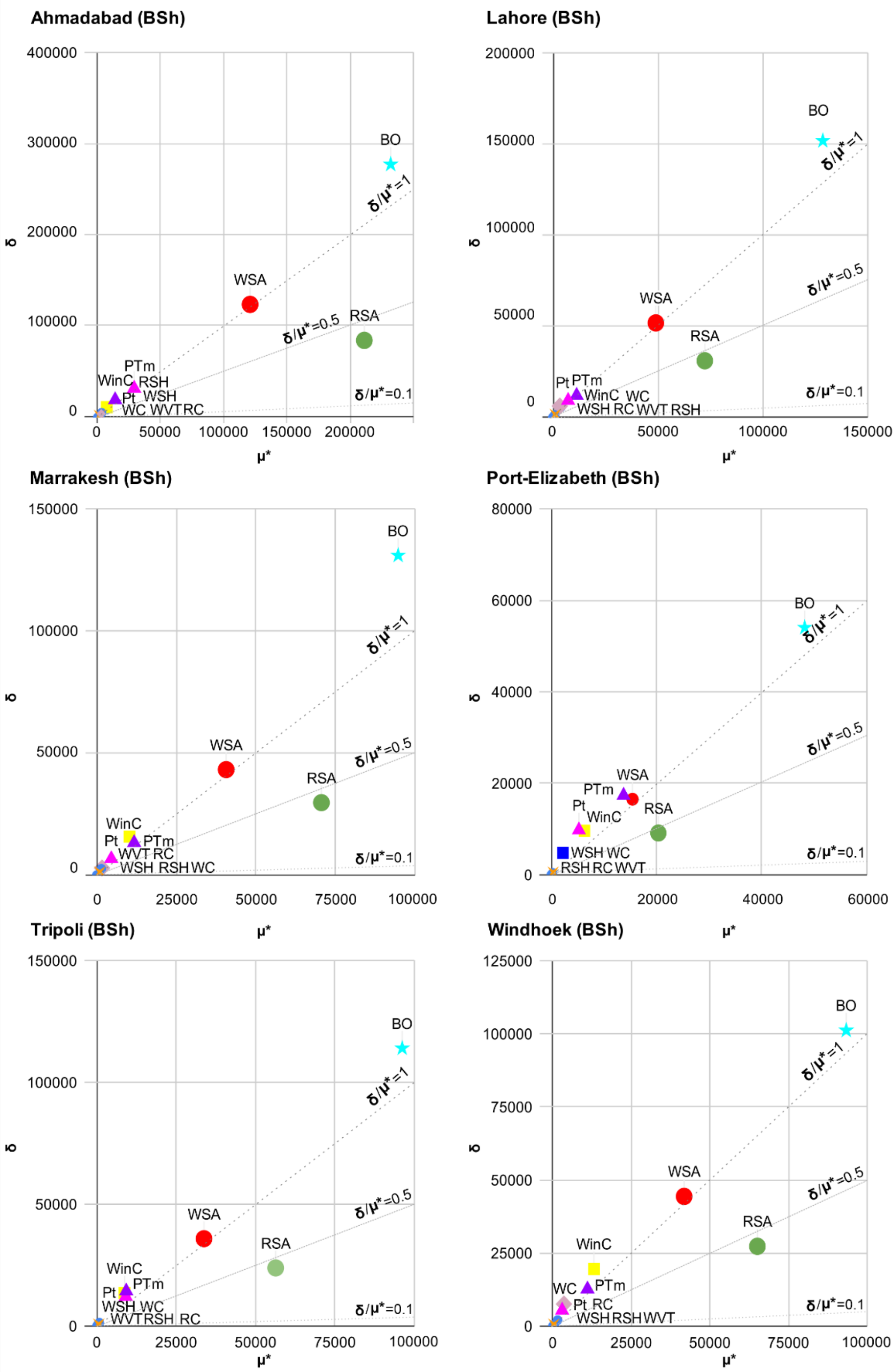

Figure 4.2: μ* and δ of the TEC in the BSh zone.

The findings showed that the most important parameters for cooling energy consumption were roof solar absorptance, roof thermal capacity, and wall solar absorptance. It was concluded that building orientation and wall and roof solar absorptance were the most crucial parameters for residential buildings.

In summary, four of the eleven parameters substantially impact TEC in the BSh zone. These parameters are BO, RSA, WSA, and PTm. Other parameters may be considered insignificant.

4.2.1.2. **Morris method results for the future climate scenario**

The Morris EE approach was used to assess the sensitivity of results to changes to the eleven parameters in the input space. According to μ*, parameters can be ranked in importance since this measure approximates total factor importance. Based on the mean sensitivity indices (μ*), the parameters in Figure 4.3 were ranked. According to μ* sensitivity index, the most significant parameters in the BSh zone were found to be BO, RSA, WSA, PTm, and RSH. Another category of parameters with quite low values comprises Pt and WC. The remaining parameters do not influence total energy consumption.

To determine the direction of indicators, the mean of the elementary effects (μ) was employed (Table 4.4). The positive sign indicates that the output value increases as the parameter value increases, whereas the negative sign (yellow color) indicates that the output value decreases as the parameter value increases. In the BSh zone, it was discovered that WSA, RSH, Pt, and WC negatively correlated with the TEC in almost all cities. Also, in some cities, RSH and RC negatively correlated with TEC. The remaining parameters showed a positive correlation with TEC.

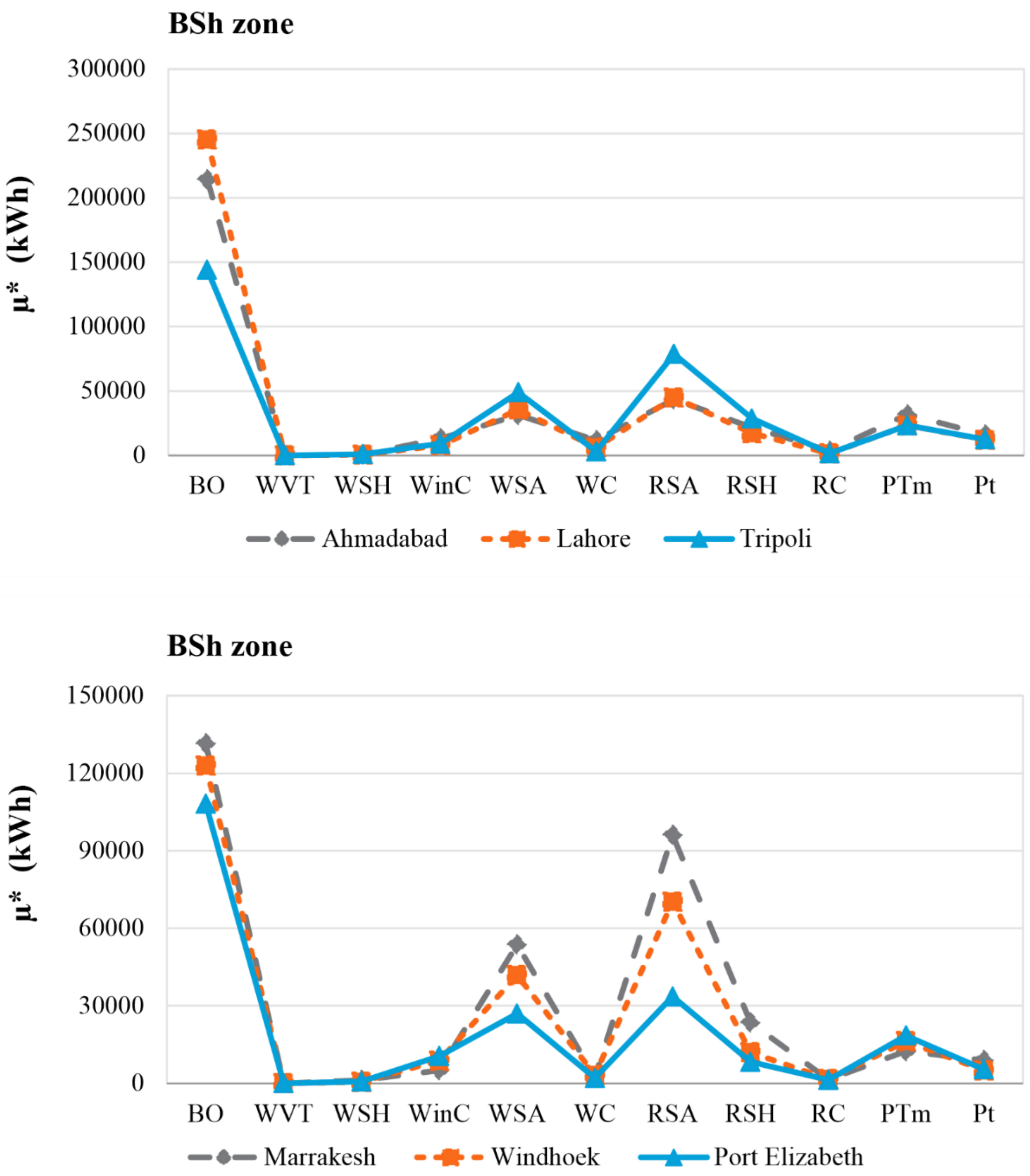

Figure 4.3: μ* indices for each input parameter relative to TEC.

Table 4.4: μ signs in the BSh zone for the future climate scenario.

Cities/ Parameters	Ahmadabad	Lahore	Marrakesh	Port Elizabeth	Tripoli	Windhoek
BO	85054	86617	41135	47838	36663	50848
WVT	0	0	0	0	0	0
WSH	-257	-206	76	108	89	34
WinC	3870	4837	1558	1742	4569	1374
WSA	-5989	-5558	-10553	-4076	-9304	-8123
WC	-4035	-1494	-1028	543	-1597	2596
RSA	3930	4978	16090	6430	12457	9998
RSH	-8480	-535	-15483	-1476	-24881	-10301
RC	-1762	10	-694	-226	-984	-538
PTm	5181	3839	5624	5518	10718	6845
Pt	-3828	-1314	-3480	1035	-2310	-731

Figure 4.4 depicts the sensitivity measurements δ and μ* in the BSh zone. An important indicator of nonlinearity is the magnitude of the interaction between the input parameters, which increases with the magnitude of δ [196]. Figure 4.4 shows that, except for RSA, most of the EDSP had a non-linear influence on TEC. BO and WSA are the design parameters with the strongest interactions or nonlinear effects on TEC in most cities in the BSh zone. The parameter RSA had a monotonic relationship with TEC as the value was between 0.5 >δ/μ* > 0.1. According to high μ* and low μ values, a non-monotonic relationship exists. To conclude, BO, RSA, WSA, PTm, RSH, Pt, and WC showed importance on the TEC in the BSh zone in the future climate scenario.

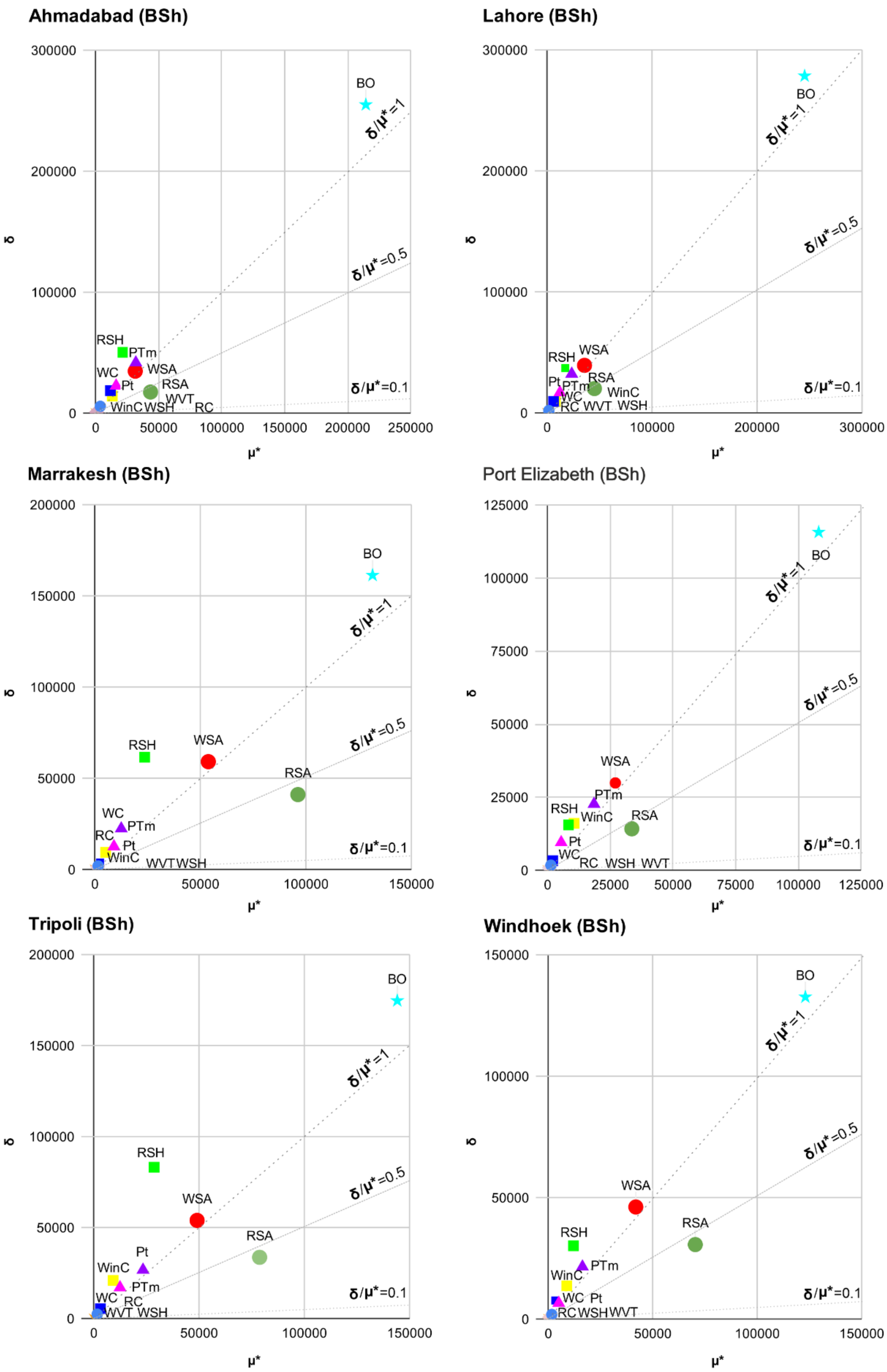

Figure 4.4: μ* and δ for the TEC in the BSh zone.

4.2.1.3. **Comparison of Morris method results**

This section presents a comparative analysis of the relative significance of EDSP based on the Morris method under current and future climate scenarios. The values of μ^* of the EDSP for TEC in the BSh zone are demonstrated in Figure 4.5. The substantial impact of BO, RSA, WSA, and PTm was indicated in the BSh zone under the current scenario, while the significant impact of BO, RSA, WSA, PTm, RSH, Pt, and WC was observed in the future. Among the analyzed parameters, the BO appears to be the most important EDSP, having the greatest sensitivity coefficients for TMY and RCP 8.5. RSA and WSA were shown to be the second and third most important parameters. However, WVT can be considered a non-important parameter for TMY and RCP 8.5. Figure 4.5 shows TEC's time-varying dynamic sensitivity coefficient in the BSh zone. Compared to the TMY, the total energy consumption for BO was substantially higher in most cities in RCP 8.5, except Ahmadabad. Concerning BO, a less significant increase was observed for RSA and WSA in Marrakesh, Port Elizabeth, and Tripoli. Nonetheless, several cities showed a downward tendency in relative significance. Figure 4.6 shows the relative variations of μ^* EDSP for TEC in radar charts (kWh) in the BSh zone. Figure 4.6 shows that the μ^* of BO was reduced by 7.6 %, RSA by 79.4 %, WSA by 74.1%, and WSH by 18.8 % in Ahmadabad in RCP 8.5. Whereas μ^* of Pt fell by 51.4 % in Marrakesh, PTm and WinC by 33.3 % and 8% in Windhoek, WSA and RSA by 37.7% and 27.2 % in Lahore, and WC decreased by 10.2% in Port Elizabeth for RCP 8.5. Another noteworthy trend of the relative relevance variations of EDSP is that the RSH had the most significant increasing tendency among almost all cities in the BSh zone in RCP 8.5. In addition, WSH increased significantly in Port Elizabeth and Windhoek in RCP 8.5.

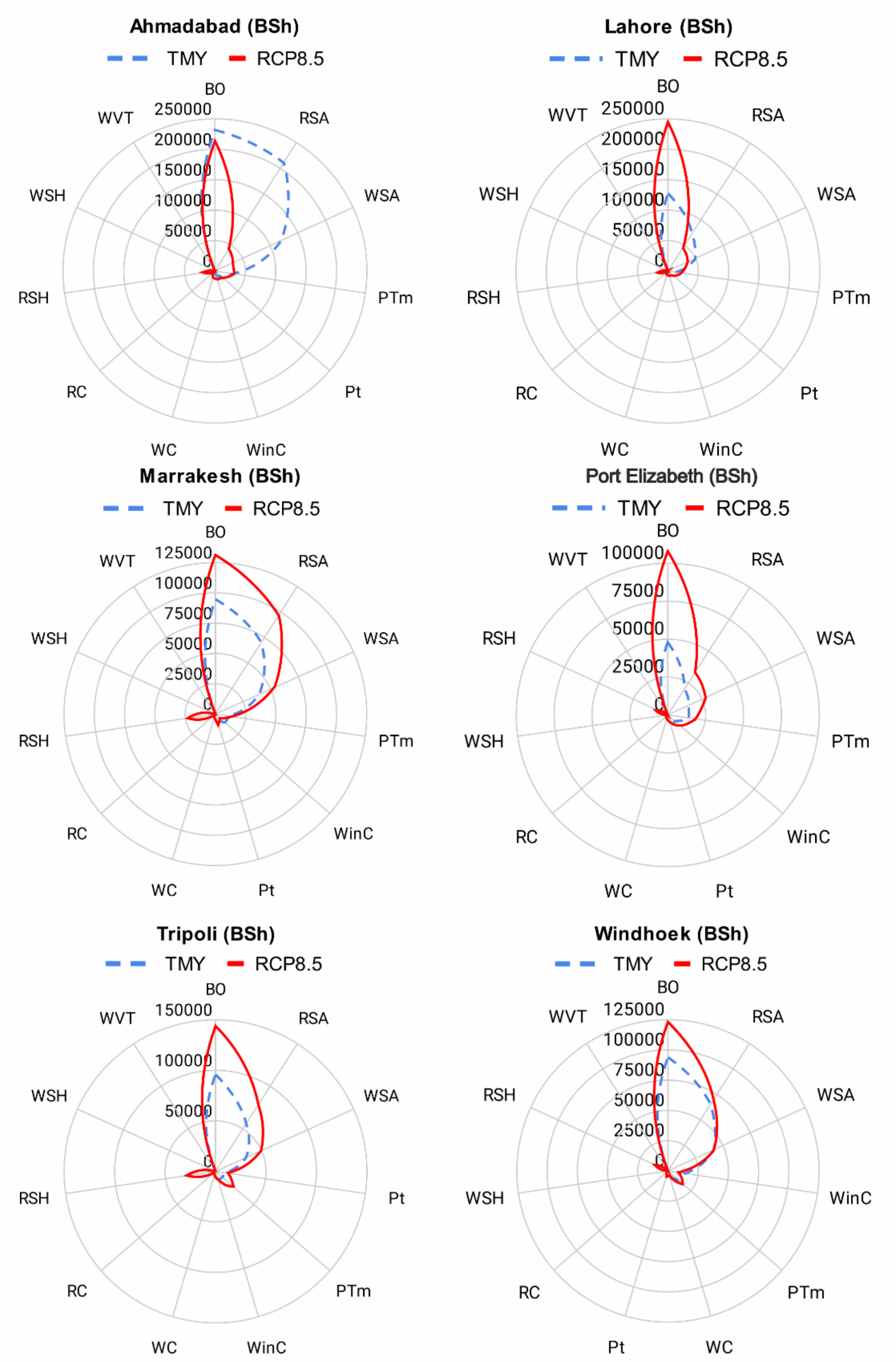

Figure 4.5: μ* of EDSP for TEC in radar charts (kWh) in the BSh zone for the current and future scenario.

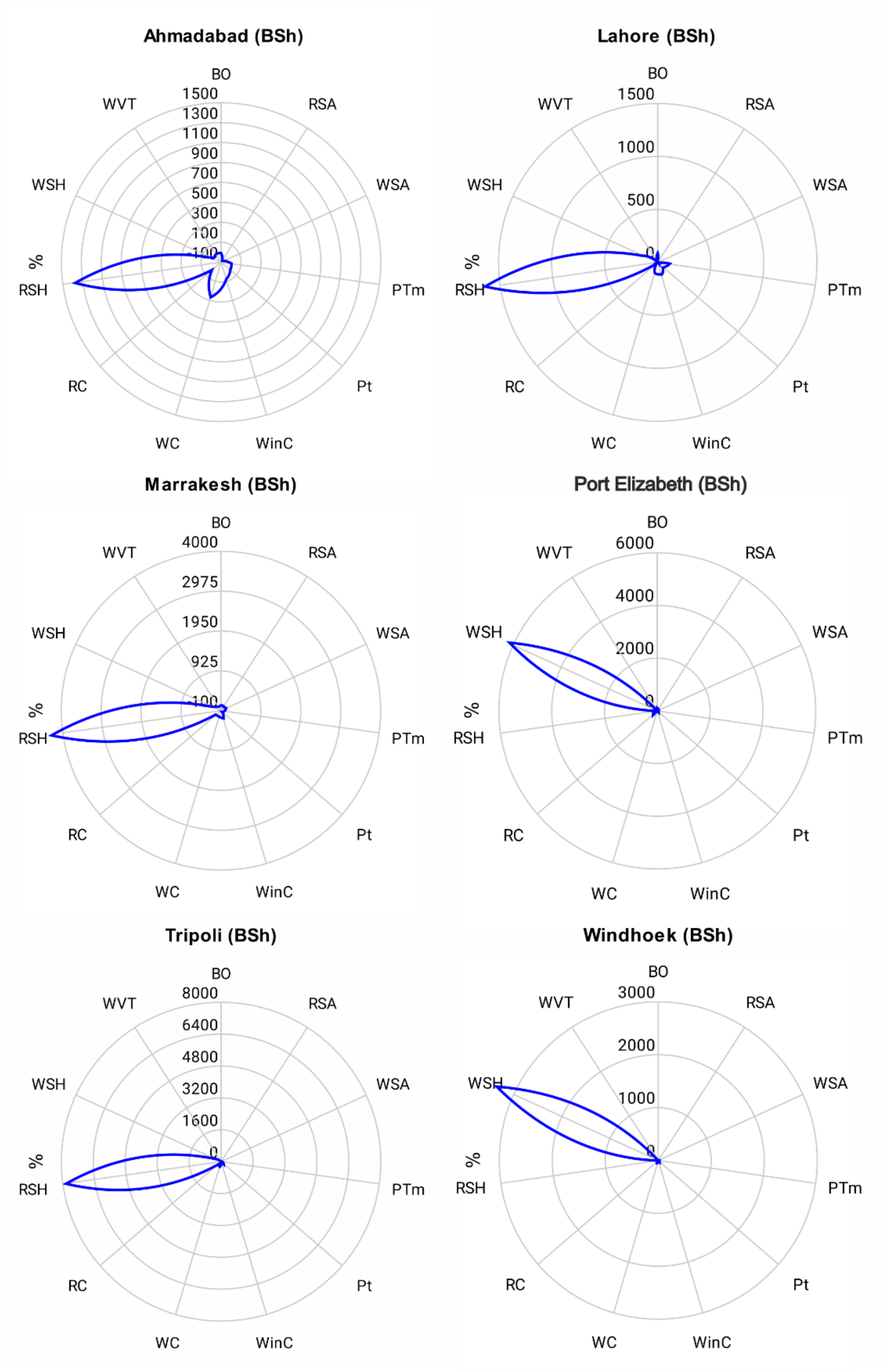

Figure 4.6: The relative variations of μ* EDSP for TEC in radar charts (kWh) in BSh zone.

The sign of the direction of μ is shown in Table 4.5 for the BSh zone under the current and future climate scenarios. It is observed that the sign of BO, WinC, RSA, and PTm, except Windhoek, was positive throughout the century in all cities. WSA and RSH were negative in all cities except Port-Elizabeth. The μ* and δ of eleven EDSP for TEC in the BSh zone for current and future climate scenarios are illustrated in Figure 4.7. It can be noted that μ* of most EDSP is over 1, showing a non-linear interaction of parameters on the TEC in both scenarios (Figure 4.7). RSA has a monotonic effect on TEC in all cities.

In conclusion, the most significant parameters were BO, RSA, and WSA in both zones for current and future climate scenarios. A declining trend in the relative significance of some parameters was anticipated for the future. The non-linear relationship between the parameters for both scenarios prevailed in both zones.

Table 4.5: μ signs in the BSh zone for the current and future climate scenarios.

Cities	**Ahmadabad**		**Lahore**		**Marrakesh**		**Port Elizabeth**		**Tripoli**		**Windhoek**	
Parameters /Scenarios	TMY	RCP 8.5	TMY	RCP 8.5	TMY	RCP 8.5	TMY	RCP 8.5	TMY	RCP 8.5	TMY	RCP 8.5
BO	71111	85054	41122	86617	19872	41135	19594	47838	30404	36663	37029	50848
WVT	0	0	0	0	0	0	0	0	0	0	0	0
WSH	184	-257	104	-206	8	76	-87.5	108	4	89	-234	34
WinC	840	3870	306	4837	1089	1558	892	1742	943	4569	1322	1374
WSA	-6865	-5989	-3703	-5558	-3050	-10553	-683	-4076	-2634	-9304	-2567	-8123
WC	985	-4035	-1410	-1494	-1214	-1028	-2082	543	-693	-1597	995	2596
RSA	45527	3930	18064	4978	17608	16090	6583	6430	14110	12457	14862	9998
RSH	-58	-8480	-93	-535	-167	-15483	1	-1476	-97	-24881	-66	-10301
RC	-1882	-1762	-394	10	69	-694	-134	-226	-145	-984	-211	-538
PTm	2530	5181	44447	3839	4227	5624	7542	5518	1113	10718	-711	6845
Pt	-5614	-3828	-1668	-1314	-851	-3480	2115	1035	-2747	-2310	1515	-731

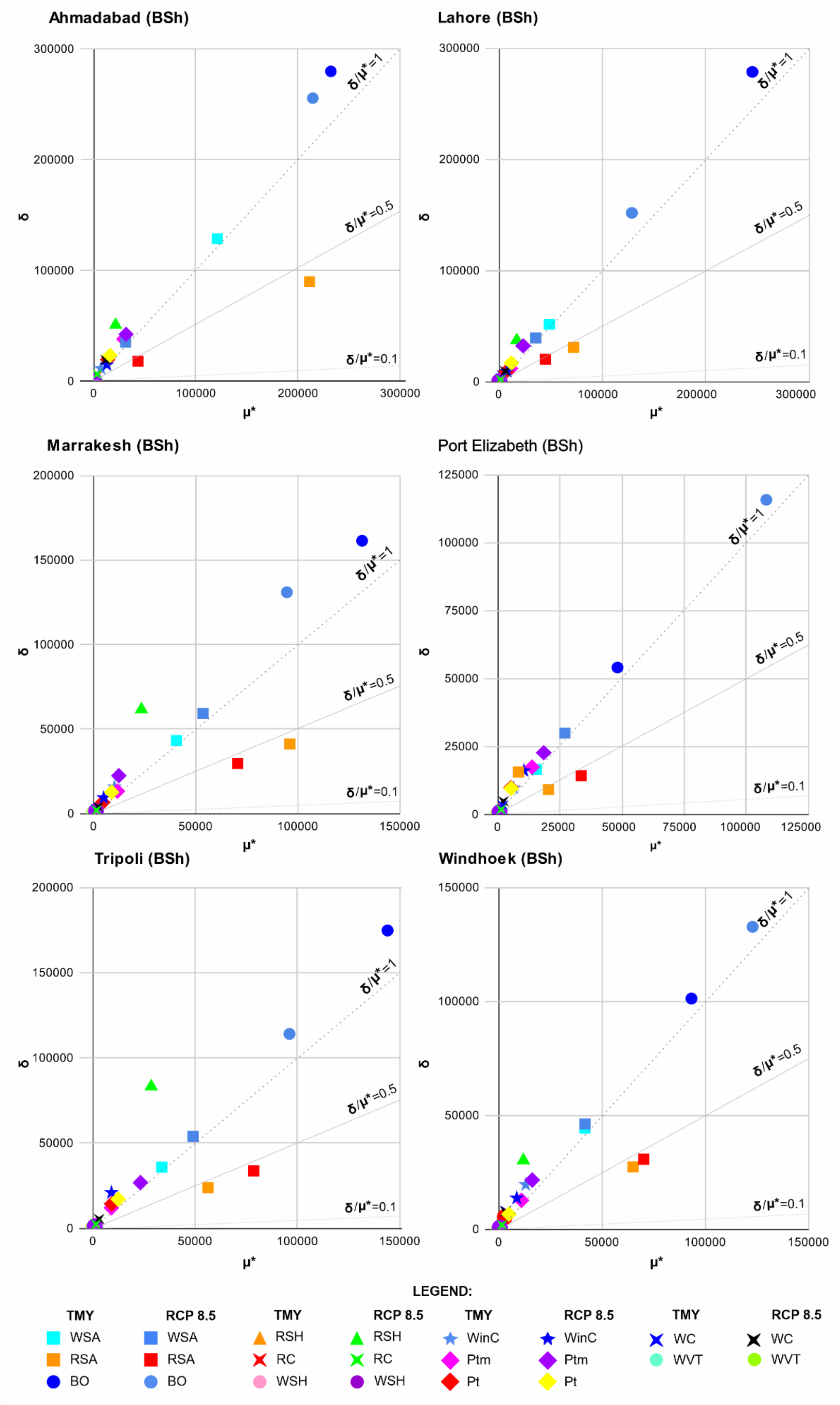

Figure 4.7: μ* and δ for the TEC in the BSh zone for current and future scenarios.

4.2.2.1. **Standardized rank regression coefficient results for the current climate scenario**

This section provides the results for TEC's standardized rank regression coefficient (SRRC) in the BSh climate zone. The SRRC was employed to determine the relative relevance of various parameters. The larger the SRRC value, the greater the significance of the parameter [197]. If the SRRC is positive, it implies that an increase in the building parameter value results in a corresponding increase in the output value. When the SRRC is negative, it shows that shifts in inputs and outputs tend to move in opposite directions [121]. The findings show only statistically significant parameters, with a significance level of 0.05.

Figure 4.8 presents the sensitivity of each EDSP related to the SRRC. According to the results, several EDSP considerably influenced the total energy consumption (TEC) in the BSh zone. Roof solar absorptance (RSA) and wall solar absorptance (WSA) were the most influential parameters in the whole climate zone, while window conductivity (WinC) was the third most influential parameter in most cities except Ahmadabad and Lahore. Apart from these parameters, PCM melting temperature (PTm) had a substantial impact on TEC in Ahmadabad, building orientation (BO) and roof conductivity (RC) had a significant impact on TEC in Lahore, while in Tripoli, roof conductivity (RC) showed significance on TEC. The other EDSP, namely PCM thickness (Pt), wall specific heat (WSH), roof specific heat (RSH), wall conductivity (WC), and window visible transmittance (WVT) showed a negligible impact on total energy consumption. The output data positively correlated with RSA, WSA, BO, and RC in all six cities, indicating that increasing these values would enhance total energy consumption. On the other hand, the WinC demonstrated a negative correlation with TEC, indicating that the energy demand decreased with the increase in the value of WinC. PTm positively correlated with TEC in most cities except Ahmadabad and Lahore. It is can be explained by that when thickness of PCM increases, latent heat cannot be utilized, as a result TEC increases.

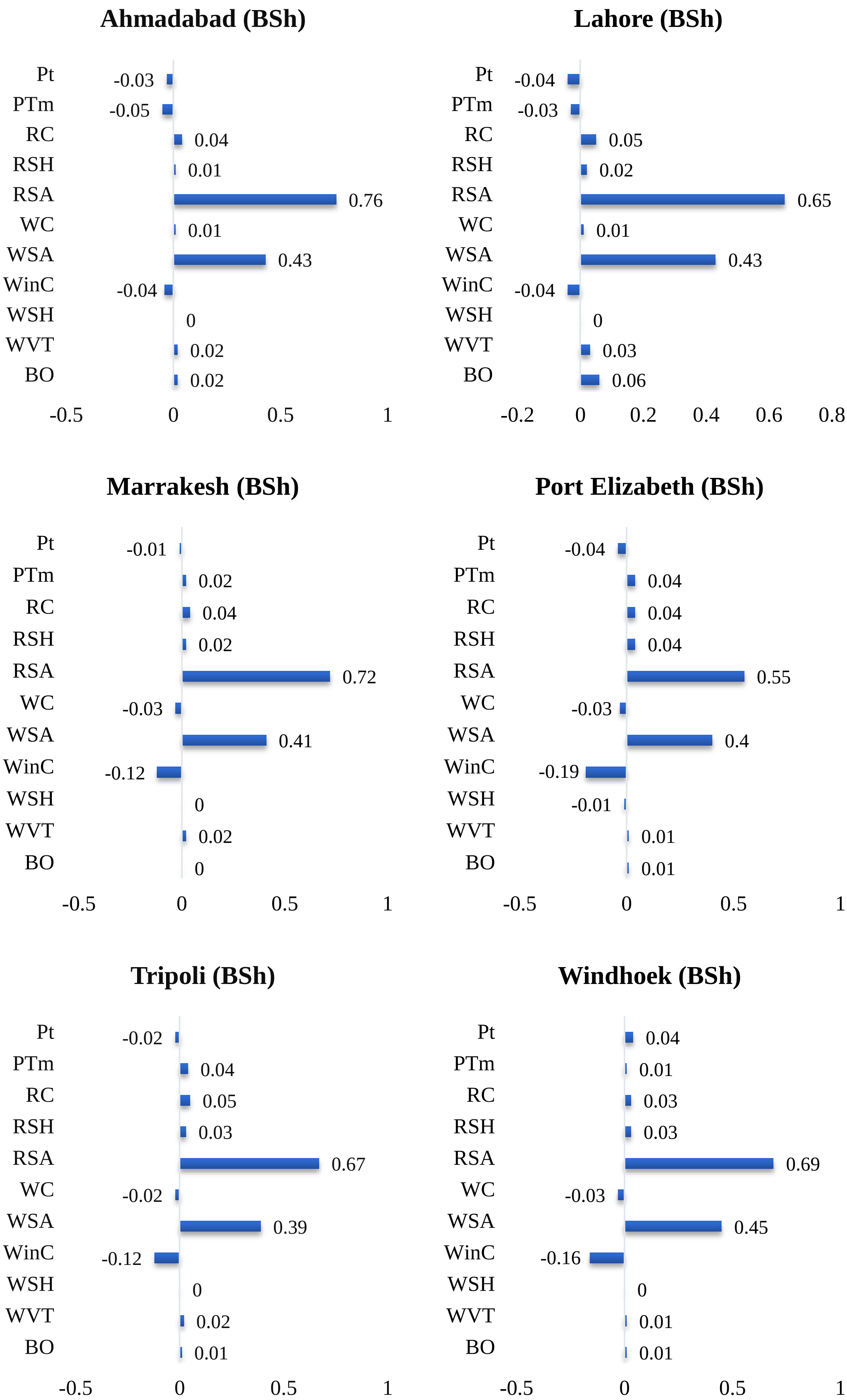

Figure 4.8: SRRC results for TEC for the BSh zone for the current climate scenario.

SRCC investigated the role of input design parameters in relation to the output parameter in several pieces of research. For instance, Gou et al. [140] performed SRRC to identify the most important parameters regarding energy consumption and thermal comfort in a newly-built residential building in China. The SRRC results indicated that east-wall solar absorptance was one of the sensitive parameters for energy consumption. Li et al. [80] examined the impact of different parameters on energy consumption and the winter discomfort of zero/low energy buildings in China. The obtained results of the SRRC indicated a significant impact of wall solar absorptance and roof solar absorptance on energy consumption. Based on the analysis of SRRC results, the RSA, WSA, and WinC parameters significantly contributed to the TEC alteration in the BSh climate zone.

4.2.2.2. **Standardized rank regression coefficient results for the future climate scenario**

This section presents the results for SRRC for TEC in the BSh zone for the future climate scenario. Figure 4.9 portrays the sensitivity of each EDSP associated with the SRRC. Based on the SRRC results, several EDSP significantly influenced TEC in the BSh zone. RSA and WSA were the dominant EDSP across the whole zone. RC was also found to be one of the significant parameter in most of the cities, except Port Elizabeth. Apart from these parameters, WinC had a substantial impact on TEC in most cities, except Lahore and Marrakesh, while BO had a considerable influence on TEC in most cities, except Marrakesh and Tripoli. Lastly, RSH, PTm, and Pt showed the importance in half of the analyzed cities in the BSh climate zone. The EDSP such as WVT, WC, and WSH displayed a minor impact on TEC. A positive correlation of RSA, WSA, RC, and RSH with TEC was observed in all six cities, implying that the rise of these values would increase TEC. Conversely, BO, PTm, WinC, and Pt showed a negative correlation with TEC in most cities, showing that the TEC decreased as the value of these parameters increased. In summary, based on the analysis of SRRC results, the RSA, WSA, RC, WinC, BO, RSH, PTm, and Pt essentially contributed to the TEC in the BSh zone.

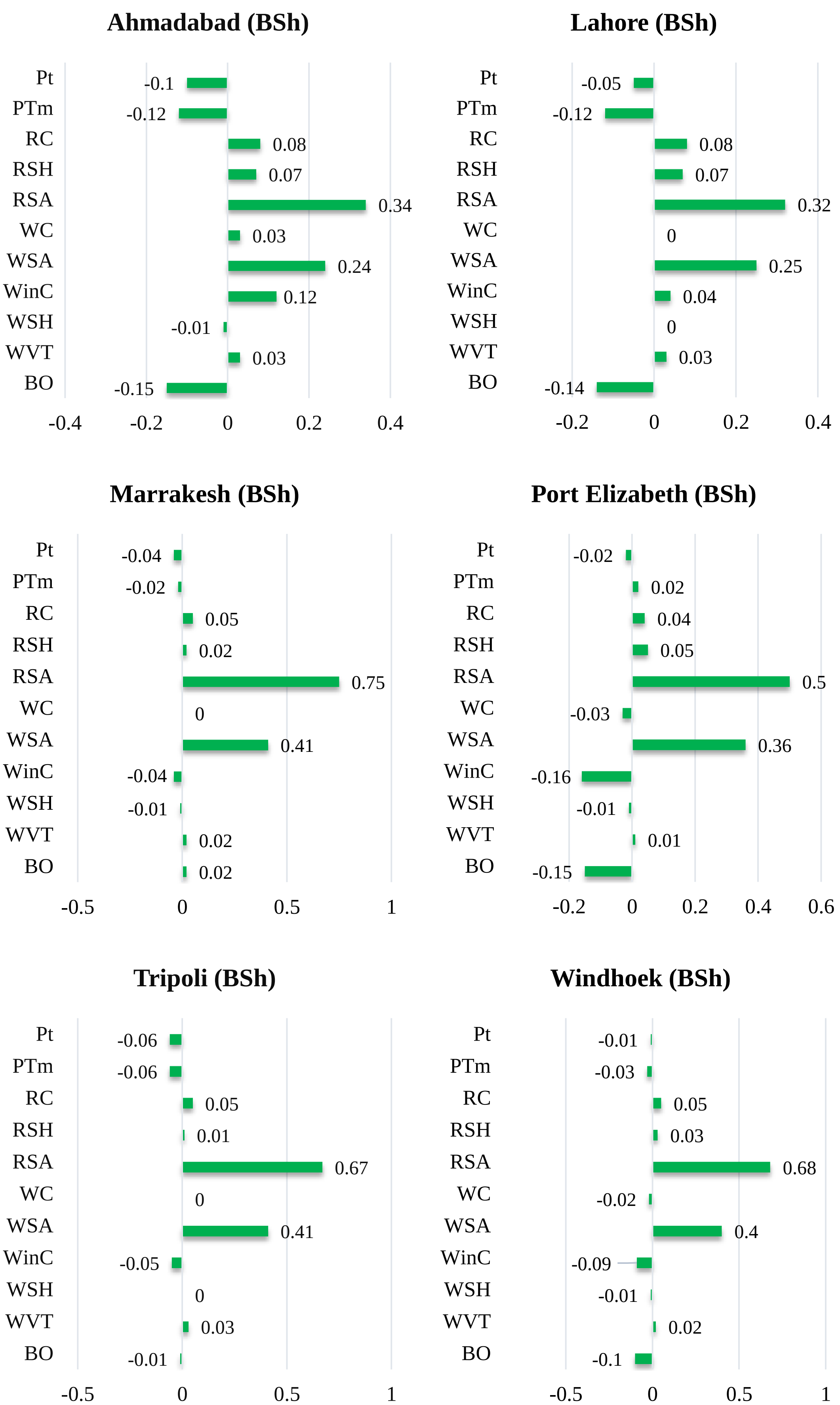

Figure 4.9: SRRC results for TEC for the BSh zone for the future climate scenario.

4.2.2.3. **Comparison of SRRC results**

The sensitivity rankings of EDSP of SRRC methods were compared for the current and future climate scenarios in the BSh zone. In Figure 4.10, the length of the bars illustrates the relative significance of the absolute values of the early design stage parameters' SRRCs and, as a result, the significance of the parameters (the longer the bar, the greater the significance of the parameter). It can be observed that for the BSh zone, the most significant parameters were RSA, WSA, and WinC for the current scenario, while RSA, WSA, RC, WinC, BO, RSH, PTm, and Pt were the most influential parameters for the future scenario.

Substantial changes in parameters relevance were defined as a difference of 0.05 in the significance level. According to the results, the relative importance of EDSP showed variations in several cities in the BSh zone in the future climate scenario. For instance, the contribution of RSA and WSA will decrease in the future. The contributions of BO and WinC varied in numerous cities. Apart from these, PTm and RSH showed variations in Ahmadabad and Lahore, while Pt showed substantial variations only in Ahmadabad. The SRRC sensitivity indices for WVT, WSH, WC, RSH, and RC have no significant changes or impact on TEC, or the changes were negligible. It can be observed from Figure 4.10 that the direction of influence of WSA, RSA, RSH, WVT, and RC remained constant throughout the century. However, the sign of BO altered in opposing directions across most locations, while the remaining parameters (WinC, WC, PTm, and Pt) showed sign transformations in a few locations in the future.

In conclusion, it was indicated that some EDSP can alter their relevance in a future climate scenario while others can remain constant. The relevance of RSA and WSA will decrease in the future. Apart from these parameters, WinC and BO showed variations in significance. The remaining parameters showed negligible alterations.

Cities/ Parameters	Ahmadabad	Lahore	Marrakesh	Port-Elizabeth	Tripoli	Windhoek
BO	0.02	0.06	0	0.01	0.01	0.01
WVT	0.02	0.03	0.02	0.01	0.02	0.01
WSH	0	0	0	-0.01	0	0
WinC	-0.04	-0.04	-0.12	-0.19	-0.12	-0.16
WSA	0.43	0.43	0.41	0.4	0.39	0.45
WC	0.01	0.01	-0.03	-0.03	-0.02	-0.03
RSA	0.76	0.65	0.72	0.55	0.67	0.69
RSH	0.01	0.02	0.02	0.04	0.03	0.03
RC	0.04	0.05	0.04	0.04	0.05	0.03
PTm	-0.05	-0.03	0.02	0.04	0.04	0.01
Pt	-0.03	-0.04	-0.01	-0.04	-0.02	0.04

a)

Cities/ Parameters	Ahmadabad	Lahore	Marrakesh	Port-Elizabeth	Tripoli	Windhoek
BO	-0.15	-0.14	0.02	-0.15	-0.01	-0.1
WVT	0.03	0.03	0.02	0.01	0.03	0.02
WSH	-0.01	0	-0.01	-0.01	0	-0.01
WinC	0.12	0.04	-0.04	-0.16	-0.05	-0.09
WSA	0.24	0.25	0.41	0.36	0.41	0.4
WC	0.03	0	0	-0.03	0	-0.02
RSA	0.34	0.32	0.75	0.5	0.67	0.68
RSH	0.07	0.07	0.02	0.05	0.01	0.03
RC	0.08	0.08	0.05	0.04	0.05	0.05
PTm	-0.12	-0.12	-0.02	0.02	-0.06	-0.03
Pt	-0.1	-0.05	-0.04	-0.02	-0.06	-0.01

b)

Figure 4.10: SRRC of the BSh zone for a) current scenario; b) future scenario.

4.2.3.1. **Partial rank correlation coefficient results for the current climate scenario**

The PRCC approach sorts the inputs and outputs in increasing order and replaces their values with their rankings. Whenever the PRCC of a parameter is high (near 1), it indicates that the parameter has a significant effect on the model output [79]. A PRCC of eleven EDSP for the total energy consumption is presented in Figure 4.11 to observe their potential influence. According to PRCC results, the most important parameters in the BSh zone were the RSA, WSA, WinC, and RC. Apart from these parameters, Pt showed the importance in the four cities located in the BSh zone.

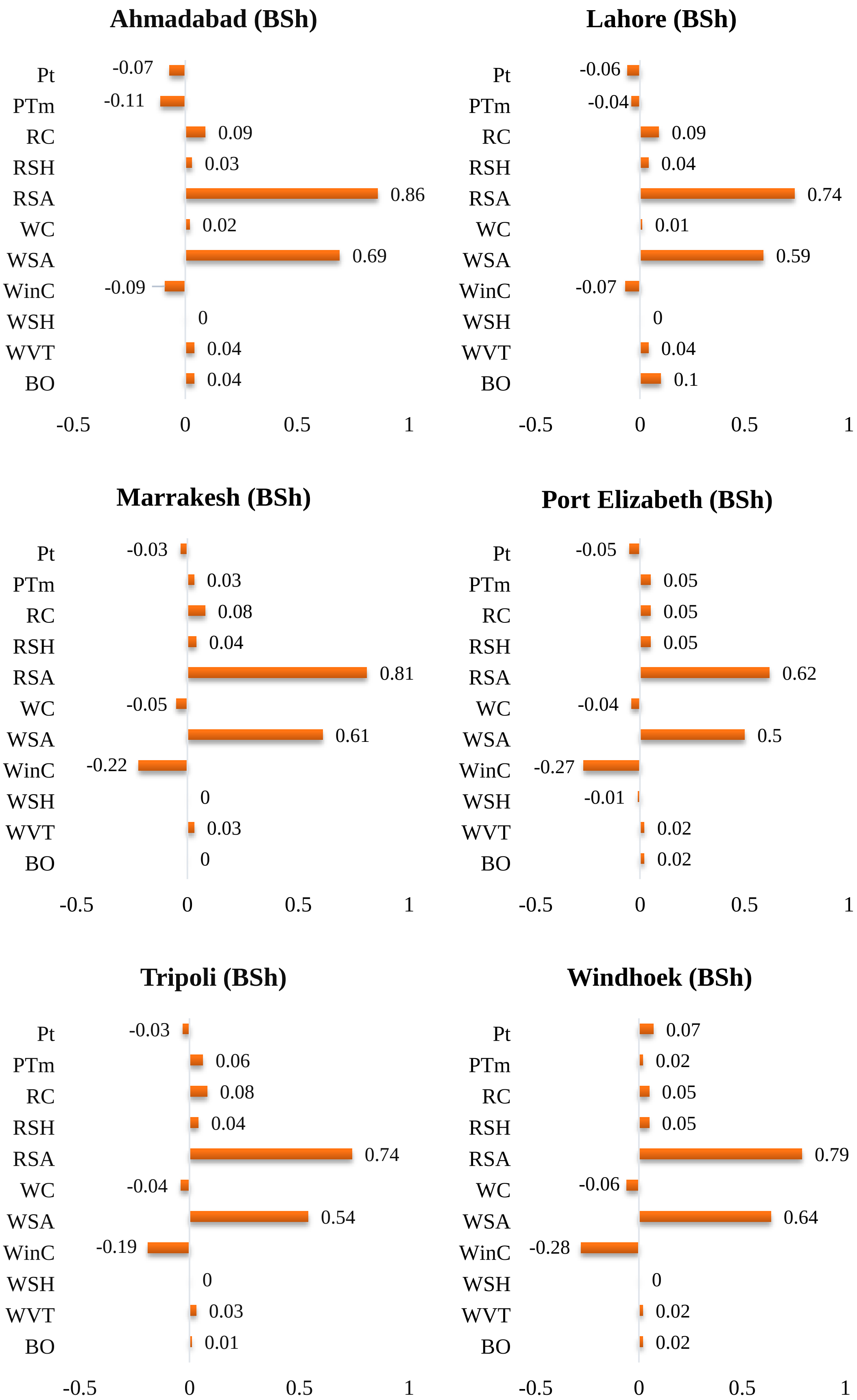

Figure 4.11: PRCC results for TEC for the BSh zone for the current climate scenario.

While PTm was found to be important in Ahmadabad, Port Elizabeth, and Tripoli. Also, RSH showed sensitivity in Port Elizabeth and Windhoek, while WC was influential for the TEC in Marrakesh and Windhoek. PRCC indexes of other EDSP are less than 0.05, indicating relatively weak impacts on total energy consumption. The positive correlation of RSA, WSA, and RC with TEC was observed in all cities, whereas WinC and Pt are negatively correlated with TEC in almost all cities. In summary, RSA, WSA, WinC, RC, RSH, Pt, WC, and PTm were significant parameters in the BSh zone. Since the values of PRCC are higher than SRRC, non-linear impacts are present [80].

4.2.3.2. **Partial rank correlation coefficient results for the future climate scenario**

This section presents the results of the PRCC for eleven EDSP in the BSh zone for future climate scenarios. The relative importance of design parameters for the BSh zone is depicted in Figure 4.12. According to the results, the most significant parameters in all cities were RSA and WSA, followed by RC and WinC (except Lahore), respectively. Apart from these parameters, BO, RSH, and Pt showed relative importance to TEC in four cities. Also, PTm was found to be important in three cities of the BSh zone, namely Ahmadabad, Lahore, and Tripoli. A positive correlation with TEC was observed for RSA, WSA, RC, and RSH, while Pt demonstrated a negative correlation with TEC in all selected cities. A negative correlation with TEC was dominant for BO and WinC. In summary, for the future scenario, RSA, WSA, RC, WinC, BO, RSH, Pt, and PTm are the most significant parameters in the BSh zone.

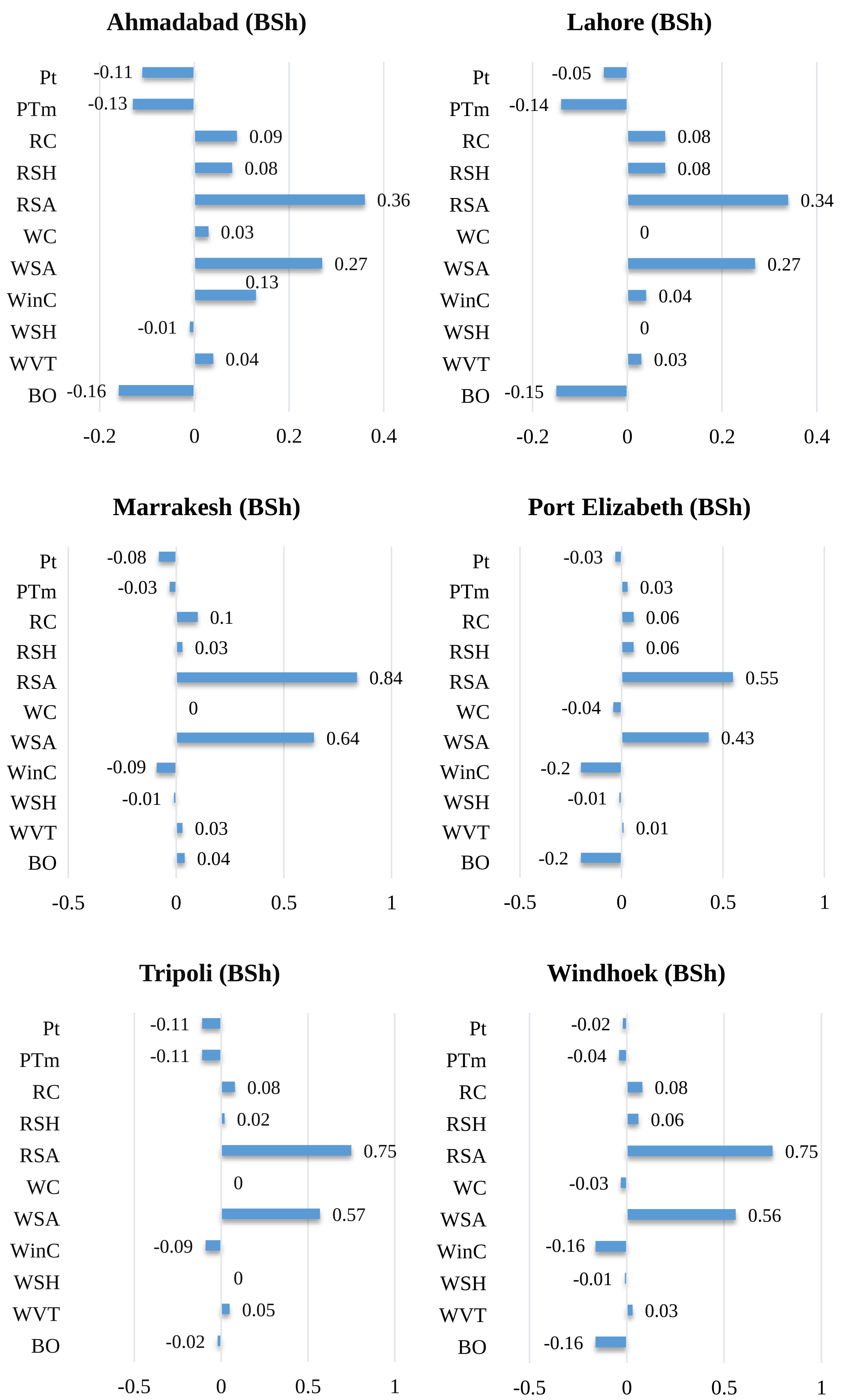

Figure 4.12: PRRC results for TEC for the BSh zone for the future climate scenario.

4.2.3.3. **Comparison of PRCC results**

A comparison of sensitivity indices of PRCC results for the current and future climate scenarios was executed in the BSh zone. The relative relevance of the absolute values of the EDSP is indicated in Figure 4.13. The significant parameters in the BSh zone in the current scenario were found to be RSA, WSA, WinC, RC, RSH, Pt, and PTm. RSA, WSA, RC, WinC, BO, RSH, Pt and PTm will be significant in the future. In several cities in the BSh zone, the importance of WSA and RSA was reduced under the future climate scenarios. Also, significant alterations in the relative importance of WinC were demonstrated in most cities. There were alterations in the PRCC indices of BO in Ahmadabad, Lahore, Port Elizabeth, and Windhoek, as well as alterations in the PTm in Lahore and Tripoli and Pt in Marrakesh and Tripoli. The signs of direction of RSA, WSA, WVT, RSH, RC, WC, and WSH remained unchanged throughout the century. In most cities, the BO sign's direction changed to the negative in the future climate scenario. Apart from these parameters, minor variations of the direction sign were indicated for WinC, PTm, and Pt.

In summary, the importance of relevance and the direction of several design parameters varied throughout the century. The decrease of relevance of WSA and RSA were observed in future. The sign of direction was constant during the century for RSA, WSA, WVT, RSH, RC, WC, and WSH in the BSh zone.

Cities/ Parameters	Ahmadabad	Lahore	Marrakesh	Port-Elizabeth	Tripoli	Windhoek
BO	0.04	0.1	0	0.02	0.01	0.02
WVT	0.04	0.04	0.03	0.02	0.03	0.02
WSH	0	0	0	-0.01	0	0
WinC	-0.09	-0.07	-0.22	-0.27	-0.19	-0.28
WSA	0.69	0.59	0.61	0.5	0.54	0.64
WC	0.02	0.01	-0.05	-0.04	-0.04	-0.06
RSA	0.86	0.74	0.81	0.62	0.74	0.79
RSH	0.03	0.04	0.04	0.05	0.04	0.05
RC	0.09	0.09	0.08	0.05	0.08	0.05
PTm	-0.11	-0.04	0.03	0.05	0.06	0.02
Pt	-0.07	-0.06	-0.03	-0.05	-0.03	0.07

a)

Cities/ Parameters	Ahmadabad	Lahore	Marrakesh	Port-Elizabeth	Tripoli	Windhoek
BO	-0.16	-0.15	0.04	-0.2	-0.02	-0.16
WVT	0.04	0.03	0.03	0.01	0.05	0.02
WSH	-0.01	0	-0.01	-0.01	0	-0.01
WinC	0.13	0.04	-0.09	-0.2	-0.09	-0.16
WSA	0.27	0.27	0.64	0.43	0.57	0.56
WC	0.03	0	0	-0.04	0	-0.03
RSA	0.36	0.34	0.84	0.55	0.75	0.75
RSH	0.08	0.08	0.03	0.06	0.02	0.06
RC	0.09	0.08	0.1	0.06	0.08	0.08
PTm	-0.13	-0.14	-0.03	0.03	-0.11	-0.05
Pt	-0.11	-0.05	-0.08	-0.03	-0.11	-0.02

b)

Figure 4.13: PRCC of the BSh zone for a) current scenario; b) future scenario.

4.2.4.1. **Ranking of the first stage of MSA in the current climate scenario**

In this section, the ranking results from the first-stage sensitivity analysis were compared. Table 4.6 indicates the relative importance of each EDSP in terms of its influence on the TEC derived by the SRRC, PRCC, and Morris approaches in the BSh zone. The cells in Table 4.6 are colored from light blue (high value) to dark blue (low value) to provide a rapid overview. The average value of ranking results from three global sensitivity analyses was calculated to obtain the most significant EDSP.

The results of the ranking significance for eleven EDSP that affect TEC were almost the same for SRRC and PRCC. A slight variation in ranks for these methods was noted in Ahmadabad, Marrakesh, and Tripoli. Based on the SRRC and PRCC rankings, the most important parameters in the BSh zone were RSA, WSA, and WinC. Based on the SRRC rankings, the most important parameters in the BSh zone were RSA, WSA, and WinC, while for PRCC rankings, the most important parameters were RSA, WSA, WinC, RC, RSH, Pt, PTm, and WC. The BO, RSA, WSA, and PTm were the most significant parameters for the Morris method. By comparing the SRRC and PRCC rankings in the BSh zone, it is evident that RSA and WSA were the top two most significant parameters while WinC was the third most influential parameter in most of the cities. According to Morris method, the three most important parameters are RSA, WSA, and BO. SRRC and PRCC identified BO as an unimportant parameter; however, the Morris method identified it as the first top crucial parameter. This alteration can be explained by the nonlinear relationship between cooling energy and building orientation. Building windows are typically oriented in various orientations, deviating from the base case and making the orientation strategy less important for reducing cooling energy [15]. This indicates that using merely the SRRC and PRCC, for instance, may eliminate BO, which has been identified as a highly sensitive parameter in prior research [39,182,198]. In addition, the performed analysis revealed that the Morris method's parameter ranking differed, while the SRRC and PRCC showed a similarity in most cases. One probable explanation for the different ranking order is a variation in sample size. Yang et al. [29] performed a comparative analysis of four different sensitivity analysis methods (treed Gaussian process, Fourier Amplitude Sensitivity Test, standardized regression coefficient, and Morris method) and found that the difference in Morris method ranking is due to the need for more simulation runs to generate accurate results. A detailed investigation is required to establish the precise reason for the difference between Morris and the other techniques.

Table 4.6: Ranking of SRRC, PRCC, and Morris methods in the BSh zone for the current climate scenario.

Cities	**Ahmadabad**			**Lahore**			**Marrakesh**			**Port Elizabeth**			**Tripoli**			**Windhoek**		
Pr/Ms***	S*	P*	M*	S*	P*	M*	S*	P*	M*	S*	P*	M*	S*	P*	M*	S*	P*	M*
RSA	1	1	2	1	1	2	1	1	2	1	1	2	1	1	2	1	1	2
WVT	8	8	11	7	7	11	6	7	11	10	10	11	7	8	11	9	9	11
WSA	2	2	3	2	2	3	2	2	3	2	2	3	2	2	3	2	2	3
WinC	5	4	6	5	5	6	3	3	5	3	3	5	3	3	6	3	3	4
Pt	6	6	5	6	6	4	9	9	6	7	7	6	9	9	4	4	4	7
RSH	9	9	9	9	8	9	7	6	9	4	4	10	6	7	9	6	6	10
WSH	11	11	10	11	11	10	11	11	10	11	11	9	11	11	10	11	11	9
PTm	3	3	4	8	9	5	8	8	4	6	6	4	5	5	5	10	10	5
WC	10	10	7	10	10	7	5	5	7	8	8	7	8	6	7	5	5	6
BO	7	7	1	3	3	1	10	10	1	9	9	1	10	10	1	8	8	1
RC	4	5	8	4	4	8	4	4	8	5	5	8	4	4	8	7	7	8

Note:
Ms   - Sensitivity analysis methods (S* - SRRC, P* - PRCC, M* - Morris methods);*
*Pr** - EDSP;*
Light colors represent the highest ranking of parameters;
Dark colors represent the lowest ranking of parameters.

Several researchers employed global sensitivity analysis methods to prioritize design parameters in buildings that lacked PCM. Li et al. [10] implemented MSA to identify the most relevant input parameters influencing overall energy use and winter thermal discomfort. Out of the fourteen parameters tested, the authors determined that the building orientation, roof solar absorptance, and wall solar absorptance had the greatest impact. Consequently, relying on a single sensitivity analysis method to identify crucial design parameters may overlook significant factors.

To summarize, the primary parameters for the first stage sensitivity analysis in the BSh zone were RSA, WSA, WinC, BO, RC, PTm, Pt, and WC, while the other parameters can be considered insignificant. Additionally, rankings for different EDSP may vary significantly among cities in the same climatic zone, as demonstrated in Table 4.6.

4.2.4.2. **Ranking of the first stage of MSA in the future climate scenario**

This section presents the ranking results obtained from the first-stage sensitivity analysis for the future climate scenario. Table 4.7 shows the relative relevance of each EDSP in terms of its effect on the TEC determined by the SRRC, PRCC, and Morris methods in the BSh zone. SRRC and PRCC results showed that the most significant parameters in the BSh zone were RSA, WSA, BO, WinC, RC, PTm, Pt and RSH, while the Morris method indicated BO, RSA, WSA, PTm, RSH, Pt, and WinC as the most significant parameters. The parameter ranking was based on the average value of the three methods. Based on the results, the ranking of Morris method for RSA, WVT, WSH, WC, BO, and RC showed stability across all cities in the BSh zone. The ranking of BO is consistent for SRRC and PRCC methods in all selected cities. The remaining parameters showed instability in parameter rankings in all cities.

The ranking of each parameter of the SRRC and PRCC was identical in most cities, while Lahore and Port Elizabeth showed slight variations in parameter rankings. In addition, the ranking of Morris had an almost different ranking compared to the SRRC and PRCC. As a result, to ensure the identification of all crucial design parameters, relying solely on a single sensitivity analysis technique is not recommended, as it may result in overlooking important parameters. Using a single sensitivity approach may result in neglecting the most critical parameters, which are regarded as being very sensitive. Based on the findings, eventually, eight design parameters were selected for the BSh zone (RSA, WSA, BO, WinC, PTm, RSH, RC, and Pt.)

Table 4.7: Ranking of SRRC, PRCC, and Morris methods in the BSh zone for the future climate scenario.

Cities	**Ahmadabad**			**Lahore**			**Marrakesh**			**Port Elizabeth**			**Tripoli**			**Windhoek**		
Pr/Ms***	S*	P*	M*	S*	P*	M*	S*	P*	M*	S*	P*	M*	S*	P*	M*	S*	P*	M*
RSA	1	1	2	1	1	2	1	1	2	1	1	2	1	1	2	1	1	2
WVT	9	9	11	9	9	11	7	7	11	10	10	11	7	7	11	8	9	11
WSA	2	2	4	2	2	3	2	2	3	2	2	3	2	2	3	2	2	3
WinC	4	4	7	8	8	7	4	4	7	3	4	5	5	5	7	4	4	6
Pt	6	6	6	7	7	6	5	5	6	9	9	7	4	4	6	11	10	7
RSH	8	8	5	6	5	5	8	8	4	5	5	6	9	9	4	6	6	5
WSH	11	11	10	10	10	10	10	10	10	11	11	10	10	10	10	10	11	10
PTm	5	5	3	4	4	4	9	9	5	8	8	4	3	3	5	7	7	4
WC	10	10	8	11	11	8	11	11	8	7	7	8	11	11	8	9	8	8
BO	3	3	1	3	3	1	6	6	1	4	3	1	8	8	1	3	3	1
RC	7	7	9	5	6	9	3	3	9	6	6	9	6	6	9	5	5	9

4.2.4.3. **Comparison of rankings of the first stage of MSA**

The sensitivity rankings of EDSP obtained from three sensitivity analysis methods (SRRC, PRCC, and Morris) were compared for the current and future climate scenarios in the BSh zone (Table 4.8). The color and length of the cells show the relative magnitude of the parameters' importance: the redder the color, the more significant the parameter; the greener the color, the less significant the parameter. According to the results, the ranking of RSA and WSA showed no substantial change in the future for the PRCC and SRRC in the BSh zone. The SRRC ranking of PTm revealed a tendency for declining relevance in three cities, whereas growing importance was demonstrated by the ranking of BO, except Lahore, where it was found to be stable. Other cities showed variations in the SRRC rankings. Based on PRCC rankings, PTm importance decreased in all three cities, whereas WinC importance decreased in all cities except Ahmadabad. BO became more significant throughout the zone, except for Lahore, where it was stable, while the ranks of other parameters fluctuated. According to the Morris approach, there was no change in the ranks of RSA, WSA, WVT, and BO in the BSh zone, however, there were minor changes in the rating of WSH in Port Elizabeth and Windhoek. Aside from these parameters, the rankings for WC and RC decreased throughout all cities, while in certain cities, the rankings for WinC and Pt remained constant. In some cities, the impact of WinC was insignificant; the reason for this can be the increased heat gain and cooling loads, which can result in higher energy consumption and decreased comfort. However, the impact of WinC depends on different factors, including the building orientation, the glazing properties, and the use of shading devices. The impact of WC on the energy consumption of the building can be slow because of high level of thermal insulation, air tightness of the building envelope, the efficiency of HVAC system. The rankings of RSH increased in all cities, while the rankings of PTm showed variability in all cities.

In summary, the rankings of SRRC and PRCC are expected to change in the future for most parameters in the BSh zone. However, the RSA and WSA showed no significant change in the future. PTm demonstrated a decrease in significance for SRRC and PRCC rankings in half the cities, while BO demonstrated an increase in significance for SRRC and PRCC in almost all the cities. For the Morris method, several parameters showed constant ranking in the BSh zone.

Table 4.8: Ranking of SRRC, PRCC, and Morris methods in the BSh zone for the current and future scenarios.

Cities	Ahmadabad						Lahore						Marrakesh					
Weather data	TMY			RCP 8.5			TMY			RCP 8.5			TMY			RCP 8.5		
Pr**/Ms*	S*	P*	M*	S*	P*	M*	S*	P*	M*	S*	P*	M*	S*	P*	M*	S*	P*	M*
RSA	1	1	2	1	1	2	1	1	2	1	1	2	1	1	2	1	1	2
WVT	8	8	11	9	9	11	7	7	11	9	9	11	6	7	11	7	7	11
WSA	2	2	3	2	2	4	2	2	3	2	2	3	2	2	3	2	2	3
WinC	5	4	6	4	4	7	5	5	6	8	8	7	3	3	5	4	4	7
Pt	6	6	5	6	6	6	6	6	4	7	7	6	9	9	6	5	5	6
RSH	9	9	9	8	8	5	9	8	9	6	5	5	7	6	9	8	8	4
WSH	11	11	10	11	11	10	11	11	10	10	10	10	11	11	10	10	10	10
PTm	3	3	4	5	5	3	8	9	5	4	4	4	8	8	4	9	9	5
WC	10	10	7	10	10	8	10	10	7	11	11	8	5	5	7	11	11	8
BO	7	7	1	3	3	1	3	3	1	3	3	1	10	10	1	6	6	1
RC	4	5	8	7	7	9	4	4	8	5	6	9	4	4	8	3	3	9

Cities	Port-Elizabeth						Tripoli						Windhoek					
Weather data	TMY			RCP 8.5			TMY			RCP 8.5			TMY			RCP 8.5		
Pr**/Ms*	S*	P*	M*	S*	P*	M*	S*	P*	M*	S*	P*	M*	S*	P*	M*	S*	P*	M*
RSA	1	1	2	1	1	2	1	1	2	1	1	2	1	1	2	1	1	2
WVT	10	10	11	10	10	11	7	8	11	7	7	11	9	9	11	8	9	11
WSA	2	2	3	2	2	3	2	2	3	2	2	3	2	2	3	2	2	3
WinC	3	3	5	3	4	5	3	3	6	5	5	7	3	3	4	4	4	6
Pt	7	7	6	9	9	7	9	9	4	4	4	6	4	4	7	11	10	7
RSH	4	4	10	5	5	6	6	7	9	9	9	4	6	6	10	6	6	5
WSH	11	11	9	11	11	10	11	11	10	10	10	10	11	11	9	10	11	10
PTm	6	6	4	8	8	4	5	5	5	3	3	5	10	10	5	7	7	4
WC	8	8	7	7	7	8	8	6	7	11	11	8	5	5	6	9	8	8
BO	9	9	1	4	3	1	10	10	1	8	8	1	8	8	1	3	3	1
RC	5	5	8	6	6	9	4	4	8	6	6	9	7	7	8	5	5	9

Ms - Sensitivity analysis methods (S* - SRRC, P* - PRCC, M* - Morris methods);*
*Pr** - EDSP;*
Red colors represent the highest ranking of parameters;
Green colors represent the lowest ranking of parameters.

4.2.5. **Results of second stage sensitivity analysis for current and future climate scenarios**

The first stage sensitivity analyses showed that combining several EDSP essential for TEC reduction could result in optimal TEC performance. As a result, a local sensitivity approach was employed to investigate the impact of each input parameter on TEC for the current and future climate scenarios in the BSh zone. The comparative analysis is also presented in this section.

The most significant EDSP obtained from the first-stage sensitivity analysis were evaluated using Local sensitivity analysis (LSA). LSA is utilized to assess the effect of EDSP on TEC. To examine the relationship between the design parameters and TEC, the range of values for each parameter from first stage sensitivity was altered while the other remained fixed. The eight most important design parameters acquired from the first stage of SA are used to calculate the local sensitivity indices (LSI). For the BSh zone, the most significant parameters for the current climate scenario were: RSA, WSA, WinC, PTm, Pt, BO, WC, and RC. Figure 4.14 presents the results of the LSA of eight EDSP on TEC based on the LSI in the BSh zone. The most important parameter selection was based on the average value of the LSI method in six cities. Generally, the higher the LSI value, the more important the design parameter is to TEC. For all cities, similar impacts were observed. The most significant parameters were the RSA, WSA, BO, WinC, and PTm. The impact of RC, WC, and Pt was negligible. Figure 4.15 presents the results of the LSI of EDSP in the BSh zone for the future climate scenario. According to the results, BO had the highest value relative to TEC. Apart from this parameter, the dominant influence of RSA was observed. Further, the significant impact of WSA, WinC, and PTm was indicated in this zone. The five most significant parameters were selected for further optimization in the BSh zone by adopting MSA. These parameters are RSA, WSA, BO, WinC, and PTm.

The results of the comparative analysis for the BSh zone are presented in Figure 4.16. According to obtained results, for the BSh zone, the magnitude of the significance of RSA and WSA is reduced in the future when compared with the current scenario. When comparing current and future scenarios, in some cities, WinC, PTm, Pt, and BO showed an increase in significance, while in other cities, they showed a decrease in significance. The remaining parameters were indicated as insignificant in the future. In summary, the five most significant parameters were selected for further optimization in both climate scenarios: RSA, WSA, BO, WinC, and PTm.

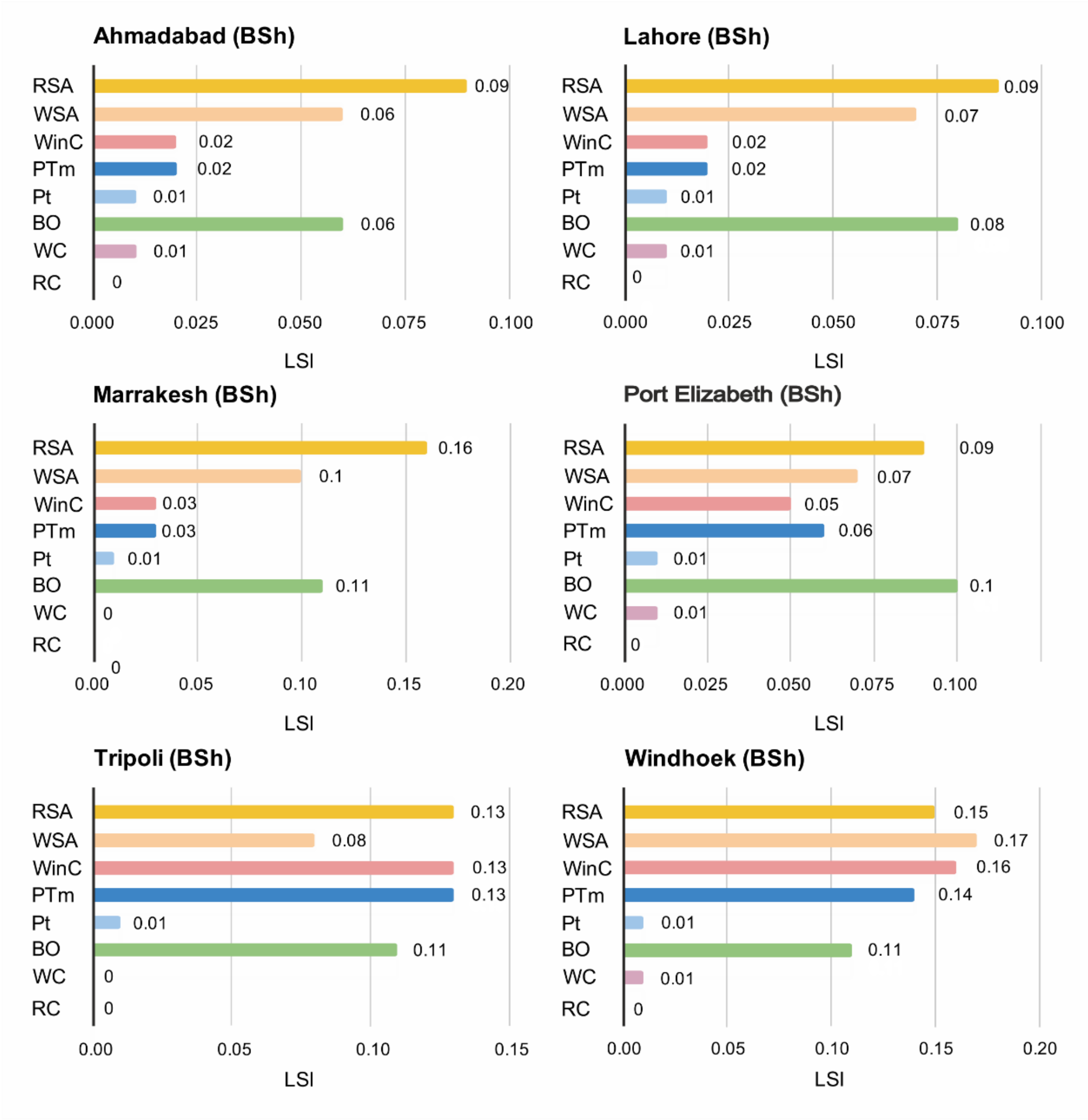

Figure 4.14: LSI for TEC in the BSh zone for the current climate scenario.

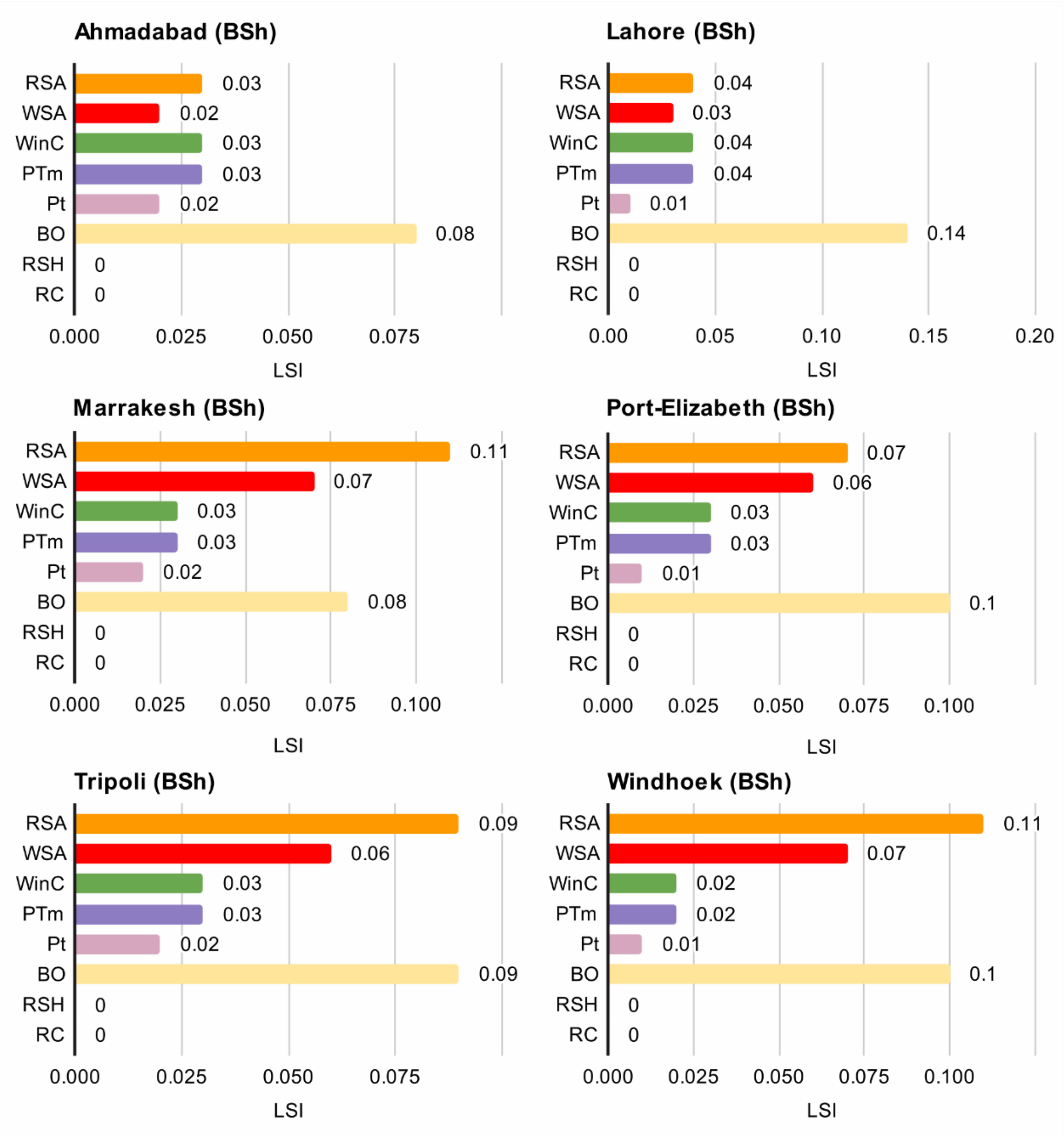

Figure 4.15: LSI for TEC in the BSh zone for the future climate scenario.

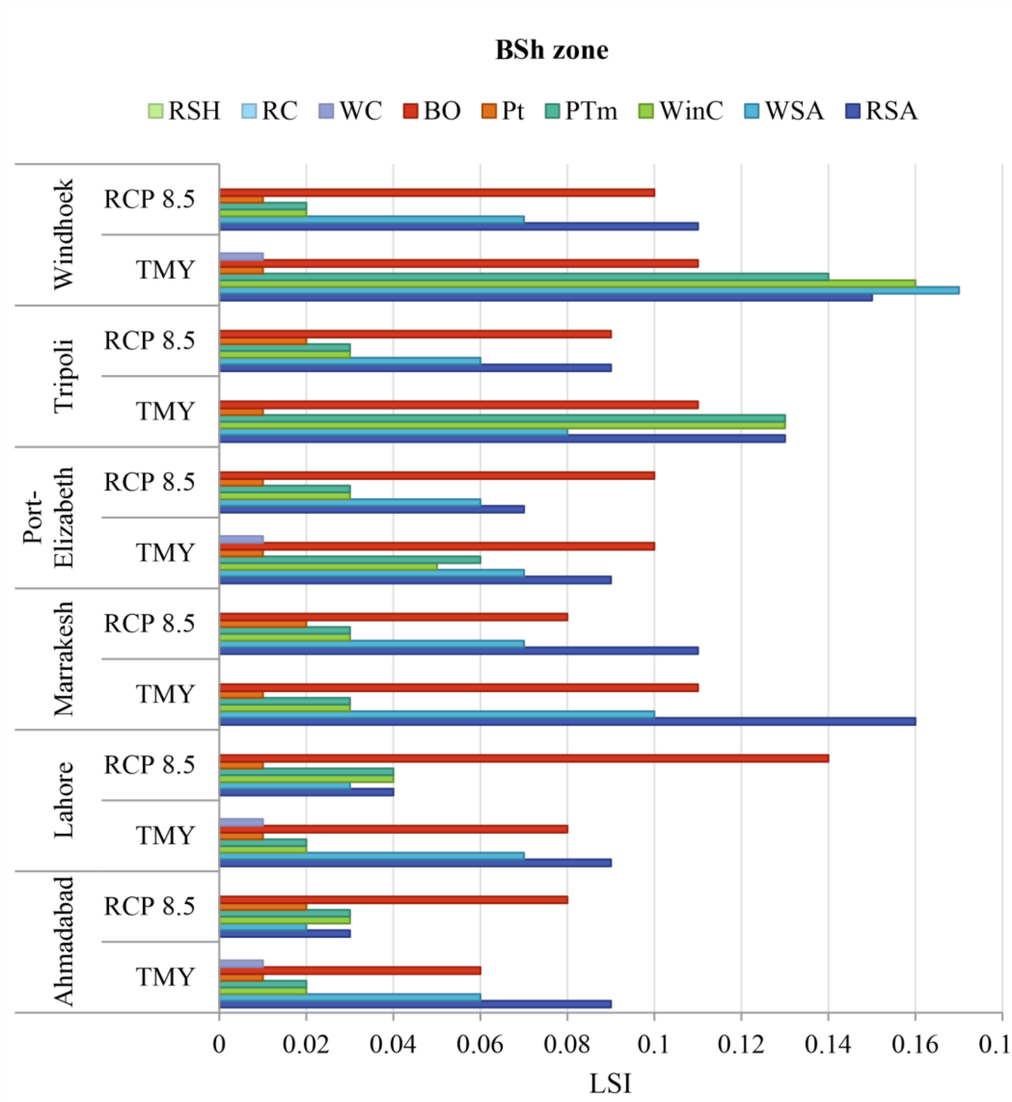

Figure 4.16: LSI for TEC in BSh zone for current and future climate scenarios.

4.3. Single-optimization results for current and future climate scenarios

This section presents the optimization outcomes for BSh zones under current and future climate scenarios. Five EDSP are chosen from the MSA for further optimization. The parameters that were not determined to be sensitive for objective function were set to be fixed.

4.3.1. **Single-optimization results for the current climate scenario**

This section provides the results for single-objective optimization in the BSh zone. The most important parameters are listed in Table 4.9.

Table 4.9: Optimization parameters range and base case values for BSh zone for the current scenario.

Input parameters	**Abbreviation**	**Units**	**Probability**	**Range**	**Base case**
Building orientation	BO	°	Continuous Uniform	{0, 360}	0
Roof solar absorptance	RSA	-	Continuous Uniform	[0.1, 0.9]	0.7
Wall solar absorptance	WSA	-	Continuous Uniform	[0.1, 0.9]	0.7
Window conductivity	WinC	W/m K	Continuous Uniform	[0.1, 1]	0.9
PCM melting temperature	PTm	ºC	Continuous Uniform	[20,30]	-

The ranges of obtained optimal solutions and energy consumption values for the BSh zone are summarized in Table 4.10. The optimal building orientation value in the BSh zone is 0, except for Tripoli. The RSA value is very close to the lower limits of the range, indicating that the light color of the roof in the BSh zone is useful for improving the energy efficiency of buildings. The WSA value ranges from 0.2 to 0.4, indicating that preference should be given to the light colors of walls. WinC is toward the upper limit of the range, as prescribed in Table 4.9. The optimal value of PCM melting temperature is 24 ºC in almost all cities except for Tripoli and Windhoek. A significant reduction in TEC was observed from the energy analysis of the base case and optimized solution. TEC reductions ranged from 11% to 20.4% compared to the base case in all selected cities. The maximum reductions (20.4 %) of TEC were achieved in Windhoek, while the minimum reductions (11 %) were achieved in Port Elizabeth.

Table 4.10: Detailed values of the optimal solutions in BSh zone for the current scenario.

Cities	Optimal early design stage parameters					TEC of base case (kWh)	TEC of optimal solution (kWh)	ES (%)
	BO	RSA	WSA	WinC	PTm			
Ahmadabad	0	0.1	0.4	0.6	24	218352	192960	11.6
Lahore	0	0.1	0.4	0.6	24	172467	150010	13
Marrakesh	0	0.1	0.4	0.6	24	93423	74817	20
Port Elizabeth	0	0.1	0.4	0.6	24	53589	47740	11
Tripoli	180	0.2	0.2	0.8	27	104597	89499	14.4
Windhoek	0	0.1	0.2	0.9	30	91081	72474	20.4

According to the aforementioned discussions, optimizing the TEC of the building depends heavily on choosing the proper ranges for EDSP. In summary, for the optimized solutions, RSA and WSA were reduced compared to the base case, while WinC remained close to the base case value. Regarding BO, for the optimized solution, its value was similar to the base case scenario (zero value). The wall and roof spaces remain colder because of the low values of RSA and WSA, which absorb less heat. The proper building orientation will reduce solar heat gain while increasing daylight. The optimum PCM maximizes indoor thermal comfort and minimizes the energy consumption of the building. In most cities, the finding of this research related to the optimum melting temperature of PCM is consistent with M'hambi et al. [199] investigation. They studied the impact of PCM integration in a residential building in Benguerir city (Morocco, BSh zone), where the optimum PCM melting temperate was 25 ºC. In the research of Solgi et al. [200], PCM with a melting temperature of 29 ºC was the appropriate one in the hot-arid climate of Phoenix, whereas PCM with a melting temperature of 27 ºC was optimum for Yazd. Even though both cities are located in a hot-arid zone, the research found that the differences in PCM melting temperature were assigned to the two cities' weather conditions variations and the set-point temperature of thermostats. A reason for the small difference in the value PCM melting temperature could be the differences in elevation, solar radiation, and wind speed, according to Saffari et al. [12].

In summary, it is observed that the optimal values of BO, RSA, and WSA were close to the lower limit, while those of WinC were close to the upper limit. In almost all cities, the optimal value of PCM melting temperature was 24 ºC. It is interesting to note that in four out of six cities, the optimal values were similar. Significant energy savings due to the use of optimization were achieved in the BSh zone.

4.3.2. **Single-optimization results for the future climate scenario**

This section presents the results of single-objective optimization in the BSh zone. Table 4.11 shows the five most significant parameters.

Table 4.11: Optimization parameters range and base case values in the BSh zone for the future scenario.

Input parameters	**Abbreviation**	**Units**	**Probability**	**Range**	**Base case**
Building orientation	BO	°	Continuous Uniform	{0, 360}	0
Roof solar absorptance	RSA	-	Continuous Uniform	[0.1, 0.9]	0.7
Wall solar absorptance	WSA	-	Continuous Uniform	[0.1, 0.9]	0.7
Window conductivity	WinC	W/m K	Continuous Uniform	[0.1, 1]	0.9
PCM melting temperature	PTm	ºC	Continuous Uniform	[20,30]	-

From the presented optimization results (Table 4.12), up to 12.9% energy savings can be achieved with the optimal EDSP in the BSh zone. Another important observation from the optimization results is that two groups of similar optimal design decisions were obtained. The first group of cities, which consists of four cities from six selected cities, conveyed the same optimal values of BO, RSA, WSA, WinC, and PTm (0, 0.1, 0.2, 0.9, and 30), while the second group consisting of the two remaining cities obtained similar values of BO, RSA, WSA, WinC, and PTm (180, 0.2, 0.2, 0.2, and 28). Based on the results, RSA and WSA were in the lower limit range, indicating the demand for light-colored walls and roofs to decrease the solar heat gain. The values of WinC were on the upper side of the range, except for Ahmadabad and Lahore. Building orientation had similar values as the base case, except for Ahmadabad and Lahore. In all cities, the PTm was on the upper side of the range. In summary, according to the single optimization results, energy savings ranging between 6.6 % and 12.7 % were obtained in the BSh zone.

Table 4.12: Detailed values of the optimal solutions in BSh zone for the future scenario.

Cities	**Optimal early design stage parameters**					**TEC of base case (kWh)**	**TEC of optimal solution (kWh)**	**ES (%)**
	BO	**RSA**	**WSA**	**WinC**	**PTm**			
Ahmadabad	180	0.2	0.2	0.2	28	221808	206830	6.6
Lahore	180	0.2	0.2	0.2	28	238686	218521	8.5
Marrakesh	0	0.1	0.2	0.9	30	169166	147250	13
Port Elizabeth	0	0.1	0.2	0.9	30	108916	99972	8.2
Tripoli	0	0.1	0.2	0.9	30	164688	146437	11.1
Windhoek	0	0.1	0.2	0.9	30	140424	122360	12.9

4.3.3. **Comparative analysis of single-objective results**

This section presents the results of optimal solutions obtained from current and future scenarios for the BSh zone. Table 4.13 shows the base case results, optimized solutions, and obtained energy savings for current and future climate scenarios. It can be noted that for most of the cities, the insignificant change in measures of EDSP was recognized in the future for the BSh zone. For example, RSA increased from 0.1 to 0.2 in two cities, while WSA decreased from 0.4 to 0.2 in four cities. Also, some changes in BO were observed in Ahmadabad and Lahore in the future, where the BO changed from 0º to 180º. The WinC tended to achieve the upper bound of the range in four cities of the BSh zone, while in the remaining two cities, values were on the lower side of the range. In the future scenario, the optimized solution's PTm range was on the higher side. Compared to the base case, the TEC of the base case in the current scenario varied from 53589 kWh to 218352 kWh, while in the future scenario, the TEC altered from 108916 kWh to 221808 kWh. In the current scenario, optimal solutions ranged from 47740 kWh to 192960 kWh, whereas optimal solutions for the future ranged from 99992 kWh to 206830 kWh. The findings indicated that the energy savings were in the range of 11% and 20.4% in the current scenario, while the energy savings for the future scenario were in the range of 6.6 and 13%.

According to the above discussions, maximizing a building's TEC is largely dependent on selecting the appropriate ranges for EDSP. Compared to the current scenario, the energy savings rate in the future scenario was lower. The lower rate of energy savings can be explained by that the in RCP 8.5 scenario, the greenhouse gas emissions continue to rise throughout the century, leading to a significant increase in global temperatures and resulting in increased demand for energy for cooling purposes. Variations in the optimal EDSP ranges were observed in certain cities.

Table 4.13: Base case and optimal solutions for current and future scenarios in the BSh zone.

Cities	Early design stage parameters										TEC					
	BO (°)		RSA		WSA		WinC (W/m K)		PTm (ºC)		Base case (kWh)		Optimal solution (kWh)		Energy savings (%)	
	TMY	**RCP 8.5***	**TMY**	**RCP 8.5***	**TMY**	**RCP 8.5***	**TMY**	**RCP 8.5***	**TMY**	**RCP 8.5***	**TMY**	**RCP 8.5**	**TMY**	**RCP 8.5**	**TMY**	**RCP 8.5**
Ahmadabad	0	180	0.1	0.2	0.4	0.2	0.6	0.2	24	28	218352	221808	192960	206830	11.6	6.6
Lahore	0	180	0.1	0.2	0.4	0.2	0.6	0.2	24	28	172467	238686	150010	218521	13	8.5
Marrakesh	0	0	0.1	0.1	0.4	0.2	0.6	0.9	24	30	93423	169166	74817	147250	20	13
Port-Elizabeth	0	0	0.1	0.1	0.4	0.2	0.6	0.9	24	30	53589	108916	47740	99972	11	8.2
Tripoli	180	0	0.2	0.1	0.2	0.2	0.8	0.9	27	30	104597	164688	89499	146437	14.4	11.1
Windhoek	0	0	0.1	0.1	0.2	0.2	0.9	0.9	30	30	91081	140424	72474	122360	20.4	12.9

4.4. Economic results for the current climate scenario

An economic analysis was conducted for the optimal solutions located in the six cities of BSh zone for the current climate scenario due to the availability of the data prices. The payback period obtained for each location in the BSh zone is demonstrated in Table 4.14. The economic advantage increases with a decreasing payback period. The payback periods for Ahmadabad, Lahore, Marrakesh, Port Elizabeth, Tripoli, and Windhoek corresponded to 28.3, 42.5, 26.4, 63.7, 869.4, and 25.7 years, respectively. The minimum payback period was 25.7 years in Windhoek, while the maximum PB of 869.4 years was in Tripoli. The reason for the highest payback period in Tripoli (Libya) is the lowest energy price for electricity (0.004 $/kWh). Due to its large oil reserves and expanding renewable energy projects, Libya's energy costs are significantly subsidized by the government, and the country is completely self-sufficient in terms of power [201]. Almost all optimal solutions were feasible since the payback time was less than the typical lifespan (from 50 to 100 years) [202] of a residential building in the BSh climatic zone. In the research of M'hamdi et al. [199], the PCM integration in the residential building envelope in Benguerir city, located in Morocco (BSh zone), showed a payback period of 19.24 years.

In summary, in most cities, applying optimal solutions would result in a payback period of 25.7 - 63.7 years in the BSh zone. Since the recovery time is substantially shorter than the typical lifespan (60 to 100 years) of residential buildings, it is practical and affordable to use the optimal solutions of EDSP.

Table 4.14: Economic analysis of optimal solutions in the BSh zone for the current climate scenario.

City	Ahmadabad	Lahore	Marrakesh	Port Elizabeth	Tripoli	Windhoek
ES (kWh)	25392	22457	18606	5849	15098	18607
PB (years)	28.3	42.5	26.4	63.7	869.4	25.7

4.5. Chapter summary

This chapter focused on examining the total energy consumption of base cases, MSA, optimization and economic analyses of PCM-integrated residential buildings and the impact of climate change. The first part of the chapter presented the weather data variations under the impact of climate change and the results of base case simulations to demonstrate the total energy consumption variations in the current and future climate scenarios. The next part of the chapter presented the results of MSA and optimization to examine the relative importance of EDSP in the current and future climate scenarios in the BSh zone. Afterwards, an economic assessment of the current climate scenario was employed. The main findings from the chapter are listed below:

- Across all locations, the increasing tendency in total energy consumption can be observed in the BSh climate zone (51.7%), implying that more energy will be consumed in 2095. The average temperature was expected to increase by 5.07 ℃ in the BSh zone.
- The first stage MSA in the BSh zone in the current climate scenario revealed that the most important parameters for TEC in the BSh zone were RSA, WSA, and WinC based on SRRC, while RSA, WSA, WinC, RC, RSH, Pt, WC, and PTm were found to be significant parameters based on PRCC results. The Morris method displayed that BO, RSA, WSA, and PTm were the parameters that contributed the most to the TEC. According to the ranking of the BSh zone, the most important parameters of the first stage sensitivity analysis were: RSA, WSA, WinC, BO, RC, PTm, Pt, and WC. Furthermore, in several cities in the same climatic zone, the rankings of several EDSP may change significantly.
- Results of MSA and optimization in the future climate scenario in the BSh zone showed that the RSA, WSA, RC, WinC, BO, RSH, PTm, and Pt were the influential parameters based on the SRRC. PRCC results indicated that RSA, WSA, RC, RSH, BO, Pt, and WinC were the significant parameters on TEC. According to the Morris method, BO, RSA, WSA, PTm, RSH, Pt, and WC showed the importance of the TEC. The ranking results in the BSh zone indicated that RSA, WSA, BO, WinC, PTm, RSH, RC, and Pt were the important parameters on TEC. Compared to the SRRC and PRCC, Morris

had a completely different rating. A comparison of the rankings of current and future climate scenarios showed no substantial change in the rankings of RSA and WSA, while other parameters showed variations, and the same eight EDSP were selected for local sensitivity analysis. Some alterations to the rankings of the SRRC, PRCC, and Morris methods were indicated for the BSh zone in the future;

- Comparing the first stage of MSA under TMY and RCP 8.5, it was found that while certain parameters might remain constant, others can be relevant in future climate scenarios during the EDSP in the BSh zone. A decline in RSA and WSA significance was predicted in the BSh zone based on SRRC and PRCC results. Future adjustments to WVT, WSH, and WC were negligible. The signs of WSA, RSA, WSH, RC, and WC remained steady across the century. μ^* value was significantly larger in the BSh zone for RCP 8.5. RSH was anticipated to climb significantly in the BSh zone. The relationship of μ^* and δ in Morris EE indicated the non-linearity amongst all input parameters except the RSA, which showed a monotonic relationship;
- In the current climate scenario, the second stage of sensitivity analysis revealed that the RSA, WSA, BO, WinC, and PTm were the most significant parameters in the BSh zone. In the future climate scenario, a local sensitivity analysis revealed the five design parameters for optimization in both zones: BO, RSA, WSA, WinC, and PTm. The comparison of climatic scenarios showed that the significance of RSA and WSA decreased in the future scenario in the BSh zone, while the significance of BO, PTm, Pt, and WinC dropped in half of the cities.
- In the TMY and applying single-objective optimization, 11% to 20.4% energy reductions can be obtained in the BSh zone. The feasibility of optimal solutions was demonstrated by the payback period, which ranged from 25.7 to 63.7 years in the BSh zone. Based on these findings, it is concluded that it is practicable and feasible to apply the optimized solution of EDSP since the recovery period is significantly shorter than the typical lifespan (between 60 and 100 years) of residential buildings.
- In the RCP 8.5, by single-objective optimization, a 6.6 % to 12.7% savings in total energy load was observed by varying five EDSP in the BSh zone. According to the results, the five EDSP were equally important for current

and future climate scenarios for the BSh zone: BO, RSA, WSA, WinC, and PTm.

CHAPTER 5: CONCLUSIONS

This thesis addressed the issues discussed in Chapter 1 by proposing a framework for developing an MSA and optimization approach applied to PCM-integrated buildings. This chapter highlights the conclusions, limitations, and future recommendations.

5.1. Conclusions

This thesis proposes an MSA and single-objective optimization framework to assess the impact of EDSP on the total energy consumption under current and future climate scenarios in the BSh climate zone. MSA implemented three global sensitivity analysis approaches (SRRC, PRCC, and Morris method) in the first stage, while local sensitivity analysis was employed in the second stage. The ranking of the relative importance of parameters was calculated, and the list of the most important parameters was derived. The combination of local and global sensitivity analysis has shown to be a reasonable method for determining the most important parameters. After that, a single objective optimization was utilized. Input parameters are limited to the eleven EDSP, representing the building geometry, energy-efficiency measures, and thermophysical properties.

To define the most significant EDSP, an MSA was employed. At the first stage of MSA, the set of EDSP derived from the SRRC, PRCC, and Morris methods differed. The relative importance of design parameters obtained from first stage sensitivity analysis was compared by applying ranking. Generally, the SRRC and PRCC rankings were almost identical. Relatively small changes in the order of importance in the Morris method were observed in the BSh zone. These changes were expected since the sensitivity of design parameters may vary depending on climatic conditions. The eight most significant parameters were selected for the second stage of the MSA. Five EDSP (BO, RSA, WSA, WinC, PTm) were selected for the optimization of current and future climate scenarios.

To get the best understanding of the behavior of the EDSP in relation to the total energy consumption, the interactions between parameters were revealed. The sign of direction derived from SRRC indicated a set of EDSP with positive (RSA, WSA, BO, and RC) and negative (WinC, PTm) correlations for the current scenario in the BSh zone. The SRRC and PRCC signs of some parameters tend to change in the future. Throughout the century, the signs for WSA, RSA, RSH, and RC remained the same. For most parameters, strong non-linearity and/or interaction effects were found.

Based on the results of the MSA, a single-objective optimization was performed. The optimal solutions based on total energy consumption and lifetime constraints were obtained using Evolutionary Algorithms in conjunction with EnergyPlus and jEPlus.

Improving the TEC of the building is strongly reliant on selecting the appropriate ranges for EDSP. The combination of EDSP such as RSA, WSA, WinC, BO, and PTm showed substantial energy savings. In the current scenario, up to 20.4% of savings in total energy load was observed by varying five EDSP in the BSh zone, while up to 13% of energy savings were achieved in the future scenario.

The economic feasibility of optimal solutions was evaluated in the current scenario. Using the optimal solutions, most cities' payback periods ranged from 25.7 to 63.7 years. The recovery period is much shorter than the typical lifespan (60 to 100 years) of residential buildings, thus making it feasible and cost-effective to apply the optimal approaches from the EDSP.

The findings indicated that the total energy consumption of residential buildings would increase due to the impact of climate change; however, energy savings can be achieved through the optimization of EDSP. Up to 6.6% to 12.7% savings in total energy load were achieved by optimizing design parameters in the BSh zone in the RCP 8.5, respectively. It was noted that multiple sets of optimized parameters had been identified for the optimized designs under the impact of climate change on the zone. It is important to note that in this research, only a certain number of potential optimization parameters were considered. More optimization parameters might result in greater energy savings.

The MSA and optimization approach demonstrated to be appealing to building performance modeling techniques since it may reveal important details about the building model that would not be acquired using single methods. MSA in the early design stage can yield useful data about the EDSP with the greatest impact on the overall energy consumption and their ranges, which could be used in the later design stage. The data can aid designers in calculating anticipated energy savings and assessing the energy effectiveness of proposed energy conservation strategies. Furthermore, the findings of this research lead to some general recommendations for the early design stage of residential buildings in hot semi-arid climates. Some recommendations are presented as follows:

- According to research, when multiple SA approaches are employed, the ranking outcome for the same model might be distinct. As a result, when distributing computing materials, stakeholders are advised to use several SA methodologies to acquire a thorough knowledge of the system.
- The revealing of the most sensitive parameters concerning energy efficiency will assist in focusing on the optimization of the most significant design parameters.

- For the current scenario, using light colors on the roof and walls is recommended in the BSh zone to achieve higher energy efficiency. Because of the low RSA and WSA values, which absorb less heat, the wall and roof spaces stay cool.

5.2. Limitations of the current research

The findings in the present research are relevant to the building under investigation. The data reported in the study only serve as reference values for mid-rise apartment buildings and other related building types rather than the overall building stock. The two types of weather data (TMY and RCP 8.5) were utilized, whereas more comprehensive research would look at numerous climate model forecasts and socioeconomic situations. As a result, the outcomes reported here exclusively depend on the climatic information employed. The cost of PCM was considered to be constant throughout entire zone. As well as life-time of PCM building are regarded to be common, and the PCM melting temperature was in the range of 20℃ - 30℃. In the building energy simulations, the time-step was selected to the three minutes. Both the urban environment and urban heat island around the building were not modeled, even though it is well recognized that these factors significantly impact the dynamic thermal behavior of buildings, such as the possibility for solar heat gains or natural ventilation.

5.3. Recommendations for future research

This thesis has contributed to some fundamental findings in PCM-integrated buildings in hot semi-arid climates. Future investigations might include:

- Application of this methodology to a more complex model with the aim to examine the impact of EDSP on various building performance objectives such as thermal comfort, environmental impacts, and life cycle cost. Simultaneously examining different performance criteria contributes to a more precise and exhaustive assessment. In addition, future research might concentrate on employing other sensitivity analysis methods, different EDSP, weather conditions, and building typologies to provide detailed instructions that can be used nationwide to construct the buildings to achieve environmentally friendly buildings.
- Inclusion of different thermal characteristics of building materials to examine the impact on energy consumption is required.
- Due to the requirement for rapid feedback in the early design stage, the application of machine learning predictive models to replace the procedures of building simulations and optimization should be considered in the future;

- The employment of diverse occupancy behavior scenarios to assess the influence of climate change on the building's thermal efficiency, and examining their impact under different conditions is required.

BIBLIOGRAPHY

[1] Guo R, Gao Y, Zhuang C, Heiselberg P, Levinson R, Zhao X, et al. Optimization of cool roof and night ventilation in office buildings: A case study in Xiamen, China. Renew Energy 2020;147:2279–94. https://doi.org/10.1016/j.renene.2019.10.032.

[2] Karakurt I, Aydin G. Development of regression models to forecast the CO2 emissions from fossil fuels in the BRICS and MINT countries. Energy 2023;263:125650. https://doi.org/10.1016/j.energy.2022.125650.

[3] Martins F, Felgueiras C, Smitkova M, Caetano N. Analysis of fossil fuel energy consumption and environmental impacts in european countries. Energies 2019;12:1–11. https://doi.org/10.3390/en12060964.

[4] Share of world total final consumption by source, 2019 – Charts – Data & Statistics - IEA n.d. https://www.iea.org/data-and-statistics/charts/share-of-world-total-final-consumption-by-source-2019 (accessed February 15, 2023).

[5] Reynolds J, Rezgui Y, Kwan A, Piriou S. A zone-level, building energy optimisation combining an artificial neural network, a genetic algorithm, and model predictive control. Energy 2018;151:729–39. https://doi.org/10.1016/j.energy.2018.03.113.

[6] Ascione F, De Masi RF, de Rossi F, Ruggiero S, Vanoli GP. Optimization of building envelope design for nZEBs in Mediterranean climate: Performance analysis of residential case study. Appl Energy 2016;183:938–57. https://doi.org/10.1016/j.apenergy.2016.09.027.

[7] Harkouss F, Fardoun F, Biwole PH. Passive design optimization of low energy buildings in different climates. Energy 2018;165:591–613. https://doi.org/10.1016/j.energy.2018.09.019.

[8] UNEP. 2020 Global Status Report for Buildings and Construction. Glob Status Rep 2020:20–4.

[9] Cabeza LF, Martorell I, Miró L, Fernández AI, Barreneche C. Introduction to thermal energy storage (TES) systems. Woodhead Publishing Limited; 2015. https://doi.org/10.1533/9781782420965.1.

[10] Sharma A, Tyagi V V., Chen CR, Buddhi D. Review on thermal energy storage with phase change materials and applications. Renew Sustain Energy Rev 2009;13:318–45. https://doi.org/10.1016/j.rser.2007.10.005.

[11] Ramakrishnan S, Wang X, Sanjayan J, Wilson J. Thermal performance of buildings integrated with phase change materials to reduce heat stress risks during extreme heatwave events. Appl Energy 2017;194:410–21. https://doi.org/10.1016/j.apenergy.2016.04.084.

[12] Saffari M, de Gracia A, Fernández C, Cabeza LF. Simulation-based optimization of PCM melting temperature to improve the energy performance in buildings. Appl Energy 2017;202:420–34. https://doi.org/10.1016/j.apenergy.2017.05.107.

[13] Hester J, Gregory J, Kirchain R. Sequential early-design guidance for residential single-family buildings using a probabilistic metamodel of energy consumption. Energy Build 2017;134:202–11. https://doi.org/10.1016/j.enbuild.2016.10.047.

[14] Méndez Echenagucia T, Capozzoli A, Cascone Y, Sassone M. The early design stage of a building envelope: Multi-objective search through heating, cooling and lighting energy performance analysis. Appl Energy 2015;154:577–91. https://doi.org/10.1016/j.apenergy.2015.04.090.

[15] Chen X, Yang H, Zhang W. A comprehensive sensitivity study of major passive design parameters for the public rental housing development in Hong Kong. Energy 2015;93:1804–18. https://doi.org/10.1016/j.energy.2015.10.061.

[16] Hamdy M, Nguyen AT, Hensen JLM. A performance comparison of multi-objective optimization algorithms for solving nearly-zero-energy-building design problems. Energy Build 2016;121:57–71. https://doi.org/10.1016/j.enbuild.2016.03.035.

[17] Menberg K, Heo Y, Choudhary R. Sensitivity analysis methods for building energy models: Comparing computational costs and extractable information. Energy Build 2016;133:433–45. https://doi.org/10.1016/j.enbuild.2016.10.005.

[18] Mara TA, Tarantola S. Application of global sensitivity analysis of model output to building thermal simulations. Build Simul 2008;1:290–302. https://doi.org/10.1007/s12273-008-8129-5.

[19] Yang Z, Becerik-Gerber B. A model calibration framework for simultaneous multi-level building energy simulation. Appl Energy 2015;149:415–31. https://doi.org/10.1016/j.apenergy.2015.03.048.

[20] Domínguez-Muñoz F, Cejudo-López JM, Carrillo-Andrés A. Uncertainty in peak cooling load calculations. Energy Build 2010;42:1010–8. https://doi.org/10.1016/j.enbuild.2010.01.013.

[21] Fang Y, Cho S. Design optimization of building geometry and fenestration for daylighting and energy performance. Sol Energy 2019;191:7–18. https://doi.org/10.1016/j.solener.2019.08.039.

[22] Al-Janabi A, Kavgic M. Application and sensitivity analysis of the phase change material hysteresis method in EnergyPlus: A case study. Appl Therm Eng 2019;162:114222. https://doi.org/10.1016/j.applthermaleng.2019.114222.

[23] Kishore RA, Bianchi MVA, Booten C, Vidal J, Jackson R. Parametric and sensitivity analysis of a PCM-integrated wall for optimal thermal load modulation in lightweight buildings. Appl Therm Eng 2021;187:116568. https://doi.org/10.1016/j.applthermaleng.2021.116568.

[24] Chen X, Yang H. Sensitivity analysis and optimization of a typical passively designed residential building with hybrid ventilation in hot and humid climates. Energy Procedia 2017;142:1781–6. https://doi.org/10.1016/j.egypro.2017.12.563.

[25] Chen X, Yang H. Integrated energy performance optimization of a passively designed high-rise residential building in different climatic zones of China. Appl Energy 2018;215:145–58. https://doi.org/10.1016/j.apenergy.2018.01.099.

[26] Bre F, Silva AS, Ghisi E, Fachinotti VD. Residential building design optimisation using sensitivity analysis and genetic algorithm. Energy Build 2016;133:853–66. https://doi.org/10.1016/j.enbuild.2016.10.025.

[27] Ioannou A, Itard LCM. Energy performance and comfort in residential buildings: Sensitivity for building parameters and occupancy. Energy Build 2015;92:216–33. https://doi.org/10.1016/j.enbuild.2015.01.055.

[28] Heiselberg P, Brohus H, Hesselholt A, Rasmussen HE., Seinre E, Thomas S.

Application of Sensitivity analysis in Design of Sustanable buildings. SDBE 2007 Sustanable Dev Build Environ Chongqing Univ 2007.

[29] Yang S, Tian W, Cubi E, Meng Q, Liu Y, Wei L. Comparison of Sensitivity Analysis Methods in Building Energy Assessment. Procedia Eng 2016;146:174–81. https://doi.org/10.1016/j.proeng.2016.06.369.

[30] Zeferina V, Wood R, Xia J, Edwards R. Sensitivity analysis of a simplified office building. J Phys Conf Ser 2019;1343. https://doi.org/10.1088/1742-6596/1343/1/012129.

[31] Østergård T, Jensen RL, Maagaard SE. Building simulations supporting decision making in early design - A review. Renew Sustain Energy Rev 2016;61:187–201. https://doi.org/10.1016/j.rser.2016.03.045.

[32] Gervásio H, Santos P, Martins R, Simões da Silva L. A macro-component approach for the assessment of building sustainability in early stages of design. Build Environ 2014;73:256–70. https://doi.org/10.1016/j.buildenv.2013.12.015.

[33] Feng K, Lu W, Wang Y. Assessing environmental performance in early building design stage: An integrated parametric design and machine learning method. Sustain Cities Soc 2019;50:101596. https://doi.org/10.1016/j.scs.2019.101596.

[34] Delgarm N, Sajadi B, Azarbad K, Delgarm S. Sensitivity analysis of building energy performance: A simulation-based approach using OFAT and variance-based sensitivity analysis methods. J Build Eng 2018;15:181–93. https://doi.org/10.1016/j.jobe.2017.11.020.

[35] Basbagill J, Flager F, Lepech M, Fischer M. Application of life-cycle assessment to early stage building design for reduced embodied environmental impacts. Build Environ 2013;60:81–92. https://doi.org/10.1016/j.buildenv.2012.11.009.

[36] Ochoa CE, Capeluto IG. Advice tool for early design stages of intelligent facades based on energy and visual comfort approach. Energy Build 2009;41:480–8. https://doi.org/10.1016/j.enbuild.2008.11.015.

[37] Ciardiello A, Rosso F, Dell'Olmo J, Ciancio V, Ferrero M, Salata F. Multi-objective approach to the optimization of shape and envelope in building energy design. Appl Energy 2020;280:115984. https://doi.org/10.1016/j.apenergy.2020.115984.

[38] Acar U, Kaska O, Tokgoz N. Multi-objective optimization of building envelope components at the preliminary design stage for residential buildings in Turkey. J Build Eng 2021;42:102499. https://doi.org/10.1016/j.jobe.2021.102499.

[39] Yip S, Athienitis AK, Lee B. Early stage design for an institutional net zero energy archetype building. Part 1: Methodology, form and sensitivity analysis. Sol Energy 2021;224:516–30. https://doi.org/10.1016/j.solener.2021.05.091.

[40] Li Z, Chen H, Lin B, Zhu Y. Fast bidirectional building performance optimization at the early design stage. Build Simul 2018;11:647–61. https://doi.org/10.1007/s12273-018-0432-1.

[41] Lamrani B, Johannes K, Kuznik F. Phase change materials integrated into building walls: An updated review. Renew Sustain Energy Rev 2021;140:110751. https://doi.org/10.1016/j.rser.2021.110751.

[42] Li C, Wen X, Cai W, Yu H, Liu D. Phase change material for passive cooling in building envelopes: A comprehensive review. J Build Eng 2023;65:105763. https://doi.org/10.1016/j.jobe.2022.105763.

[43] Hussain F, Rahman MZ, Sivasengaran AN, Hasanuzzaman M. Energy storage technologies. Elsevier Inc.; 2019. https://doi.org/10.1016/B978-0-12-814645-3.00006-7.

[44] Abdin Z, Khalilpour KR. Single and polystorage technologies for renewable-based hybrid energy systems. Elsevier Inc.; 2018. https://doi.org/10.1016/B978-0-12-813306-4.00004-5.

[45] Menghare YM, Jibhakate YM. Review On Sensible Heat Storage System Principle, Performance And Analysis 2013;2:3432–5.

[46] Lawag RA, Ali HM. Phase change materials for thermal management and energy storage: A review. J Energy Storage 2022;55:105602. https://doi.org/10.1016/j.est.2022.105602.

[47] Zhang J, Cho H, Mago PJ. Energy conversion systems and Energy storage systems. INC; 2020. https://doi.org/10.1016/B978-0-12-820592-1.00007-5.

[48] Sarbu I, Sebarchievici C. A comprehensive review of thermal energy storage. Sustain 2018;10. https://doi.org/10.3390/su10010191.

[49] Lizana J, Chacartegui R, Barrios-Padura A, Valverde JM. Advances in thermal energy storage materials and their applications towards zero energy buildings: A critical review. Appl Energy 2017;203:219–39. https://doi.org/10.1016/j.apenergy.2017.06.008.

[50] Zeinelabdein R, Omer S, Gan G. Critical review of latent heat storage systems for free cooling in buildings. Renew Sustain Energy Rev 2018;82:2843–68. https://doi.org/10.1016/j.rser.2017.10.046.

[51] Luu MT, Milani D, Nomvar M, Abbas A. Computer-aided design for high efficiency latent heat storage – a case study of a novel domestic solar hot water process. vol. 40. Elsevier Masson SAS; 2017. https://doi.org/10.1016/B978-0-444-63965-3.50194-X.

[52] Topličić – Ćurčić G, Keković A, Grdić D, Đorić – Veljković S, Grdić Z. Fazno Promenljivi Materijali – Inovativni Materijali Za Poboljšanje Energetske Efikasnosti Objekata. Zb Rad Građevinskog Fak 2018;34:323–34. https://doi.org/10.14415/konferencijagfs2018.032.

[53] Phase Change Material (PCM) n.d. https://thermtest.com/phase-change-material-pcm (accessed January 13, 2023).

[54] Sharma SD, Sagara K. Latent Heat Storage Materials and Systems: A Review. Int J Green Energy 2005;2:1–56. https://doi.org/10.1081/ge-200051299.

[55] Hamby DM. A Review of Techniques for Parameter Sensitivity. Environ Monit Assess 1994;32:135–54.

[56] Kalnæs SE, Jelle BP. Phase change materials and products for building applications: A state-of-the-art review and future research opportunities. vol. 94. Elsevier B.V.; 2015. https://doi.org/10.1016/j.enbuild.2015.02.023.

[57] Zhou D, Zhao CY, Tian Y. Review on thermal energy storage with phase change materials (PCMs) in building applications. Appl Energy 2012;92:593–605. https://doi.org/10.1016/j.apenergy.2011.08.025.

[58] Al-Yasiri Q, Szabó M. Incorporation of phase change materials into building envelope for thermal comfort and energy saving: A comprehensive analysis. J Build

Eng 2021;36. https://doi.org/10.1016/j.jobe.2020.102122.

[59] Kharbouch Y. Effectiveness of phase change material in improving the summer thermal performance of an office building under future climate conditions: An investigation study for the Moroccan Mediterranean climate zone. J Energy Storage 2022;54:105253. https://doi.org/10.1016/j.est.2022.105253.

[60] Saffari M, De Gracia A, Ushak S, Cabeza LF. Economic impact of integrating PCM as passive system in buildings using Fanger comfort model. Energy Build 2016;112:159–72. https://doi.org/10.1016/j.enbuild.2015.12.006.

[61] Hagenau M, Jradi M. Dynamic modeling and performance evaluation of building envelope enhanced with phase change material under Danish conditions. J Energy Storage 2020;30:101536. https://doi.org/10.1016/j.est.2020.101536.

[62] Jin X, Medina MA, Zhang X. On the importance of the location of PCMs in building walls for enhanced thermal performance. Appl Energy 2013;106:72–8. https://doi.org/10.1016/j.apenergy.2012.12.079.

[63] Biswas K, Abhari R. Low-cost phase change material as an energy storage medium in building envelopes: Experimental and numerical analyses. Energy Convers Manag 2014;88:1020–31. https://doi.org/10.1016/j.enconman.2014.09.003.

[64] Hachem C, Athienitis A, Fazio P. Parametric investigation of geometric form effects on solar potential of housing units. Sol Energy 2011;85:1864–77. https://doi.org/10.1016/j.solener.2011.04.027.

[65] Calleja Rodríguez G, Carrillo Andrés A, Domínguez Muñoz F, Cejudo López JM, Zhang Y. Uncertainties and sensitivity analysis in building energy simulation using macroparameters. Energy Build 2013;67:79–87. https://doi.org/10.1016/j.enbuild.2013.08.009.

[66] Wei T. A review of sensitivity analysis methods in building energy analysis. Renew Sustain Energy Rev 2013;20:411–9. https://doi.org/10.1016/j.rser.2012.12.014.

[67] Østergård T, Jensen RL, Maagaard SE. Early Building Design: Informed decision-making by exploring multidimensional design space using sensitivity analysis. Energy Build 2017;142:8–22. https://doi.org/10.1016/j.enbuild.2017.02.059.

[68] Silva AS, Ghisi E. Estimating the sensitivity of design variables in the thermal and energy performance of buildings through a systematic procedure. J Clean Prod 2020;244:118753. https://doi.org/10.1016/j.jclepro.2019.118753.

[69] Kristensen MH, Petersen S. Choosing the appropriate sensitivity analysis method for building energy model-based investigations. Energy Build 2016;130:166–76. https://doi.org/10.1016/j.enbuild.2016.08.038.

[70] Pang Z, O'Neill Z, Li Y, Niu F. The role of sensitivity analysis in the building performance analysis: A critical review. Energy Build 2020;209:109659. https://doi.org/10.1016/j.enbuild.2019.109659.

[71] Pang Z, O'Neill Z. Uncertainty quantification and sensitivity analysis of the domestic hot water usage in hotels. Appl Energy 2018;232:424–42. https://doi.org/10.1016/j.apenergy.2018.09.221.

[72] Iooss B, Van Dorpe F, Devictor N. Response surfaces and sensitivity analyses for an environmental model of dose calculations. Reliab Eng Syst Saf 2006;91:1241–51. https://doi.org/10.1016/j.ress.2005.11.021.

[73] Saltelli A, Ratto M, Andres T, Campolongo F, Cariboni J, Gatelli D, et al. Global sensitivity analysis: The primer. John Wiley & Sons Ltd; 2008.

[74] Heiselberg P, Brohus H, Hesselholt A, Rasmussen H, Seinre E, Thomas S. Application of sensitivity analysis in design of sustainable buildings. Renew Energy 2009;34:2030–6. https://doi.org/10.1016/j.renene.2009.02.016.

[75] Saltelli A, Tarantola S, Campolongo F, Ratto M. Sensitivity analysis in practice: a guide to assessing scientific models (Google eBook). 2004.

[76] de Wilde P, Tian W. Identification of key factors for uncertainty in the prediction of the thermal performance of an office building under climate change. Build Simul 2009;2:157–74. https://doi.org/10.1007/s12273-009-9116-1.

[77] Nguyen AT, Reiter S. A performance comparison of sensitivity analysis methods for building energy models. Build Simul 2015;8:651–64. https://doi.org/10.1007/s12273-015-0245-4.

[78] Kishore RA, Bianchi MVA, Booten C, Vidal J, Jackson R. Optimizing PCM-integrated walls for potential energy savings in U.S. Buildings. Energy Build 2020;226. https://doi.org/10.1016/j.enbuild.2020.110355.

[79] Gagnon R, Gosselin L, Decker S. Sensitivity analysis of energy performance and thermal comfort throughout building design process. Energy Build 2018;164:278–94. https://doi.org/10.1016/j.enbuild.2017.12.066.

[80] Li H, Wang S, Cheung H. Sensitivity analysis of design parameters and optimal design for zero/low energy buildings in subtropical regions. Appl Energy 2018;228:1280–91. https://doi.org/10.1016/j.apenergy.2018.07.023.

[81] Pianosi F, Sarrazin F, Wagener T. A Matlab toolbox for Global Sensitivity Analysis. Environ Model Softw 2015;70:80–5. https://doi.org/10.1016/j.envsoft.2015.04.009.

[82] Palonen M, Hamdy M, Hasan A. Mobo a new software for multi-objective building performance optimization. Proc BS 2013 13th Conf Int Build Perform Simul Assoc 2013:2567–74.

[83] Machairas V, Tsangrassoulis A, Axarli K. Algorithms for optimization of building design: A review. Renew Sustain Energy Rev 2014;31:101–12. https://doi.org/10.1016/j.rser.2013.11.036.

[84] Evins R. A review of computational optimisation methods applied to sustainable building design. Renew Sustain Energy Rev 2013;22:230–45. https://doi.org/10.1016/j.rser.2013.02.004.

[85] Nguyen AT, Reiter S, Rigo P. A review on simulation-based optimization methods applied to building performance analysis. Appl Energy 2014;113:1043–58. https://doi.org/10.1016/j.apenergy.2013.08.061.

[86] Attia S, Hamdy M, O'Brien W, Carlucci S. Assessing gaps and needs for integrating building performance optimization tools in net zero energy buildings design. Energy Build 2013;60:110–24. https://doi.org/10.1016/j.enbuild.2013.01.016.

[87] Huang Y, Niu JL. Optimal building envelope design based on simulated performance: History, current status and new potentials. Energy Build 2016;117:387–98. https://doi.org/10.1016/j.enbuild.2015.09.025.

[88] Cui Y, Geng Z, Zhu Q, Han Y. Review: Multi-objective optimization methods and application in energy saving. Energy 2017;125:681–704.

https://doi.org/10.1016/j.energy.2017.02.174.

[89] Yang XS. Optimization and Metaheuristic Algorithms in Engineering. Metaheuristics Water, Geotech Transp Eng 2013:1–23. https://doi.org/10.1016/B978-0-12-398296-4.00001-5.

[90] Hopfe CJ, Hensen JLM. Uncertainty analysis in building performance simulation for design support. Energy Build 2011;43:2798–805. https://doi.org/10.1016/j.enbuild.2011.06.034.

[91] Liberti L, Kucherenko S. Comparison of deterministic and stochastic approaches to global optimization. Int Trans Oper Res 2005;12:263–85. https://doi.org/10.1111/j.1475-3995.2005.00503.x.

[92] Konis K, Gamas A, Kensek K. Passive performance and building form: An optimization framework for early-stage design support. Sol Energy 2016;125:161–79. https://doi.org/10.1016/j.solener.2015.12.020.

[93] Yu H, Yang W, Li Q. Multi-objective optimization of building's life cycle performance in early design stages. IOP Conf Ser Earth Environ Sci 2019;323. https://doi.org/10.1088/1755-1315/323/1/012116.

[94] Picco M, Lollini R, Marengo M. Towards energy performance evaluation in early stage building design: A simplification methodology for commercial building models. Energy Build 2014;76:497–505. https://doi.org/10.1016/j.enbuild.2014.03.016.

[95] Negendahl K, Nielsen TR. Building energy optimization in the early design stages: A simplified method. Energy Build 2015;105:88–99. https://doi.org/10.1016/j.enbuild.2015.06.087.

[96] Delgarm N, Sajadi B, Delgarm S. Multi-objective optimization of building energy performance and indoor thermal comfort: A new method using artificial bee colony (ABC). Energy Build 2016;131:42–53. https://doi.org/10.1016/j.enbuild.2016.09.003.

[97] Soares N, Gaspar AR, Santos P, Costa JJ. Multi-dimensional optimization of the incorporation of PCM-drywalls in lightweight steel-framed residential buildings in different climates. Energy Build 2014;70:411–21. https://doi.org/10.1016/j.enbuild.2013.11.072.

[98] Arıcı M, Bilgin F, Nižetić S, Karabay H. PCM integrated to external building walls: An optimization study on maximum activation of latent heat. Appl Therm Eng 2020;165. https://doi.org/10.1016/j.applthermaleng.2019.114560.

[99] Kharbouch Y, Mimet A, El Ganaoui M. A Simulation based-optimization method for energy efficiency of a multi-zone house integrated PCM. Energy Procedia 2017;139:450–5. https://doi.org/10.1016/j.egypro.2017.11.236.

[100] Herrera M, Natarajan S, Coley DA, Kershaw T, Ramallo-González AP, Eames M, et al. A review of current and future weather data for building simulation. Build Serv Eng Res Technol 2017;38:602–27. https://doi.org/10.1177/0143624417705937.

[101] Pérez-Andreu V, Aparicio-Fernández C, Martínez-Ibernón A, Vivancos JL. Impact of climate change on heating and cooling energy demand in a residential building in a Mediterranean climate. Energy 2018;165:63–74. https://doi.org/10.1016/j.energy.2018.09.015.

[102] Zou Y, Xiang K, Zhan Q, Li Z. A simulation-based method to predict the life cycle

energy performance of residential buildings in different climate zones of China. Build Environ 2021;193:107663. https://doi.org/10.1016/j.buildenv.2021.107663.

[103] IPCC. Climate Change 2014 Synthesis Report Summary Chapter for Policymakers. Ipcc 2014:31.

[104] Zou Y, Lou S, Xia D, Lun IYF, Yin J. Multi-objective building design optimization considering the effects of long-term climate change. J Build Eng 2021;44:102904. https://doi.org/10.1016/j.jobe.2021.102904.

[105] Cellura M, Guarino F, Longo S, Tumminia G. Climate change and the building sector: Modelling and energy implications to an office building in southern Europe. Energy Sustain Dev 2018;45:46–65. https://doi.org/10.1016/j.esd.2018.05.001.

[106] Berardi U, Jafarpur P. Assessing the impact of climate change on building heating and cooling energy demand in Canada. Renew Sustain Energy Rev 2020;121:109681. https://doi.org/10.1016/j.rser.2019.109681.

[107] Moazami A, Nik VM, Carlucci S, Geving S. Impacts of future weather data typology on building energy performance – Investigating long-term patterns of climate change and extreme weather conditions. Appl Energy 2019;238:696–720. https://doi.org/10.1016/j.apenergy.2019.01.085.

[108] Chan ALS. Developing future hourly weather files for studying the impact of climate change on building energy performance in Hong Kong. Energy Build 2011;43:2860–8. https://doi.org/10.1016/j.enbuild.2011.07.003.

[109] Fowler HJ, Blenkinsop S, Tebaldi C. Linking climate change modelling to impacts studies: Recent advances in downscaling techniques for hydrological modelling. Int J Climatol 2007;27:1547–78. https://doi.org/10.1002/joc.1556.

[110] Abolhassani SS, Mastani Joybari M, Hosseini M, Parsaee M, Eicker U. A systematic methodological framework to study climate change impacts on heating and cooling demands of buildings. J Build Eng 2023;63:105428. https://doi.org/10.1016/j.jobe.2022.105428.

[111] Brown C, Greene A, Block P, Giannini A. Review of downscaling methodologies for Africa climate applications. IRI Tech Rep 08-05 IRI Downscal Rep 2008:1–31.

[112] Diaz-Nieto J, Wilby RL. A comparison of statistical downscaling and climate change factor methods: Impacts on low flows in the River Thames, United Kingdom. Clim Change 2005;69:245–68. https://doi.org/10.1007/s10584-005-1157-6.

[113] Trzaska S, Schnarr E. A review of downscaling methods for climate change projections. United States Agency Int Dev by Tetra Tech ARD 2014:1–42.

[114] UK Met Office. UKCP18 Guidance: Bias correction. Met Off Hadley Cent Exet UK 2018:1–7.

[115] Belcher SE, Hacker JN, Powell DS. Constructing design weather data for future climates. Build Serv Eng Res Technol 2005;26:49–61. https://doi.org/10.1191/0143624405bt112oa.

[116] Tu T, Ishida K, Ercan A, Kiyama M, Amagasaki M, Zhao T. Hybrid precipitation downscaling over coastal watersheds in Japan using WRF and CNN. J Hydrol Reg Stud 2021;37:100921. https://doi.org/10.1016/j.ejrh.2021.100921.

[117] Colette A, Vautard R, Vrac M. Regional climate downscaling with prior statistical

correction of the global climate forcing. Geophys Res Lett 2012;39. https://doi.org/10.1029/2012GL052258.

[118] Ramakrishnan S, Wang X, Sanjayan J, Wilson J. Thermal performance of buildings integrated with phase change materials to reduce heat stress risks during extreme heatwave events. Appl Energy 2017;194:410–21. https://doi.org/10.1016/j.apenergy.2016.04.084.

[119] Nurlybekova G, Memon SA, Adilkhanova I. Quantitative evaluation of the thermal and energy performance of the PCM integrated building in the subtropical climate zone for current and future climate scenario. Energy 2021;219:119587. https://doi.org/10.1016/j.energy.2020.119587.

[120] Adilkhanova I, Memon SA, Kim J, Sheriyev A. A novel approach to investigate the thermal comfort of the lightweight relocatable building integrated with PCM in different climates of Kazakhstan during summertime. Energy 2020;217:119390. https://doi.org/10.1016/j.energy.2020.119390.

[121] Yildiz Y, Korkmaz K, Göksal özbalta T, Durmus Arsan Z. An approach for developing sensitive design parameter guidelines to reduce the energy requirements of low-rise apartment buildings. Appl Energy 2012;93:337–47. https://doi.org/10.1016/j.apenergy.2011.12.048.

[122] Rubio-Bellido C, Pérez-Fargallo A, Pulido-Arcas JA. Optimization of annual energy demand in office buildings under the influence of climate change in Chile. Energy 2016;114:569–85. https://doi.org/10.1016/j.energy.2016.08.021.

[123] Bilardo M, Ferrara M, Fabrizio E. Resilient optimal design of multi-family buildings in future climate scenarios. E3S Web Conf 2019;111. https://doi.org/10.1051/e3sconf/201911106006.

[124] Nguyen AT, Rockwood D, Doan MK, Dung Le TK. Performance assessment of contemporary energy-optimized office buildings under the impact of climate change. J Build Eng 2021;35:102089. https://doi.org/10.1016/j.jobe.2020.102089.

[125] Saltelli A, Marivoet J. Non-parametric statistics in sensitivity analysis for model output: A comparison of selected techniques. Reliab Eng Syst Saf 1990;28:229–53. https://doi.org/10.1016/0951-8320(90)90065-U.

[126] Peel MC, Finlayson BL, McMahon TA. Updated world map of the Köppen-Geiger climate classification. Hydrol Earth Syst Sci 2007;11:1633–44. https://doi.org/10.5194/hess-11-1633-2007.

[127] Kottek M, Grieser J, Beck C, Rudolf B, Rubel F. World map of the Köppen-Geiger climate classification updated. Meteorol Zeitschrift 2006;15:259–63. https://doi.org/10.1127/0941-2948/2006/0130.

[128] Meteotemplate. Climate classification n.d. https://meteotemplate.com/template/plugins/climateClassification/koppen.php (accessed October 4, 2022).

[129] Ciancio V, Salata F, Falasca S, Curci G, Golasi I, de Wilde P. Energy demands of buildings in the framework of climate change: An investigation across Europe. Sustain Cities Soc 2020;60:102213. https://doi.org/10.1016/j.scs.2020.102213.

[130] Meteo Database > Import meteo data > ASHRAE IWEC2 data n.d. https://www.pvsyst.com/help/meteo_source_ashraeiwec2.htm (accessed January 13, 2023).

[131] ASHRAE International Weather Files for Energy Calculations 2.0 (IWEC2) n.d. https://www.ashrae.org/technical-resources/bookstore/ashrae-international-weather-files-for-energy-calculations-2-0-iwec2 (accessed January 13, 2023).

[132] Zhang, Q.Y., Huang, Y.J., Siwei L. Development of typical year weather data for chinese locations. ASHRAE Trans 2002;108.

[133] Rządkowski G, GŁazewska I, Sawińska K. The gompertz function and its applications in management. Found Manag 2015;7:185–90. https://doi.org/10.1515/fman-2015-0035.

[134] White Box Technologies Weather Data n.d. http://weather.whiteboxtechnologies.com/ (accessed November 24, 2021).

[135] Moazami A, Nik VM, Carlucci S, Geving S. Impacts of future weather data typology on building energy performance – Investigating long-term patterns of climate change and extreme weather conditions. Appl Energy 2019;238:696–720. https://doi.org/10.1016/j.apenergy.2019.01.085.

[136] Guan L. Preparation of future weather data to study the impact of climate change on buildings. Build Environ 2009;44:793–800. https://doi.org/10.1016/j.buildenv.2008.05.021.

[137] Zhang C, Ong L. Sensitivity Analysis of Building Envelop Elements Impact on Energy Consumptions Using BIM. Open J Civ Eng 2017;07:488–508. https://doi.org/10.4236/ojce.2017.73033.

[138] Abanda FH, Byers L. An investigation of the impact of building orientation on energy consumption in a domestic building using emerging BIM (Building Information Modelling). Energy 2016;97:517–27. https://doi.org/10.1016/j.energy.2015.12.135.

[139] Ahangari M, Maerefat M. An innovative PCM system for thermal comfort improvement and energy demand reduction in building under different climate conditions. Sustain Cities Soc 2019;44:120–9. https://doi.org/10.1016/j.scs.2018.09.008.

[140] Gou S, Nik VM, Scartezzini JL, Zhao Q, Li Z. Passive design optimization of newly-built residential buildings in Shanghai for improving indoor thermal comfort while reducing building energy demand. Energy Build 2018;169:484–506. https://doi.org/10.1016/j.enbuild.2017.09.095.

[141] Bagheri-Esfeh H, Safikhani H, Motahar S. Multi-objective optimization of cooling and heating loads in residential buildings integrated with phase change materials using the artificial neural network and genetic algorithm. J Energy Storage 2020;32:101772. https://doi.org/10.1016/j.est.2020.101772.

[142] Delgarm N, Sajadi B, Kowsary F, Delgarm S. Multi-objective optimization of the building energy performance: A simulation-based approach by means of particle swarm optimization (PSO). Appl Energy 2016;170:293–303. https://doi.org/10.1016/j.apenergy.2016.02.141.

[143] Brickworks Building Products. Brick Technical Manual. Version 2. 2017.

[144] McKay MD, Beckman RJ, Conover WJ. A comparison of three methods for selecting values of input variables in the analysis of output from a computer code. Technometrics 2000;42:55–61. https://doi.org/10.1080/00401706.2000.10485979.

[145] Minasny B, McBratney AB. A conditioned Latin hypercube method for sampling in

the presence of ancillary information. Comput Geosci 2006;32:1378–88. https://doi.org/10.1016/j.cageo.2005.12.009.

[146] Helton JC, Johnson JD, Sallaberry CJ, Storlie CB. Survey of sampling-based methods for uncertainty and sensitivity analysis. Reliab Eng Syst Saf 2006;91:1175–209. https://doi.org/10.1016/j.ress.2005.11.017.

[147] Iman RL. Latin Hypercube Sampling. Encycl Quant Risk Anal Assess 2008. https://doi.org/10.1002/9780470061596.risk0299.

[148] Petelet M, Iooss B, Asserin O, Loredo A. Latin hypercube sampling with inequality constraints. AStA Adv Stat Anal 2010;94:325–39. https://doi.org/10.1007/s10182-010-0144-z.

[149] Shields MD, Zhang J. The generalization of Latin hypercube sampling. Reliab Eng Syst Saf 2016;148:96–108. https://doi.org/10.1016/j.ress.2015.12.002.

[150] Menberg K, Heo Y, Augenbroe G, Choudhary R. New extension of Morris method for sensitivity analysis of building energy models. Build Simul Optim 2016 2016.

[151] Narkuniene A, Poskas P, Kilda R, Bartkus G. Uncertainty and sensitivity analysis of radionuclide migration through the engineered barriers of deep geological repository: Case of RBMK-1500 SNF. Reliab Eng Syst Saf 2015;136:8–16. https://doi.org/10.1016/j.ress.2014.11.011.

[152] Wang C, Peng M, Xia G. Sensitivity analysis based on Morris method of passive system performance under ocean conditions. Ann Nucl Energy 2020;137:107067. https://doi.org/10.1016/j.anucene.2019.107067.

[153] Goel S, Rosenberg M, Athalye R, Xie Y. Enhancements to ASHRAE Standard 90.1 Prototype Building Models. Pacific Northwest Natl Lab 2014.

[154] Deru M, Field K, Studer D, Benne K, Griffith B, Torcellini P, et al. U.S. Department of Energy commercial reference building models of the national building stock. Publ 2011:1–118. https://doi.org/NREL Report No. TP-5500-46861.

[155] Shiming D, Zheng L, Minglu Q. Indoor thermal comfort characteristics under the control of a direct expansion air conditioning unit having a variable-speed compressor and a supply air fan. Appl Therm Eng 2009;29:2187–93. https://doi.org/10.1016/j.applthermaleng.2008.10.011.

[156] Asadi E, da Silva MG, Antunes CH, Dias L. A multi-objective optimization model for building retrofit strategies using TRNSYS simulations, GenOpt and MATLAB. Build Environ 2012;56:370–8. https://doi.org/10.1016/j.buildenv.2012.04.005.

[157] Asadi S, Amiri SS, Mottahedi M. On the development of multi-linear regression analysis to assess energy consumption in the early stages of building design. Energy Build 2014;85:246–55. https://doi.org/10.1016/j.enbuild.2014.07.096.

[158] ISO 7730. Ergonomics of the thermal environment — Analytical determination and interpretation of thermal comfort using calculation of the PMV and PPD indices and local thermal comfort criteria. Int Stand 2005;Third edit.

[159] Sarri A, Bechki D, Bouguettaia H, Al-Saadi SN, Boughali S, Farid MM. Effect of using PCMs and shading devices on the thermal performance of buildings in different Algerian climates. A simulation-based optimization. Sol Energy 2021;217:375–89. https://doi.org/10.1016/j.solener.2021.02.024.

[160] Tabares-Velasco PC, Christensen C, Bianchi M. Verification and validation of

EnergyPlus phase change material model for opaque wall assemblies. Build Environ 2012;54:186–96. https://doi.org/10.1016/j.buildenv.2012.02.019.

[161] Alam M, Jamil H, Sanjayan J, Wilson J. Energy saving potential of phase change materials in major Australian cities 2014;78:192–201.

[162] Markarian E, Fazelpour F. Multi-objective optimization of energy performance of a building considering different configurations and types of PCM. Sol Energy 2019;191:481–96. https://doi.org/10.1016/j.solener.2019.09.003.

[163] Fumo N, Mago P, Luck R. Methodology to estimate building energy consumption using EnergyPlus Benchmark Models. Energy Build 2010;42:2331–7. https://doi.org/10.1016/j.enbuild.2010.07.027.

[164] Wang H, Lu W, Wu Z, Zhang G. Parametric analysis of applying PCM wallboards for energy saving in high-rise lightweight buildings in Shanghai. Renew Energy 2020;145:52–64. https://doi.org/10.1016/j.renene.2019.05.124.

[165] Bano F, Sehgal V. Finding the gaps and methodology of passive features of building envelope optimization and its requirement for office buildings in India. Therm Sci Eng Prog 2019;9:66–93. https://doi.org/10.1016/j.tsep.2018.11.004.

[166] Naderi E, Sajadi B, Behabadi MA, Naderi E. Multi-objective simulation-based optimization of controlled blind specifications to reduce energy consumption, and thermal and visual discomfort: Case studies in Iran. Build Environ 2019;169:106570. https://doi.org/10.1016/J.BUILDENV.2019.106570.

[167] Naji S, Aye L, Noguchi M. Multi-objective optimisations of envelope components for a prefabricated house in six climate zones. Appl Energy 2021;282:116012. https://doi.org/10.1016/j.apenergy.2020.116012.

[168] R: What is R? n.d. https://www.r-project.org/about.html (accessed January 13, 2023).

[169] Markarian E, Fazelpour F. Multi-objective optimization of energy performance of a building considering different configurations and types of PCM. Sol Energy 2019;191:481–96. https://doi.org/10.1016/j.solener.2019.09.003.

[170] Kuznik F, Virgone J. Experimental assessment of a phase change material for wall building use. Appl Energy 2009;86:2038–46. https://doi.org/10.1016/j.apenergy.2009.01.004.

[171] Cui H, Memon SA, Liu R. Development, mechanical properties and numerical simulation of macro encapsulated thermal energy storage concrete. Energy Build 2015;96:162–74. https://doi.org/10.1016/j.enbuild.2015.03.014.

[172] Souayfane F, Biwole PH, Fardoun F. Thermal behavior of a translucent superinsulated latent heat energy storage wall in summertime. Appl Energy 2018;217:390–408. https://doi.org/10.1016/j.apenergy.2018.02.119.

[173] Helton JC, Iman RL. Sensitivity analysis of a model for the environmental movement of radionuclides. Health Phys 1982;42:565–84. https://doi.org/10.1097/00004032-198205000-00002.

[174] Guo J, Li M, Jin Y, Shi C, Wang Z. Energy Prediction and Optimization Based on Sequential Global Sensitivity Analysis: The Case Study of Courtyard-Style Dwellings in Cold Regions of China. Buildings 2022;12. https://doi.org/10.3390/buildings12081132.

[175] Yildiz Y, Arsan ZD. Identification of the building parameters that influence heating and cooling energy loads for apartment buildings in hot-humid climates. Energy 2011;36:4287–96. https://doi.org/10.1016/j.energy.2011.04.013.

[176] Conover WJ. Practical Non-Parametric Statistics. Biometrics 1981;37:621. https://doi.org/10.2307/2530578.

[177] Iman RL, Conover WJ. Small sample sensitivity analysis techniques for computer models, with an application to risk assessment. Commun Stat - Theory Methods 1980;9:1749–842. https://doi.org/10.1080/03610928008827996.

[178] Iooss B, Lemaître P. A review on global sensitivity analysis methods. Oper Res Comput Sci Interfaces Ser 2015;59:101–22. https://doi.org/10.1007/978-1-4899-7547-8_5.

[179] Campolongo F, Cariboni J, Saltelli A. An effective screening design for sensitivity analysis of large models. Environ Model Softw 2007;22:1509–18. https://doi.org/10.1016/j.envsoft.2006.10.004.

[180] Zeferina V, Wood FR, Edwards R, Tian W. Sensitivity analysis of cooling demand applied to a large office building. Energy Build 2021;235:110703. https://doi.org/10.1016/j.enbuild.2020.110703.

[181] Morris Screening Method — gsa-module 0.5.3 documentation n.d. https://gsa-module.readthedocs.io/en/stable/implementation/morris_screening_method.html (accessed March 15, 2023).

[182] Hu Y, Guo R, Heiselberg PK, Johra H. Modeling PCM Phase Change Temperature and Hysteresis in Ventilation Cooling and Heating Applications. Energies 2020;13:6445.

[183] Bamdad K, Cholette ME, Omrani S, Bell J. Future energy-optimised buildings — Addressing the impact of climate change on buildings. Energy Build 2021;231:110610. https://doi.org/10.1016/j.enbuild.2020.110610.

[184] Maier HR, Razavi S, Kapelan Z, Matott LS, Kasprzyk J, Tolson BA. Introductory overview: Optimization using evolutionary algorithms and other metaheuristics. Environ Model Softw 2019;114:195–213. https://doi.org/10.1016/j.envsoft.2018.11.018.

[185] Whole Building Design | WBDG - Whole Building Design Guide n.d. https://wbdg.org/resources/whole-building-design (accessed February 15, 2023).

[186] Wolpert DH, Macready WG. No free lunch theorems for optimization. IEEE Trans Evol Comput 1997;1:67–82. https://doi.org/10.1109/4235.585893.

[187] Zhang Y. “Use jEPlus as an efficient building design optimisation tool.” CIBSE ASHRAE Tech Symp Imp Coll 18 19 April 2012, London, UK 2012.

[188] Electricity prices around the world | GlobalPetrolPrices.com n.d. https://www.globalpetrolprices.com/electricity_prices/ (accessed May 29, 2022).

[189] Wang R, Lu S, Feng W. A three-stage optimization methodology for envelope design of passive house considering energy demand, thermal comfort and cost. Energy 2020;192:116723. https://doi.org/10.1016/j.energy.2019.116723.

[190] House Window Prices & Costs for New & Replacement Windows n.d. https://windowpriceguide.com/prices (accessed May 3, 2023).

[191] MetalsDepot® - Buy Steel Sheet Online - Any Quantity, Any Size! n.d.

https://www.metalsdepot.com/steel-products/steel-sheet (accessed May 3, 2023).

[192] Material Cost Guides and Calculators - Homewyse n.d. https://homewyse.com/costs/ (accessed May 29, 2022).

[193] Home Insulation Prices, Costs & Types n.d. https://insulationguides.com/ (accessed May 3, 2023).

[194] Silva AS, Almeida LSS, Ghisi E. Decision-making process for improving thermal and energy performance of residential buildings: A case study of constructive systems in Brazil. Energy Build 2016;128:270–86. https://doi.org/10.1016/j.enbuild.2016.06.084.

[195] Garcia Sanchez D, Lacarrière B, Musy M, Bourges B. Application of sensitivity analysis in building energy simulations: Combining first- and second-order elementary effects methods. Energy Build 2014;68:741–50. https://doi.org/10.1016/j.enbuild.2012.08.048.

[196] Maučec D, Premrov M, Leskovar VŽ. Use of sensitivity analysis for a determination of dominant design parameters affecting energy efficiency of timber buildings in different climates. Energy Sustain Dev 2021;63:86–102. https://doi.org/10.1016/j.esd.2021.06.003.

[197] De Wilde P, Tian W. Predicting the performance of an office under climate change: A study of metrics, sensitivity and zonal resolution. Energy Build 2010;42:1674–84. https://doi.org/10.1016/j.enbuild.2010.04.011.

[198] Manual R. SimLab 2.2 Reference manual n.d.

[199] M'hamdi Y, Baba K, Tajayouti M, Nounah A. Energy, environmental, and economic analysis of different buildings envelope integrated with phase change materials in different climates. Sol Energy 2022;243:91–102. https://doi.org/10.1016/j.solener.2022.07.031.

[200] Solgi E, Fayaz R, Kari BM. Cooling load reduction in office buildings of hot-arid climate, combining phase change materials and night purge ventilation. Renew Energy 2016;85:725–31. https://doi.org/10.1016/j.renene.2015.07.028.

[201] Worldwide Electricity Pricing | Energy Cost Per KWh in 230 Countries n.d. https://www.cable.co.uk/energy/worldwide-pricing/ (accessed January 20, 2023).

[202] Yau YH, Chew BT. A review on predicted mean vote and adaptive thermal comfort models. Build Serv Eng Res Technol 2014;35:23–35. https://doi.org/10.1177/0143624412465200.

Appendices

Appendix A – SRRC code in R program

```
# SRRC Sensitivity analysis (SA)
# Data extracted from jEPLus software in xslx file (All combined re
# weather file
# PCM
# For data use:

exceldata = read_excel("E:/FOR THESIS/FOR SIM 15.10.2022/RESULTS IN


dfdata = data.frame(exceldata)
dfdata

# for SA download following packages

library(sensitivity)
library(boot)

# The number for bootstrapping is 100
n <- 100

# The inputs is in X
# x1,x2. the variables names for SA

options(max.print=10000)
x1<-dfdata[,1]
x2<-dfdata[,2]
x3<-dfdata[,3]
x4<-dfdata[,4]
x5<-dfdata[,5]
x6<-dfdata[,6]
x7<-dfdata[,7]
x8<-dfdata[,8]
x9<-dfdata[,9]
x10<-dfdata[,10]
x11<-dfdata[,11]


X <- data.frame(x1,x2,x3,x4,x5,x6,x7,x8,x9,x10,x11)

# Outputs is in y

y <- dfdata[,12]
# sensitivity analysis


x <- src(X, y, rank=TRUE, nboot = 100,conf=0.95)
print(x)

plot(x, ylim = c(-1,1))
```

Appendix B – Published articles

Lead Author - Assemgul Saurbayeva:

Sensitivity analysis and optimization of PCM integrated buildings in a tropical savanna climate (Assemgul Saurbayeva, Shazim Ali Memon, Jong Kim).

Journal of Building Engineering,

Q1, impact factor 7.144,

Volume 64,

2023,

105603,

ISSN 2352-7102,

https://doi.org/10.1016/j.jobe.2022.105603)